DESIGN AND CHARACTERIZATION OF CIRCULARLY POLARIZED CAVITY-BACKED SLOT ANTENNAS IN AN IN-HOUSE-CONSTRUCTED ANECHOIC CHAMBER

by

Mangalam Chandak

A thesis submitted in partial fulfillment
of the requirements for the degree

of

MASTER OF SCIENCE

in

Electrical Engineering

Approved:

Dr. Reyhan Baktur Major Professor	Dr. Edmund Spencer Committee Member
Dr. Jacob Gunther Committee Member	Dr. Mark R. McLellan Vice President for Research and Dean of the School of Graduate Studies

UTAH STATE UNIVERSITY
Logan, Utah

2012

Abstract

Design and Characterization of Circularly Polarized Cavity-Backed Slot Antennas in an In-House-Constructed Anechoic Chamber

by

Mangalam Chandak, Master of Science

Utah State University, 2012

Major Professor: Dr. Reyhan Baktur
Department: Electrical and Computer Engineering

Small satellites are satellites that weight less than 500 kg. Compared to larger satellites, a small satellite, especially a cube satellite, has limited surface area. The limited surface area casts challenges for allocating essential parts, such as antennas, for the satellite. Therefore, antennas that are conformal to the satellite surface have distinct advantages over other types of antennas that need significant mounting area. One of the very effective conformal antennas is cavity-backed slot antennas that can be integrated around solar cells and do not compete for extra surface area. The previous study performed on cavity-backed slot antennas was mainly a feasibility study and did not address realistic concerns such as effective feeding methods for the antennas. This thesis work is aimed at providing more detailed study on achieving high quality circular polarization (CP) and simplified feed design to initiate effective integration of the antenna with solar panel.

In order to accurately characterize an antenna, an effective antenna range in an anechoic chamber is important. Utah State University had an effective near-field range; however, there was not an fully shielded anechoic chamber. As another objective of this thesis work, a state-of-the-art anechoic chamber has been constructed, calibrated, and utilized to measure

different antenna parameters. This thesis also shows correct methods to measure important antenna properties such as CP and antenna efficiency.

(104 pages)

Public Abstract

Design and Characterization of Circularly Polarized Cavity-Backed Slot Antennas in an In-House-Constructed Anechoic Chamber

by

Mangalam Chandak, Master of Science

Utah State University, 2012

Major Professor: Dr. Reyhan Baktur
Department: Electrical and Computer Engineering

Small satellites have become important vehicles for space exploration. One of the challenges on these satellites is their limited surface area, which creates problems in allocating resources for devices such as antennas. Also, an effective satellite communication system often requires circularly polarized antennas. Therefore, integrating cross slot antennas around solar cells to form a multifunctional solar panel is one of the best solutions for small satellites. The cross geometry provides circular polarization and the slot configuration does not compete for any additional surface space. The main goal of this thesis was to design, fabricate, and test such type of slot antennas. Although a cross slot antennas have been designed the integrated with solar cells before, the previous study was limited in terms of the quality of the circular polarization as well as the effectiveness of the excitation method. This thesis work is aimed to address improve on all those limitations.

In order to accurately test the antenna, there needs an environment that mimics free space that allows an antenna understand to radiate into infinite unbounded pace. Such an environment can be achieved by designing an anechoic chamber, where most electromagnetic radiation from outside can be shielded, and radiation from an antenna inside can be fully absorbed. The second objective of this thesis work was to design and construct a fully

shielded state-of-the-art anechoic chamber at Utah State University. The details such as material selection, assembly, and construction of accessories for the antenna testing system are documented in this thesis. The detailed correct antenna measurement method, as well as a number of antenna measurement results, is discussed and presented.

To my beloved parents and my brother for their love and continuous support

Acknowledgments

I would like to express my gratitude towards my advisor, Dr. Reyhan Baktur, for all her support, encouragement, guidance, and efforts. I would like to thank her for providing me the opportunity to work on a topic that interests me and for also providing me with support throughout my master's program. During this time, I learned a lot from her and will always cherish the work I did in her research group. I would also like to express my deep appreciation to the other members of my committee, Dr. Edmund Spencer and Dr. Jacob Gunther, for their help and time in making my thesis a better creation.

I would like to thank my colleagues in my research group at Utah State University for all their support and help in simulation and fabrication of antennas and their help with my thesis work. I would also like give special thanks to the employees of the ECE Department Store for all their help in making this thesis a reality by their readiness to help and by making sure that I always had whatever I needed to finish this work. I would like to thank my wonderful family for all their support, love, effort, and encouragement during this time of my life. Their faith in me made it possible. I would also like to thank all my friends in Logan for their support and hospitaility.

Mangalam Chandak

Contents

List of Tables

List of Figures

Chapter 1

Introduction

1.1 Thesis Overview

A small satellite is a satellite which has a mass less than 500 Kgs. It is generally employed in missions that large satellites cannot accomplish. These satellites are generally small in size with very limited surface area. Thus the needs and requirements of small satellites is different from other satellites. The limited surface area on such a satellite is generally used for placing solar cells so that the satellite can work smoothly. Due to the limited surface area and solar cells on the satellite, the antennas placed on the satellite need to be conformal and less disturbing. Also, conformal antennas such as slot or patch have various advantages over other kind of antennas such as a dipole antenna, and thus are best suited for use on small satellites.

Dipole antennas are the most used antennas on a small satellite, but with its inherent disadvantages such as its deployment mechanism and its property limitation due to its mounting position, it is not the best choice to be used [1]. To overcome these defects, different types of conformal antennas, mostly patch antennas [2] and slot antennas were proposed. Although, these antennas removed a lot of the drawbacks of the previous antennas, they still had a lot of troubles. The slot antennas proposed had a lot of back radiation and had low gain while the suggested patch antennas hindered the operation of the solar cells on the small satellites and thus were not advisable. To overcome the drawbacks of standard patch antennas, transparent patch antennas were suggested [3]. Although these patch antennas allowed for better operation of solar cells and had higher gains, they belonged to a different class and had some of their limitations too. Limitations like customized solar cells, higher transparency depending on the substrate or cover glass of the antenna, linear polarization and others, make this kind of antennas hard to use on a small satellite. Thus, cavity-backed

slot antennas [4] were suggested as an alternative to the current antennas on small satellite. The previous study done on cavity backed slot antennas [4] was only a feasibility study of these kind of antennas and their operation and had its own limitations such as complicated feed design, etc. Also, the measurement process used before for the test of different antennas was not accurate enough due to the absence of the anechoic chamber which creates a "free space" condition to measure the antennas. Without these kind of conditions the measurement results obtained will not be precise and will have a lot of spurious readings in it. These spurious readings arise due to the presence of reflecting surfaces around the room which interfere with the working of the antenna.

Thus, the objectives of this thesis work are:

- Detailed study on cavity backing and use of reflector for crossed slot antenna,
- Improved and simplified sesigns of slots and feeds in cavity backed crossed slot antenna to achieve good circular polarization(CP),
- Construction and calibration of anechoic chamber to be used to measure future antennas,
- Accurate measurement of various parameters which help in accurately characterizing an antenna.

1.2 Introduction of Background Terminology, Design, and Measurement Technology

This section explains some of the common terminology used in conformal antenna design and antenna measurments in this thesis.

1.2.1 Conformal Antennas

A conformal antenna is an antenna that conforms to some prescribed shape. The purpose is to build an antenna that is integrated with the structure to perform various functions such as making it less disturbing [5]. Its shape is determined by considerations other than

electromagnetic. Generally, a conformal antenna is planar, cylindrical, or spherical with the radiating elements integrated into the structure or design to make it an effective antenna. Conformal antennas are gradually becoming very important and desirable types of antennas, especially in the field of aerodynamics and hydrodynamics, due to its various advantages over other kinds of antennas. These antennas offer considerable size and location flexibility in comparison to what can be accomplished by using traditional antenna structures. Conformal antennas exhibit uniquely thin and unobtrusive profiles, reduced sizes, and improved performances, making them well suited for use in different kinds of systems [5]. One of the major uses of conformal antennas is in the field of satellite communications. The conformal antennas integrated into the surface of the satellite for communication purposes have distinct advantages over other types of antennas used such as dipole antennas. The most common type of conformal antennas used for communication purposes are slot antennas and patch antennas.

1.2.2 Slot Antennas

Slot antennas can also be called as complimentary forms of wire or dipole antennas as the pattern and impedance data of these forms can be used to predict pattern and impedance of a slot antenna, according to Babinet's principle [6]. A slot antenna usually consists of a metal surface in which a slot is cut out and which when operated at a particular frequency by using different feeding methods such as coaxial feed, microstrip line feed, etc., radiates electromagnetic waves similar to a dipole antenna. In a slot antenna the current is not confined to the edges of the slot, but spread out over the entire metal surface. The radiation pattern of dipole and slot are the same but with the E field and H field interchanged [7]. They are typically used at frequencies of 300MHz to 30GHz. The slot sizes are approximately half wavelength long similar to a dipole antenna. The radiation pattern of a slot antenna is generally bidirectional and is determined by the shape and size of the slot (i.e., it will radiate equally in both the directions) [8]. A simple slot antenna does not have any side lobes, and is thus a pretty efficient radiator. Slot antenna is also affected by the size of its ground plane and its radiation pattern depends on the finite size

it has [9]. One of the major advantages of slot antenna besides its size, design simplicity, low profile, and robustness is that it can be easily made conformal to a structure. Due to the advantages, it can be used for a variety of applications such as in cube satellites where having other kinds of antennas can interfere with the operation of solar cells by casting a shadow on them or covering up the area where the solar cells are located. The slot antennas are generally placed in the gap between the solar cells in the cube satellite, and thus do not require any extra space in the cube satellite surface, therefore allowing for efficient use of the limited surface area available on the cube satellite [4]. One other practical advantage of slot antenna is that the feed section which energizes the slot may be placed below the large metal surface in which the slot is cut. Thus nothing needs to be extended from the surface. Due to the various advantages provided by slot antennas it is being used more frequently for more and more applications now a days and varies according to the application required. Slot antennas are also easily adaptable to VHF and UHF range of frequencies.

1.2.3 Circular Polarization

Polarization of an antenna in a given direction is defined as the polarization of the radiated wave of the antenna, which is that property of an electromagnetic wave describing the time-varying direction and relative magnitude of the electric field vector as observed along the direction of propagation [6]. Polarization is basically of two types: i.e., linear polarization and elliptical polarization with circular polarization being a special case of elliptical polarization [6]. Most of the satellite communication systems favor circular polarization, therefore making it important to design antennas with CP capability.

There are various advantages of having circular polarization. A circularly polarized signal allows establishing and maintaining communication links easier, it is more resistant to signal degradation, multipath distortion is reduced, the signal is much better at penetrating and bending around obstructions and circular polarized antennas send and receive in all the planes so the signal strength is not lost, but is transferred to a different plane and is still utilized.

In general, the electric field of the wave travelling in z direction may have both an x

component and a y component. At a fixed value of z the electric field vector E rotates as a function of time, the tip of the vector describes an ellipse called the polarization ellipse [10]. The ratio of the major to minor axes of the polarization ellipse is called the Axial Ratio (A.R.) [10]. Thus, for a electromagnetic wave

$$A.R. = \frac{OA}{OB}, \tag{1.1}$$

where OA = Major Axis of the ellipse;

OB = Minor Axis of the ellipse.

The special case of elliptical polarization corresponding to circular polarization is when OA = OB and A.R. = 1.

Circular polarization using slot antennas can be achieved as long as we have two slots which are orthogonal to each other and the phase shift between them is 90 degrees. Thus for slot antennas, when we measure circular polarization, we use two criteria. The first is to compare the E-plane and H-plane; they should be similar. The second one is to check the Axial Ratio which should have a magnitude of 1 or near to 1 and the time phase angle of 90 degree [7]. The sense of rotation is always determined by rotating the phase leading component toward the phase lagging component and observing the field rotation as the wave is viewed as it travels away from the observer. This gives the time phase angle, also. If the rotation is clockwise, the wave is right-hand circularly polarized; if the rotation is anticlockwise, the wave is left-hand circularly polarized [6]. In circular polarization the difference between right-hand circular polarization level and left-hand circular polarization level is called cross-polarization level.

1.3 Summary of Methods Adopted

1.3.1 Cavity-Backed Slot Antennas with Circular Polarization

The need for a cavity-backed slot antenna with circular polarization arises because a

simple slot antenna is linearly polarized and has a bidirectional radiation pattern with low gain. The back radiation of a slot antenna can affect the circuitry inside if the slot antenna is made on the surface of devices such as cube satellites [1]. A cavity-backed slot antenna with circular polarization eliminates most of the disadvantages of a simple slot antenna and the various advantages provided by circularly polarized radiation of these antennas makes these kinds of antenna even more desirable for future use. A type of cavity backed slot antenna is shown in Fig. 1.1. A cavity-backed slot antenna (as shown in Fig. 1.1) has a top metallic ground plane on top of a substrate of a certain thickness, on which the slot is cut-out in different shapes. We use a rectangular slot here. A metallic plane is then placed at bottom of the substrate and the substrate is covered from all the sides with the same material which serves as the bottom layer to make it a cavity-backed antenna. Different methods are then used to feed this type of antenna such as coaxial feed, CPW feed, strip lines, etc.

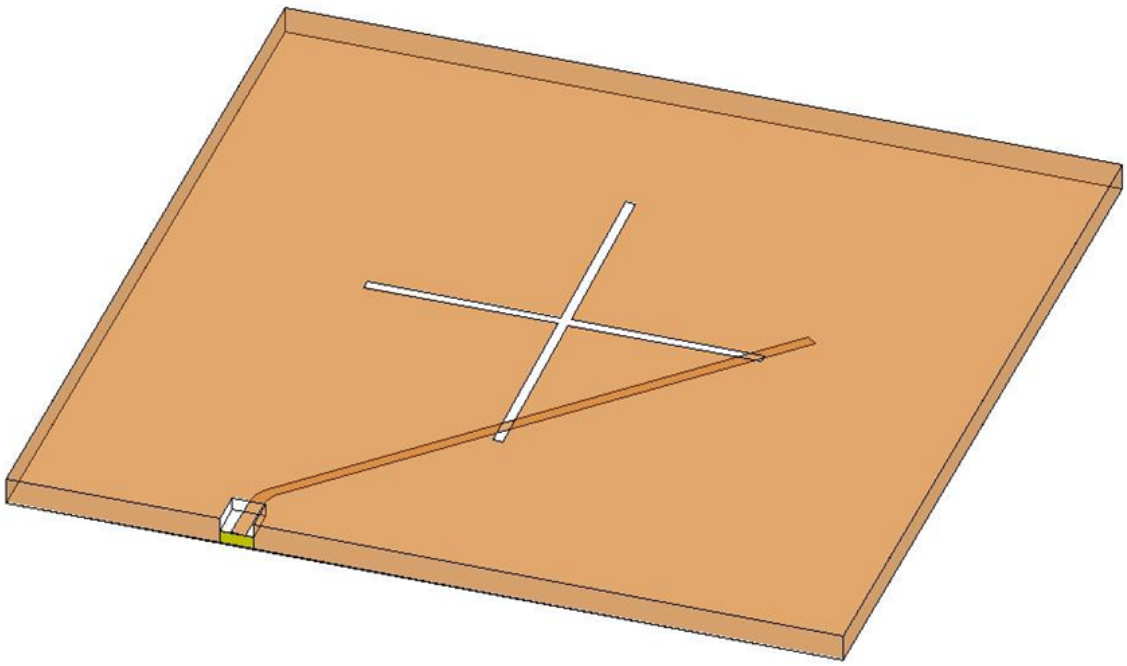

Fig. 1.1: A type of cavity-backed slot antenna.

1.3.2 Feeding Method Using Strip Lines

Strip line is used as a feeding method for the cavity-backed slot antennas because it can be easily integrated in the design of cavity-backed antennas and is thus much easier to use than other methods. A strip line is a smooth metallic strip sandwiched between two parallel ground planes [11]. The material between the two parallel ground planes is called a dielectric. The width of the line, thickness and dielectric constant of the substrate determine the characteristic impedance of the strip line [11]. Some advantages of using a strip line is that it is non-dispersive, has no cutoff frequency, better bandwidth and greater noise immunity. Also, the circuits that use micro-strip line will become better in a strip line configuration as a micro-strip line is quasi TEM while a strip line acts as transverse electromagnetic transmission line(i.e., it operates in the TEM mode) [12]. Strip line has a slower propagation speed compared to a micro-strip line as it is sandwiched between two dielectrics due to which the effective dielectric constant in strip line remains the same as that of the insulator. A strip line has a much lesser width compared to a micro-strip line for a given characteristic impedance as it has two ground planes.

1.3.3 Anechoic Chamber

One of the most important things to achieve after the antenna is designed and fabricated is an accurate characterization of the antenna concerned. The accurate characterization of the antenna depends on some important factors:

- The more data we can collect, the more accurately we can characterize our antenna's performance;
- Antennas pick up increasingly low-level signals, so we need better measurement sensitivity to characterize high performance antennas.

Therefore, based on these factors, to accurately characterize an antenna an anechoic chamber is used while doing measurements for a specific antenna. An Anechoic Chamber improves the ability to measure high performance antennas, improves the capability to

measure low-level signals easily and helps in collecting more data to improve accuracy of characterization. An anechoic chamber meaning no-echoic or echo-free chamber is a room designed to stop reflections of either sound waves or electromagnetic waves [7,13]. They are also insulated from external sources of noise. The combination of both aspects means that it simulates a quiet free space of infinite dimension, which is useful when exterior influences will otherwise give false results [13]. An anechoic chamber can be as small as a compartment to as large as a aircraft hanger depending on the size of the object to be tested and the frequency range of the signals used, although scaled models can also be used by testing at shorter wavelengths. Thus, it is important to find the range and the lowest frequency of the antennas being tested before deciding on the anechoic chamber to be used for measurement purposes. The anechoic chamber constructed at Utah State University is large enough to accurately measure antennas in the frequency range of 2GHz and above. The chamber is first calibrated for accurate measurements based on the frequency of antenna and the antenna is then hooked up in the test site for measurement using the near field range from NSI. The measurement data at multiple frequency points and multiple antenna angles is then collected and processed to display antenna pattern and gain. Measurement of input match or standard wave ratio is done and the data is compared to the design specifications to measure its accuracy.

1.3.4 Pattern Measurement and Gain Measurement

Pattern measurement is the relative power density of the electromagnetic wave transmitted by the antenna in a given direction [7]. Pattern measurement is done to view and validate the radiation pattern of an antenna in far field region of free space. It is accomplished keeping in mind the radiation pattern expected of an antenna, and the simulated and measured results are compared for accuracy and similarity based on the application desired. Radiation pattern of an antenna is defined as "a mathematical function or a graphical representation of the radiation properties of the antenna as a function of space coordinates, which in most cases is determined in the far field region and is represented as a function of directional coordinates" [6]. Thus to measure the radiation pattern, the Antenna Under

Test (AUT) is kept in the far field range for that antenna. Since the far field range of the antenna can be pretty large, near field techniques to measure the radiation pattern of the antenna in the far field were developed which allow the measurement of the field on a surface close to the antenna (typically 3 to 10 times of its wavelength) [6]. This measurement is then predicted to be the same at far field range. There are three different types of near field measurements:

- Planar Near Field Measurements,
- Cylindrical Near Field Measurements,
- Spherical Near Field Measurements.

The measurement type used for measuring the AUT in this thesis is the Spherical Near Field measurement which measures the electric field on a spherical surface close to the AUT. To convert these measurements to far field, spherical harmonics are then used which helps in getting a number of far field and aperture parameters [14]. Pattern measurements are also used to calculate the cross polarization level and axial ratio of the antenna which shows whether the antenna is circularly polarized or linearly polarized. A figure of the setup required for such a measurement is shown in Figs. 1.2 and 1.3 which show the transmistter and receiver scanner setup of NSI, respectively.

Gain is one of the most important parameters to define the performance of an antenna. Gain of an antenna (in a given direction) is defined as the ratio of the intensity in a given direction, to the radiation intensity that would be obtained if the power accepted by the antenna were to be radiated isotropically [15].

$$Gain = 4 \times \pi \times \frac{RadiationIntensity}{TotalInputPower} \tag{1.2}$$

Gain measurement is thus important as it is related to both efficiency and directivity of the antenna. It helps in realizing the difference between theoretically possible gain and the gain which is practically possible which is mostly lower than the theoretical one and

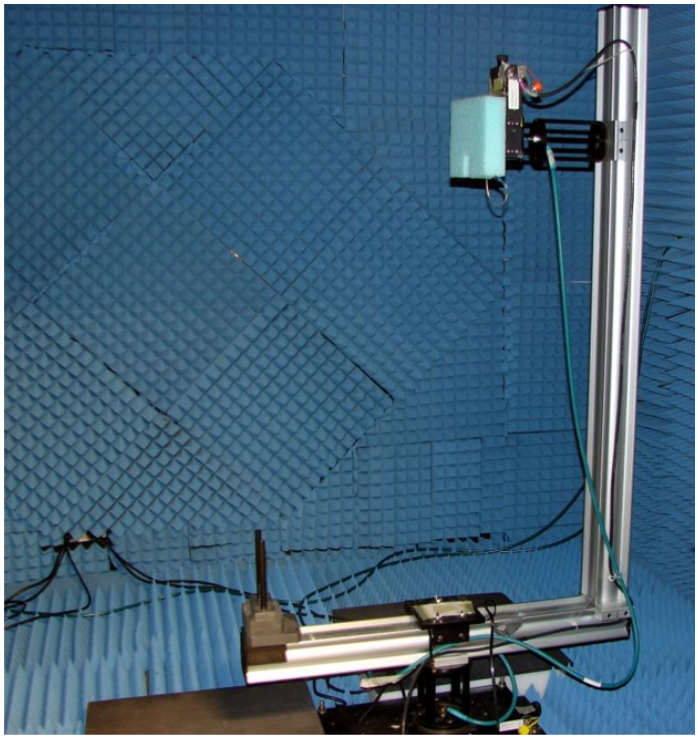

Fig. 1.2: Transmitter scanner setup.

Fig. 1.3: Receiver scanner setup.

helps us is in evaluating an antenna much better. Gain calculation in simulation of AUT is straightforward and most of the new tools do it while simulating the antenna, but in measurement for an AUT it can be only done after the pattern measurement is done and the highest amplitude values are known. Two of the methods used to do gain measurement for an AUT with NSI are:

- Comparison Gain Measurement,
- Direct Gain Measurement.

Direct gain measurement is used as the method to calculate the gain of the antenna in this thesis as it does not require an antenna of comparative parameters and can be easily modified to be used for other kinds of antennas. The gain measured by this method is correct to the accuracy of ± 0.5dB for all practical antennas. This gain value can be later used to calculate the efficiency of the antenna for practical purposes.

1.4 Contributions

The main contribution of this thesis is studying, designing, fabricating, and measuring different types of cavity-backed slot antennas that radiate in only one direction and have high gain. These type of cavity-backed slot antennas have a good CP and are conformal to structures. We also show that the feed design is very simple to make and avoids the complications that generally arises in these kinds of antenna to achieve CP. It also shows the various advantages and disadvantages of different types of antennas made. Another contribution is the construction and the calibration of the anechoic chamber needed to measure antennas in nominally free space condition. In addition, this thesis also describes how different measurements are done to characterize the antenna and how are their results studied.

Chapter 2

Crossed Slot Antennas with Circular Polarization

Slot antennas have advantages of being planar and having relatively small size of the radiating elements. They are also good candidates when considering solar cell integration into the antenna [4]. Since CP is so important for applications now, to achieve it requires two orthogonal slots with appropriate phase shift between them. This chapter presents cross slot antennas with simplified feed structures in order to achieve circular polarization from the antenna and to realize solar cell integration more easily when designed into antenna arrays. Simple printed transmission line feed structures such as strip-line and micro-strip line are used to feed these antennas, as they remove many drawbacks of the other feed designs [12]. In addition, in order to have the antenna radiate in only one direction or to only one side of the ground plane, a reflector and cavity backing is added and its effects and results are shown. These cross slot antennas with cavity backing are improvements over other cavity-backed antennas designed before because of their CP polarization, radiation pattern, and efficiency. The design frequency for these antennas ranges from 2.4GHz -2.6GHz with each antenna having a return loss greater than -20dB and AR of less than 1 dB in simulation and less then 3dB in fabrication. All the antennas are Right-Hand Circularly Polarized (RHCP).

2.1 Study of Reflector Backing and Cavity Backing

Before designing a CP antenna, it is important to perform a study on the difference between reflector backing and cavity backing. Such a study helps us to determine reasonable and more optimal antenna geometry.

The antenna geometry to be studied is as follows. A single slot antenna is placed on the top plane of a Rogers 4003C substrate ($\epsilon_r = 3.55$, thickness = 1.524mm, and dielectric loss

tangent of 0.0027) and the bottom plane of the substrate has a printed feeding microstrip line of width = 2.424mm (Fig. 2.1). The metal on the top plane is grounded. Then, a reflector metal plane is placed at a distance of d1 below the substrate. The reflector is suspended and the media between the reflector and the substrate is air. The ground, substrate, and the reflector are of the same size 10cm × 10cm. The slot is designed to be 48 mm by 1 mm to resonate at the vicinity of 2.5GHz.

A series of studies have been performed for various reflector position by changing d1. It is found that the main difference between placing a reflector instead of shorting the reflector with the top ground plane to form a cavity backing [4] is reflector backing structure results in a higher back lobe on the antenna radiation pattern. There is no significant change on S11 and radiation pattern that has been observed for different d1. It should be noted that every time when d1 is changed, the position of the microstrip line has to be modified in order to maintain a good matching for the slot antenna. Also, the slot geometry has been kept the same for all these case study. A number of results for S11 and antenna patterns for various d1 (in mm and free-space wavelength) are shown in Fig. 2.2 - Fig. 2.17.

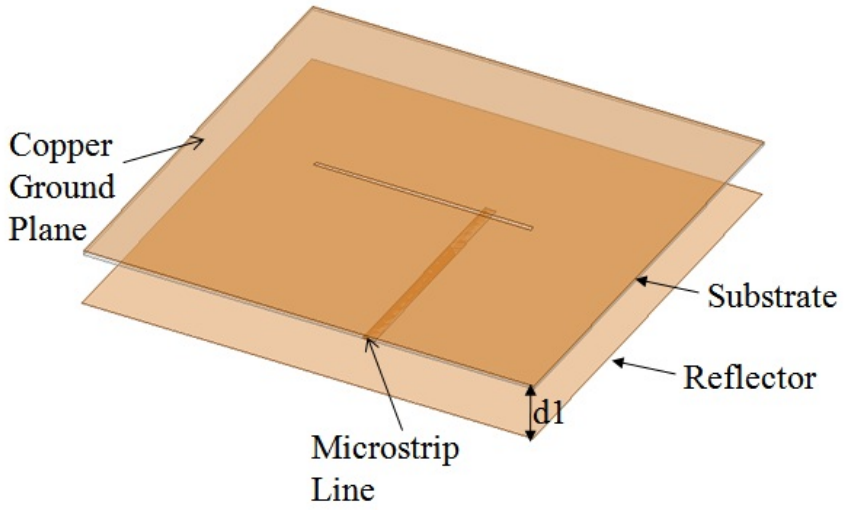

Fig. 2.1: Design of a simple slot antenna with reflector.

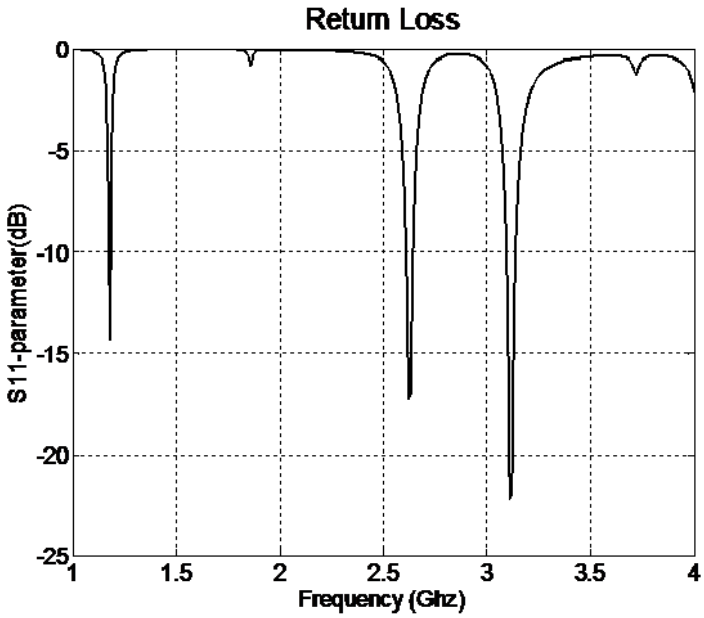

Fig. 2.2: S11 for slot antenna with d1 = 1mm ($\lambda/120$).

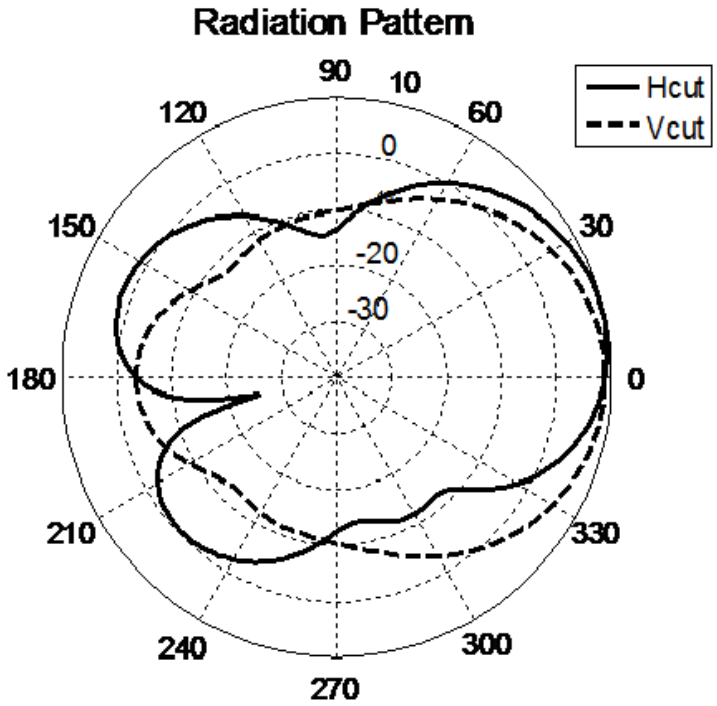

Fig. 2.3: Radiation pattern for slot antenna with d1 = 1mm ($\lambda/120$).

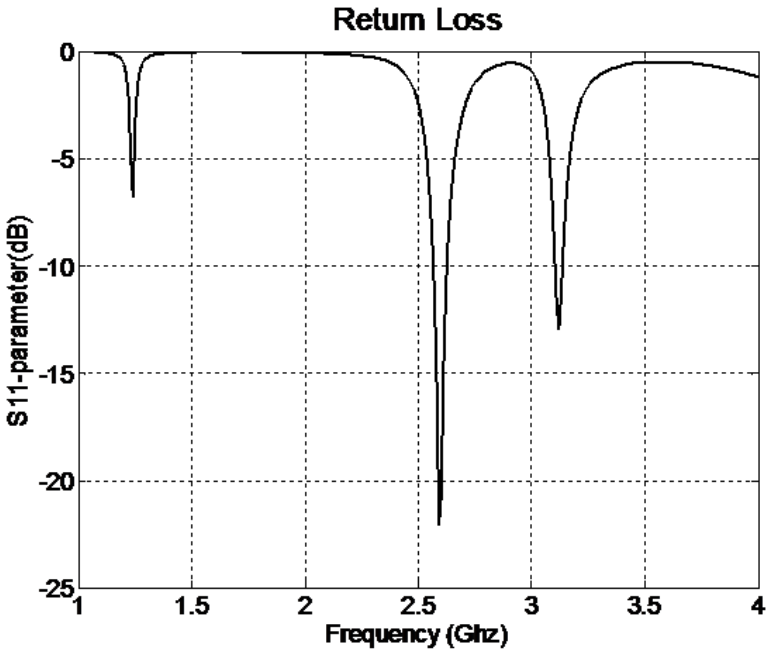

Fig. 2.4: S11 for slot antenna with d1 = 3mm ($\lambda/40$).

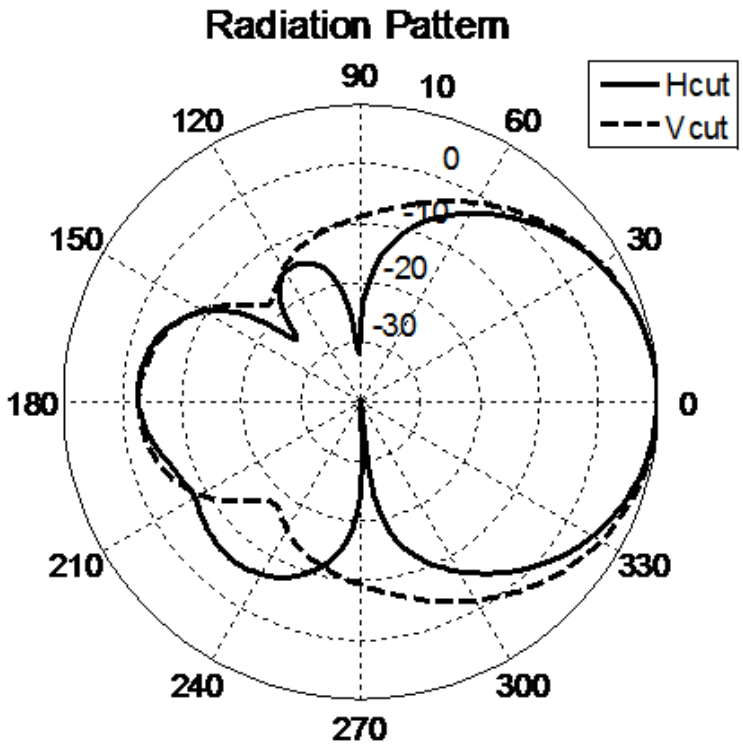

Fig. 2.5: Radiation pattern for slot antenna with d1 = 3mm ($\lambda/40$).

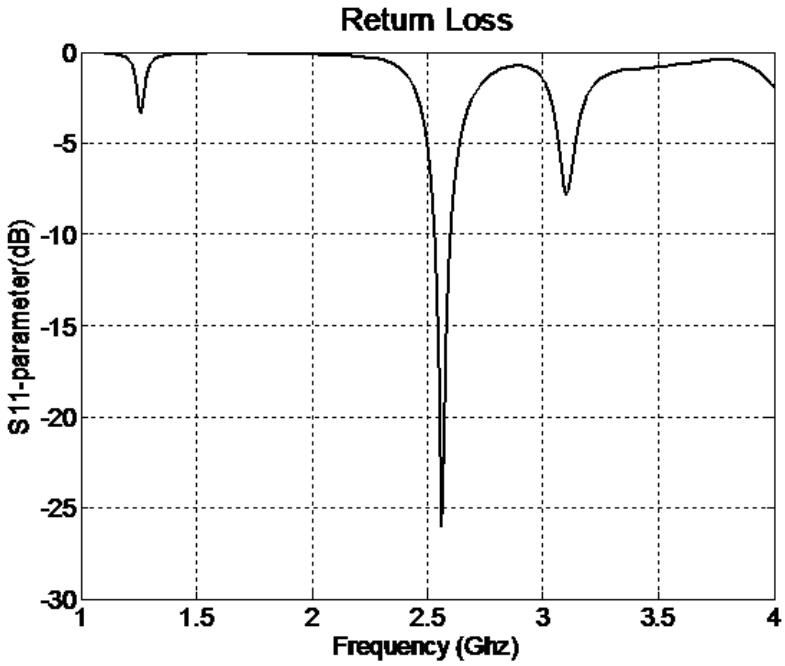

Fig. 2.6: S11 for slot antenna with d1 = 5mm ($5\lambda/120$).

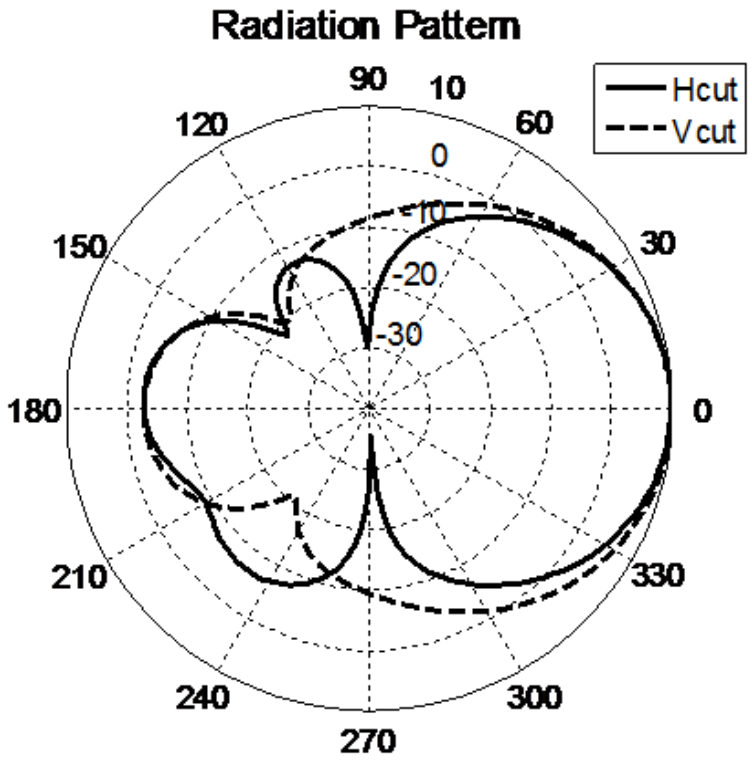

Fig. 2.7: Radiation pattern for slot antenna with d1 = 5mm ($5\lambda/120$).

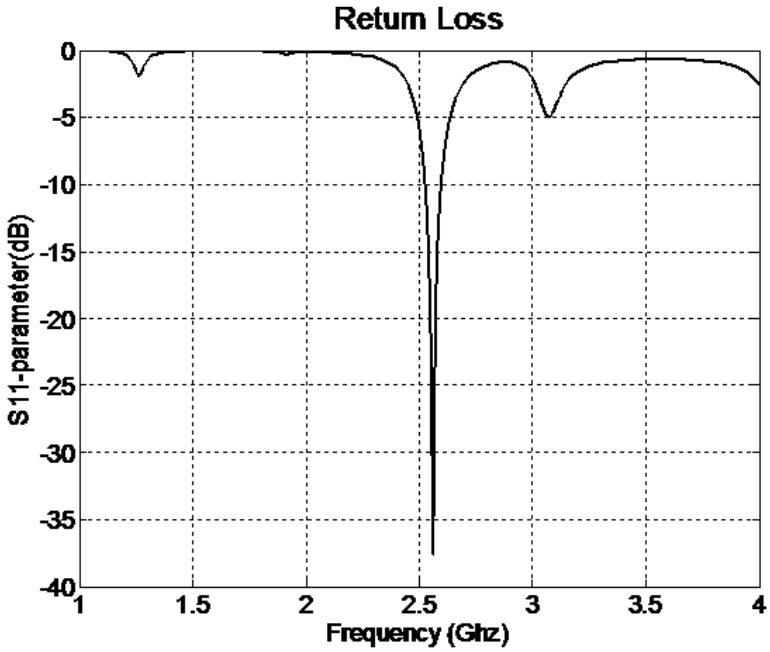

Fig. 2.8: S11 for slot antenna with d1 = 7mm ($7\lambda/120$).

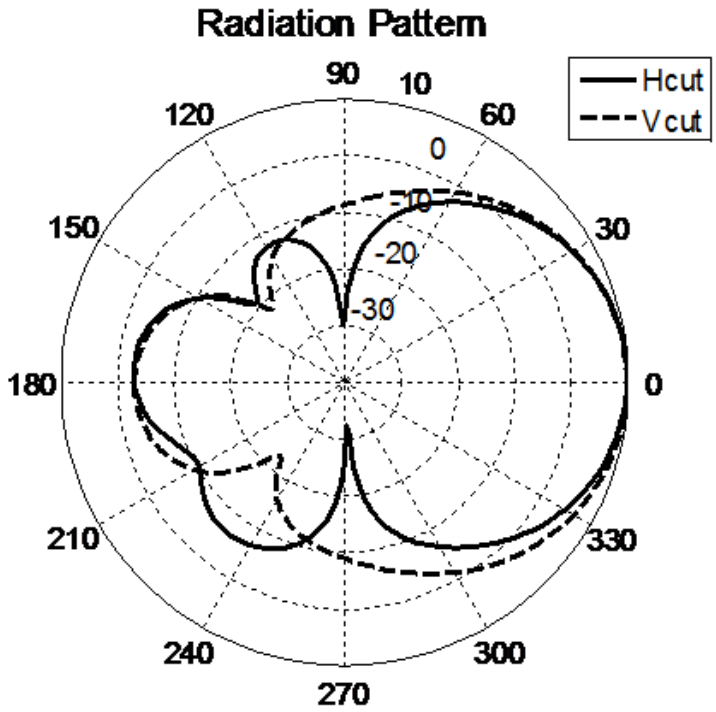

Fig. 2.9: Radiation pattern for slot antenna with d1 = 7mm ($7\lambda/120$).

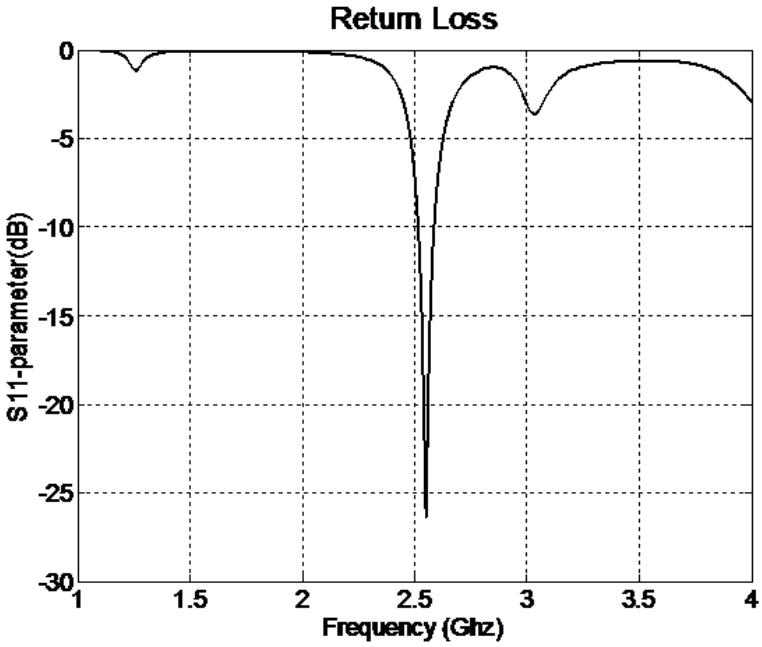

Fig. 2.10: S11 for slot antenna with d1 = 9mm ($3\lambda/40$).

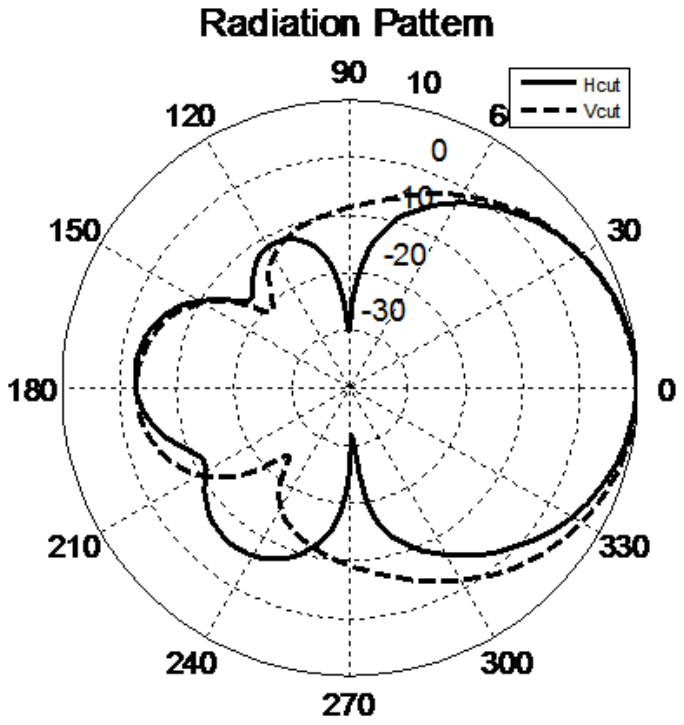

Fig. 2.11: Radiation pattern for slot antenna with d1 = 9mm ($3\lambda/40$).

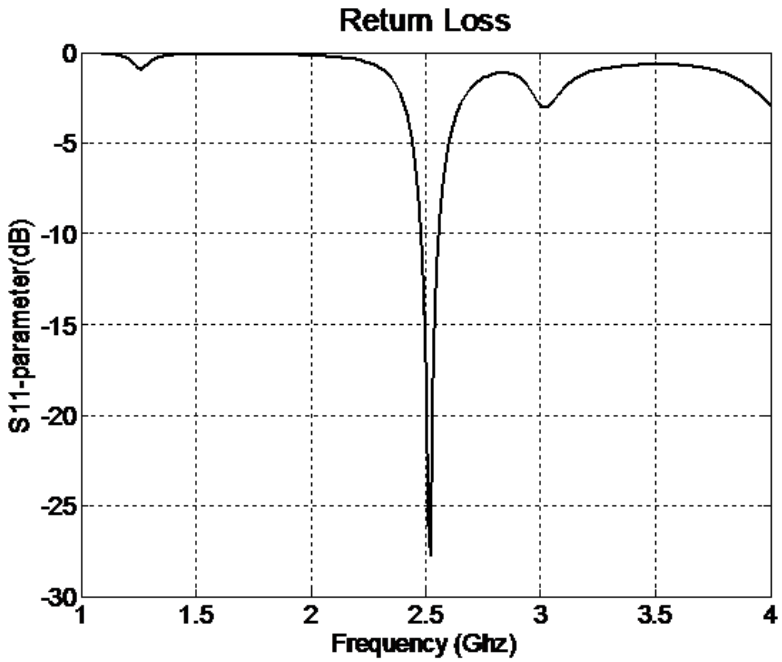

Fig. 2.12: S11 for slot antenna with d1 = 11mm ($11\lambda/120$).

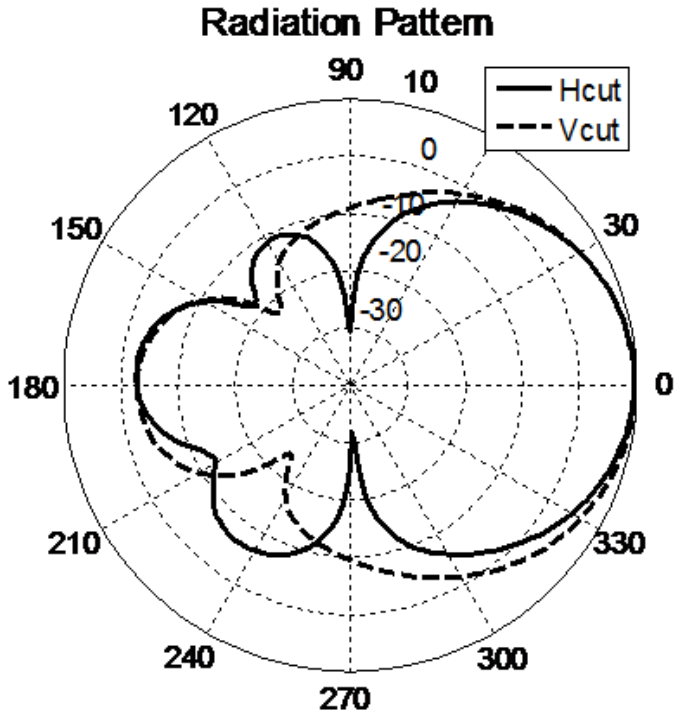

Fig. 2.13: Radiation pattern for slot antenna with d1 = 11mm ($11\lambda/120$).

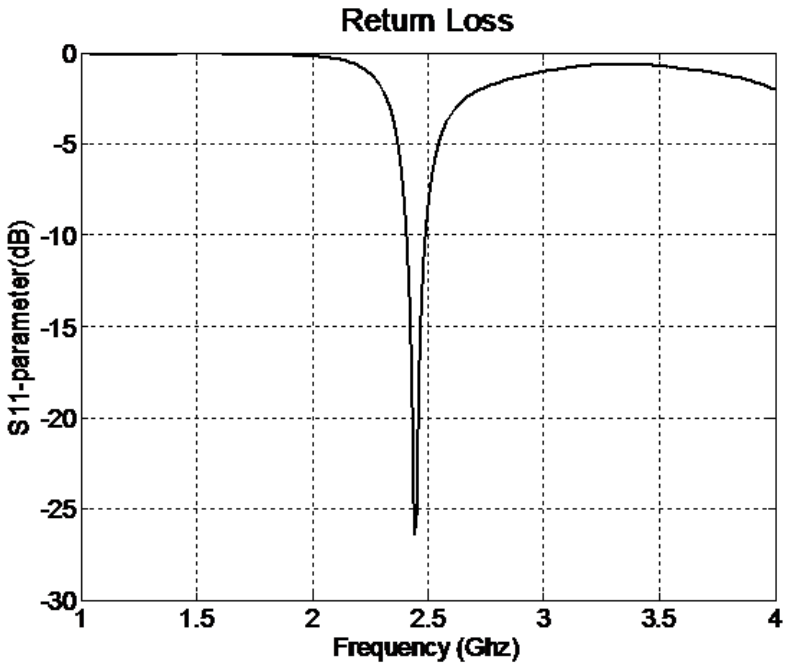

Fig. 2.14: S11 for slot antenna with d1 = 30mm ($\lambda/4$).

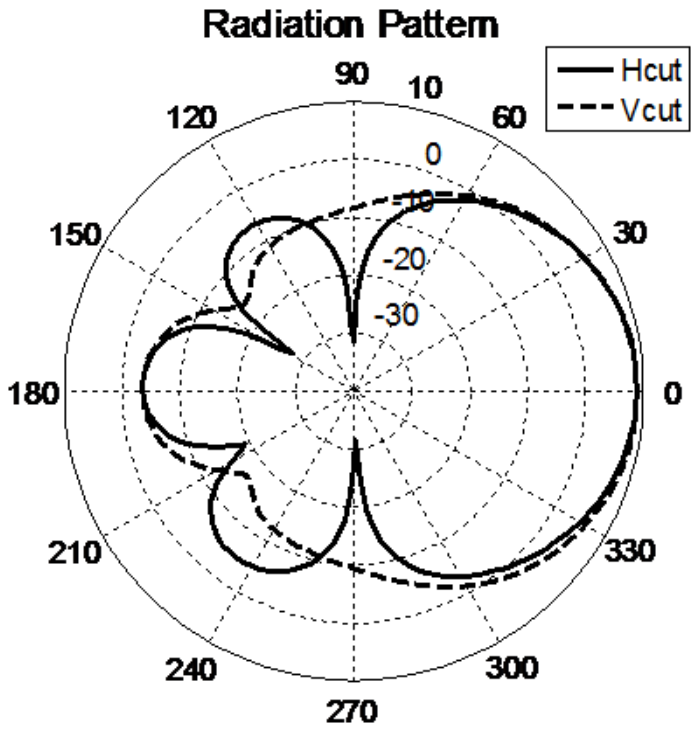

Fig. 2.15: Radiation pattern for slot antenna with d1 = 30mm ($\lambda/4$).

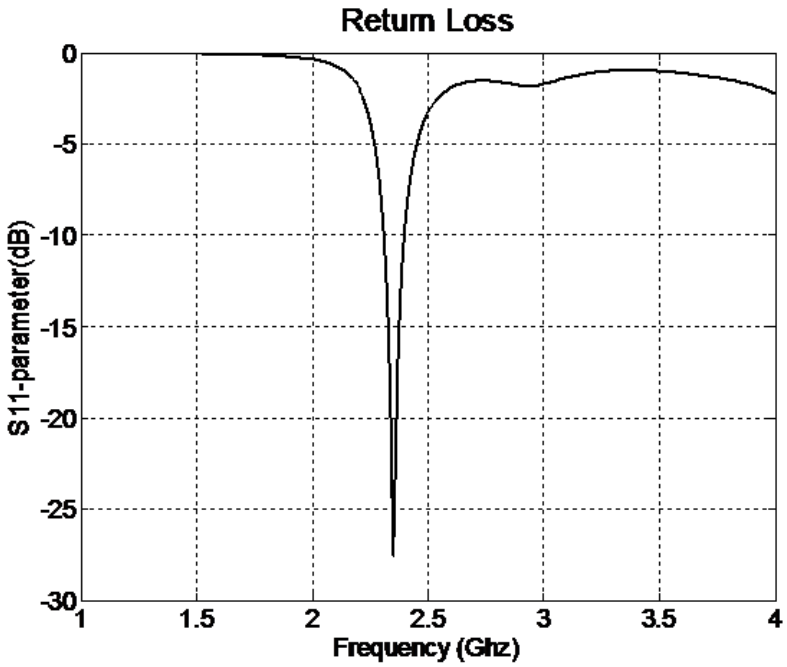

Fig. 2.16: S11 for slot antenna with d1 = 60mm ($\lambda/2$).

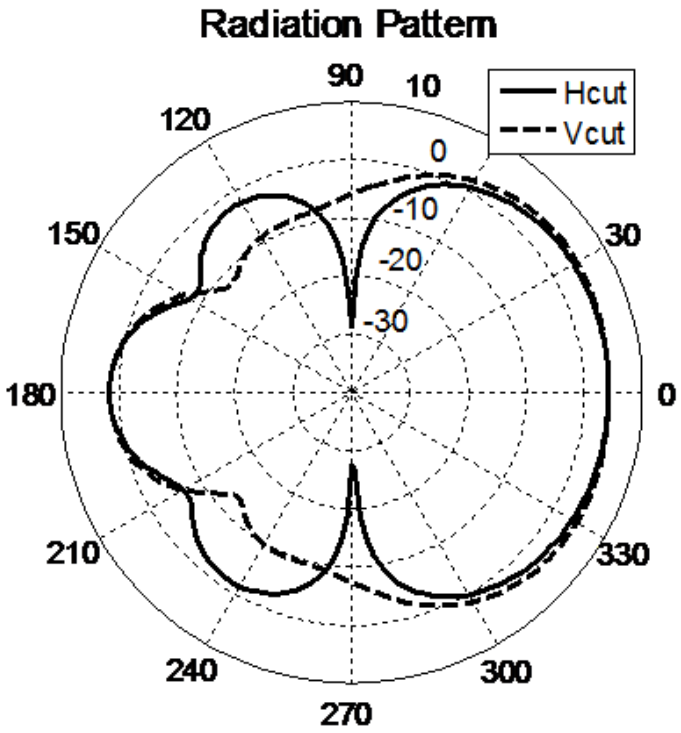

Fig. 2.17: Radiation pattern for slot antenna with d1 = 60mm ($\lambda/2$).

2.2 A Simple Crossed Slot Antenna with Circular Polarization

The design of this antenna is based on the one proposed by Katayama with the main difference being the frequency of operation of this antenna and the fixed and much bigger size of ground plane used [16, 17]. This antenna introduces a much simpler feed design which is used for achieving CP in a slot antenna. The antenna geometry is shown in Fig. 2.18 and is composed of two slots and a micro-strip line feed. On the top of the substrate the two orthogonal slots are etched on a copper ground plane and below the substrate the feed line is printed.

From Fig. 2.18 we see that the two slots etched have different lengths (l_{s1} and l_{s2}) and the same width (w_{s1}). Different lengths for the slots were used here to achieve a good CP from the antenna. The slots are perpendicular to each other at 90 degrees. The micro-strip line is at 45 degrees with both the slots, and the phase shift needed is achieved through the offset distance (O_{s1}). Open stubs matching is used for impedance matching through the stub l_{f1}. All these design parameters were input into the Ansoft HFSS to determine and fine-tune the antenna.

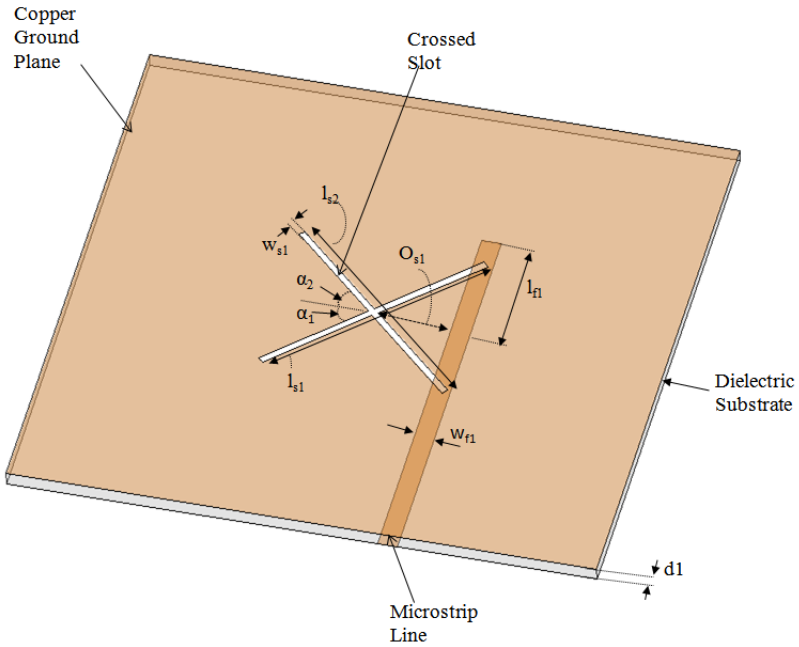

Fig. 2.18: Antenna geometry of a simple crossed slot antenna.

2.2.1 Design

The design frequency of the above antenna was chosen to be 2.50GHz. The substrate used for making this antenna is Roger's 4003C, which has a relative permittivity of ϵ_r = 3.55 and a dielectric loss tangent of 0.0027. The thickness of the substrate is 1.524mm, thus making it the thickness of the antenna. The width and length of the feeding micro-strip line is 3.446mm and 72.5mm, respectively, to provide a 50Ω impedance. The size of the antenna is 10cm × 10cm based on the requirements. The length of the two slots were designed to be l_{s1}= 43 mm and l_{s2} = 44 mm, with the width w_{s1} = 1.2 mm. The angle between the two slots is an exact 90 degrees making them orthogonal to each other. The offset of the micro-strip line from the center of the crossed slot to the center axis of the micro-strip line is O_{s1} = 12.8 mm and the inclination angle α_1 was chosen such that the AR is minimized for the CP antenna. The stub length was found to be l_{f1} = 21.5 mm for open stub matching. All these parameters were simulated in Ansoft's HFSS to determine the workings of the antenna designed.

2.2.2 Results

The simulated results for this antenna are shown in Fig. 2.19 - Fig. 2.21. From Fig. 2.19 we see that the return loss at the resonance frequency is very good and also has a nice bandwidth. The return loss at the frequency of interest in this antenna is below 25dB. Since the antenna was designed to be circularly polarized, the AR shown in Fig. 2.20, is measured in simulation to be less than 1 dB at the frequency of interest, the cross polarization level is found to be in excess of 25dB, and has a high fractional bandwidth of about 5% which proves that cross slot antennas can produce very good CP as shown in Fig. 2.20. The radiation pattern is shown in Fig. 2.21. The measured gain value in simulation is less than 3.5 dB which will become even less when this antenna is fabricated. It is seen that this antenna has a bidirectional radiation pattern (i.e., it radiates equally well in both the directions, does not have a very wide radiation pattern, and has a low gain which makes it unsuitable for use in many of the applications concerned).

This antenna, due to its radiation pattern, is not a good match for a lot of uses which

require a much more sophisticated antenna and better integration into the system to be useful. Also, since the gain of the antenna is considered low, a lot of applications will be uncertain about using such an antenna.

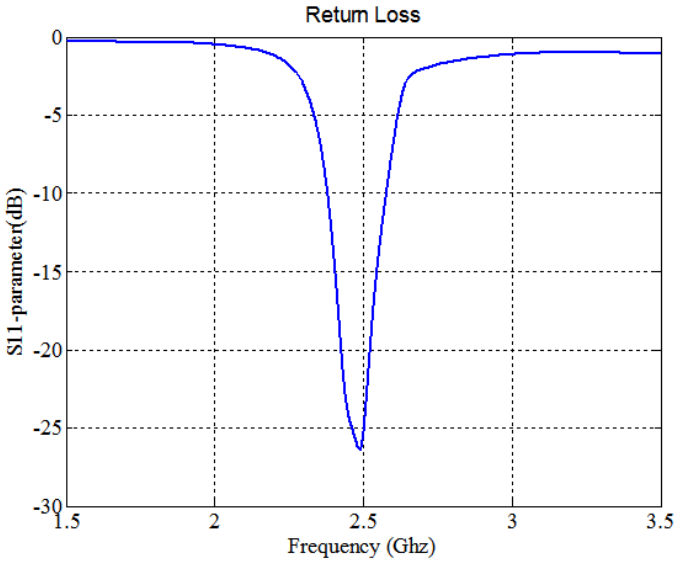

Fig. 2.19: S11 for simple crossed slot antenna.

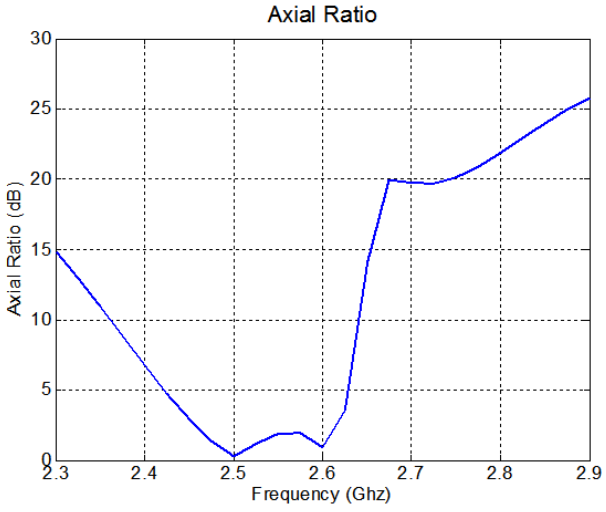

Fig. 2.20: Axial ratio for simple crossed slot antenna.

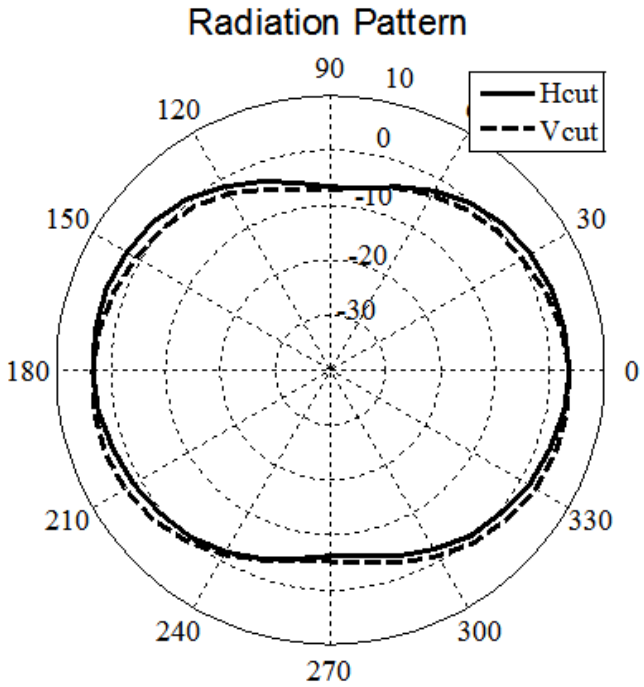

Fig. 2.21: Radiation pattern for simple crossed slot antenna.

2.3 A Reflector-Backed Crossed Slot Antenna with Circular Polarization

The design, simulation, and results of a reflector-backed crossed slot antenna is shown here. The need for this antenna arose as a cross slot antenna which radiated well in only one direction with very less back radiation and had a much higher gain while still having CP was needed. Thus, a reflector was added below the antenna to achieve it, inspired by Vaccaro's design, while still maintaining the simple feed arrangement of the previous antenna [18,19]. The adding of a reflector below the antenna changes the properties of antenna design and its characteristics.

The antenna geometry is shown in Fig. 2.22. Two slots are etched on the top of the substrate with a micro-strip line feed below it just like in the previous antenna. The difference is the presence of a reflector below the antenna which is separated at some distance from the antenna and is made of copper and has the same length and width as that of the substrate. The reflector will be used to try to make the antenna unidirectional. There is change in values of slots and feeding line in this design compared to the previous design to

account for the presence of the reflector, the changes caused by it, and to achieve CP in this antenna.

The cross slots on top are of different lengths (l_{s3} and l_{s4}) but of same width (w_{s2}). Different lengths are again used here for the purpose of achieving a good CP. The offset distance O_{s2} between the center of the slots and the center of the micro-strip line is used to achieve the phase shift while stub l_{f2} is used for impedance matching. The reflector of this antenna is at a distance of d2 below the antenna and is placed such that a good matching can be obtained.

2.3.1 Design

The design frequency of this antenna is 2.5GHz and the substrate used to make it is Roger's 4003C, which is same as the one used before with the same thickness.

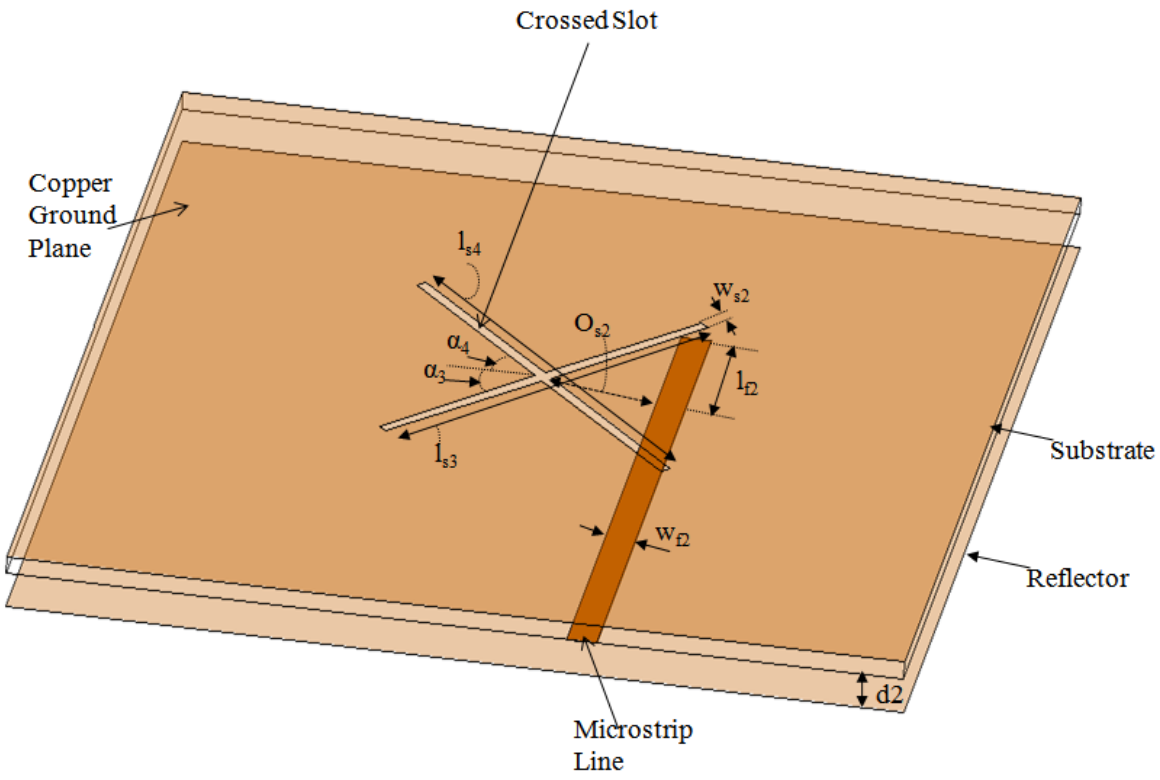

Fig. 2.22: Antenna geometry of a reflector-backed crossed slot antenna.

The width and length of the micro-strip line used to achieve a 50Ω impedance is 3.446mm and 65mm, respectively. The size of the substrate and the reflector is the same 10cm × 10cm and makes it the size of the antenna. The length and the width of the two slots is l_{s3} = 42,l_{s4} = 46.7mm and w_{s2} = 1.2mm, respectively, and the two slots in this case are at an angle of 90 degrees with each other. The offset distance O_{s2} is 12.4mm. The stub length of micro-strip line used is l_{f2} = 15mm. The distance of the reflector from the antenna for good matching is d2 = 3mm. All these parameters were simulated in Ansoft's HFSS to find out the working of the antenna.

2.3.2 Results

The results which were obtained are shown in Fig. 2.23 - Fig. 2.25. The figures show the S11 parameter, the radiation pattern, the gain, and the AR which were attained by simulation. Figure 2.23 shows that the return loss, or S11, is below 20dB which is considered good and has sufficient bandwidth at the frequency of interest. The AR measured, as shown in Fig. 2.24, is found to be near 1.4 dB which is considered fine when determining the CP of the antenna as the cross polarization level is pretty high and exceeds 20dB, though the fractional bandwidth is reduced. Figure 2.25 shows the radiation pattern of the antenna. Although the simulated gain of this antenna has improved to be much higher than that of a simple cross slot antenna due to the presence of a reflector below the antenna, the radiation pattern is still not good enough. The antenna still radiates a lot in the back direction, (i.e., it does not have a good front to back ratio as required and it still has a narrow beam width which is not suitable for use in many applications). Also, the working of this antenna is affected by the presence of a reflector below it.

Thus, a reflector-backed cross slot antenna was simulated to see if we could remove the shortcomings of a simple cross slot antenna and it was found that although it did increase the gain compared to the simple cross slot antenna, the radiation pattern was still not good enough for use. Also, the design of the antenna is complicated comparatively and is not easily integrable while the CP is affected by the presence of the reflector plane below it.

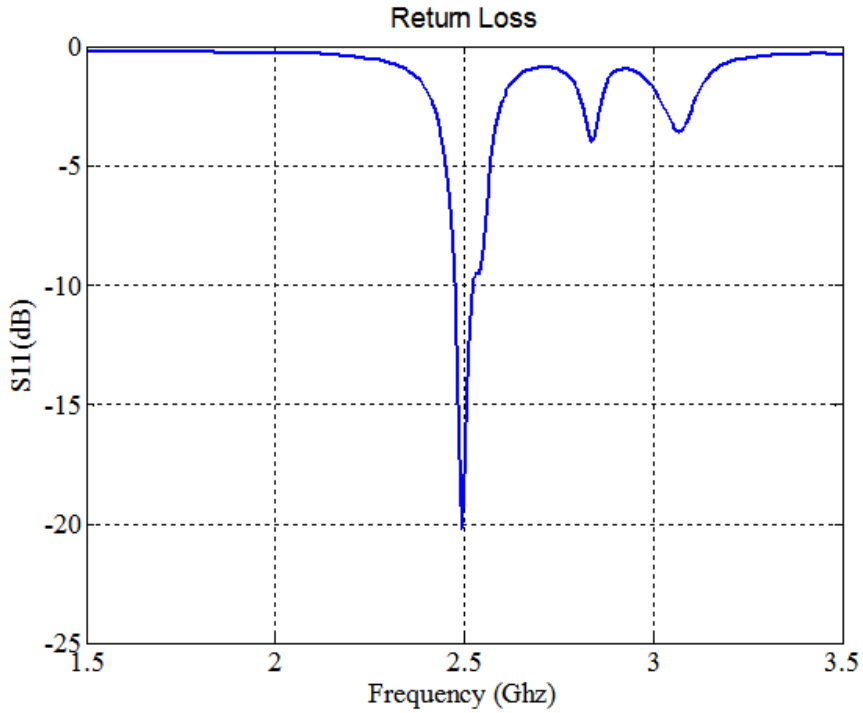

Fig. 2.23: S11 for reflector-backed crossed slot antenna.

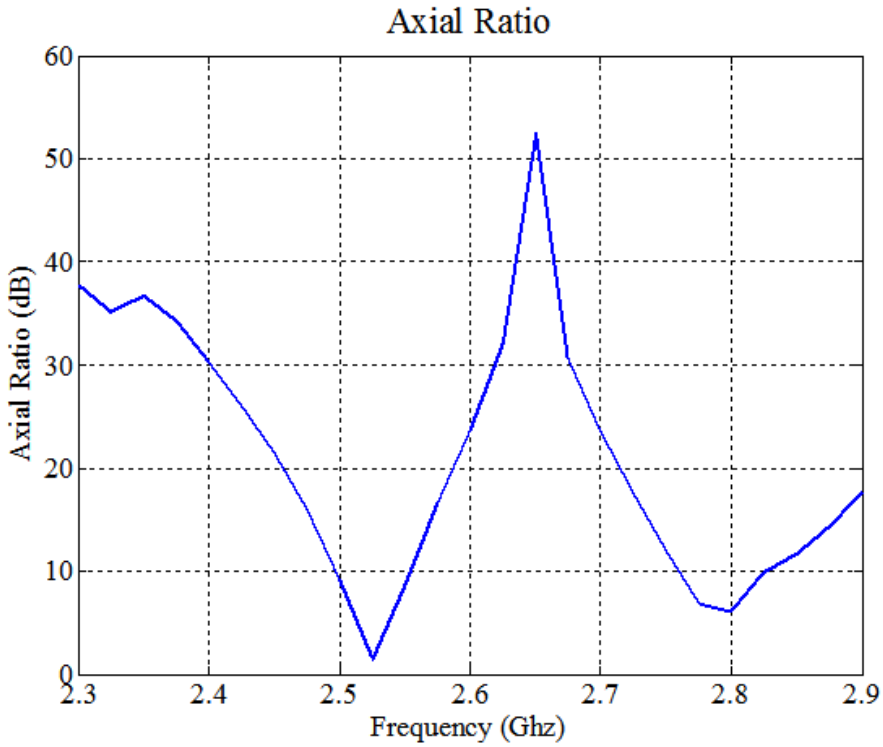

Fig. 2.24: Axial ratio for reflector-backed crossed slot antenna.

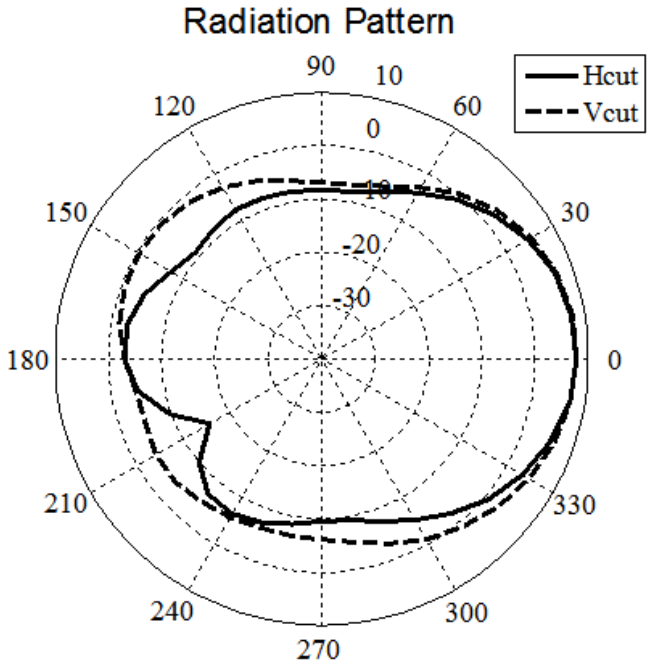

Fig. 2.25: Radiation pattern for reflector-backed crossed slot antenna.

2.4 Cavity-Backed Crossed Slot Antennas with Straight Strip Line Feeding

Cavity backing of slot antennas can significantly improve the antennas performance, and its various characteristics for example it allows for a much better unidirectional radiation pattern than other slot antennas [4,20]. Cavity-backed slot antennas, shown below with a simplified feeding method, were designed and fabricated for these purposes. Since these antennas are cavity backed, the simple feeding method used here is a straight strip-line feed. This feed allows us to achieve a superior CP from the antenna, an excellent return loss, a good radiation pattern, high gain, and easier combination into antenna arrays. Moreover, being planar and radiating in only one direction allows for better integration of these antennas into the structures required.

Two different CP antennas operating at frequencies of 2.46 GHz and 2.60 GHz were designed, fabricated, and measured, respectively. The structure of both of these antennas are the same, with the difference being in the design parameters of the antennas. The design parameters varied due to the change of the operating frequency of the antenna which is one of the most important considerations for the working of the antenna. Both the antennas

are RHCP and have a high cross polarization level.

2.4.1 Antenna Geometry

The antenna structure is shown in Figs. 2.26 and 2.27. The feed used in this antenna, as mentioned above, is a strip line. There are two substrates. This feed line is sandwiched between two substrates of the same thickness. All four sides of the substrates are then shorted together to achieve cavity backing for the antennas. As shown in Fig. 2.27, the antennas are composed of two slots and a strip line. The orthogonal slots in X-shape are etched on the center of the first substrate and the feed line to be sandwiched is printed on the second substrate. The bottom of the second substrate is the ground plane. The top plane and the bottom plane were then shorted by putting conductive tapes on the walls.

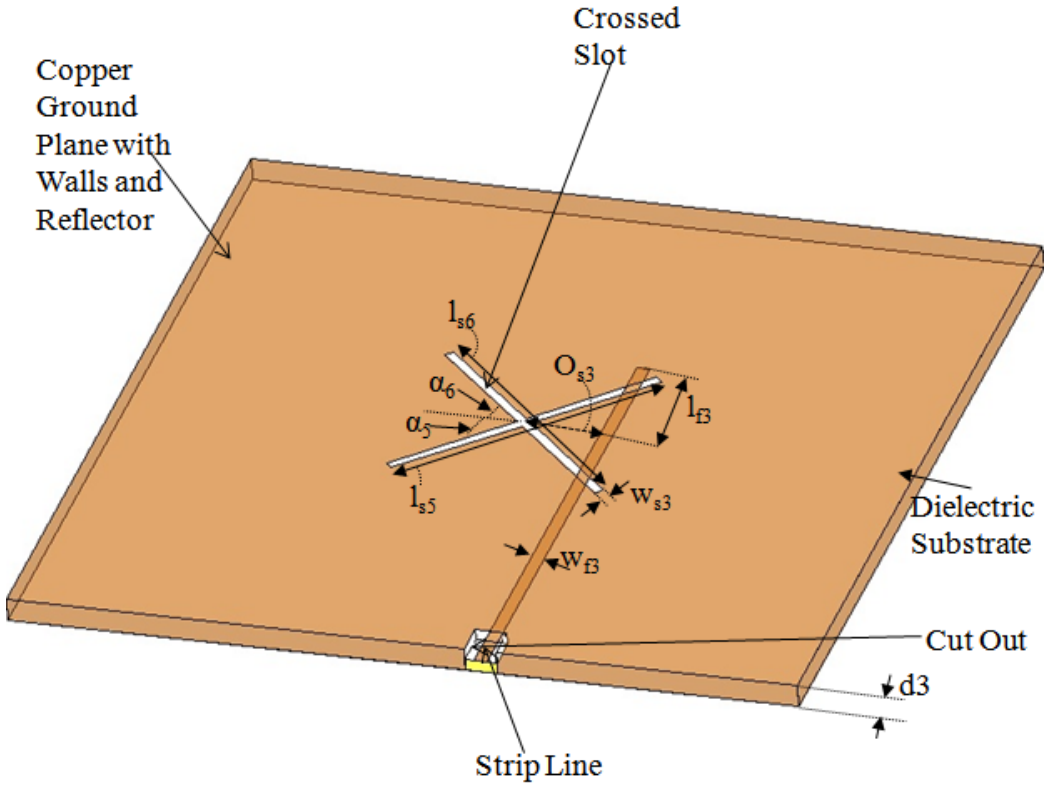

Fig. 2.26: Antenna geomtery for cavity-backed crossed slot antennas with straight strip line feeding.

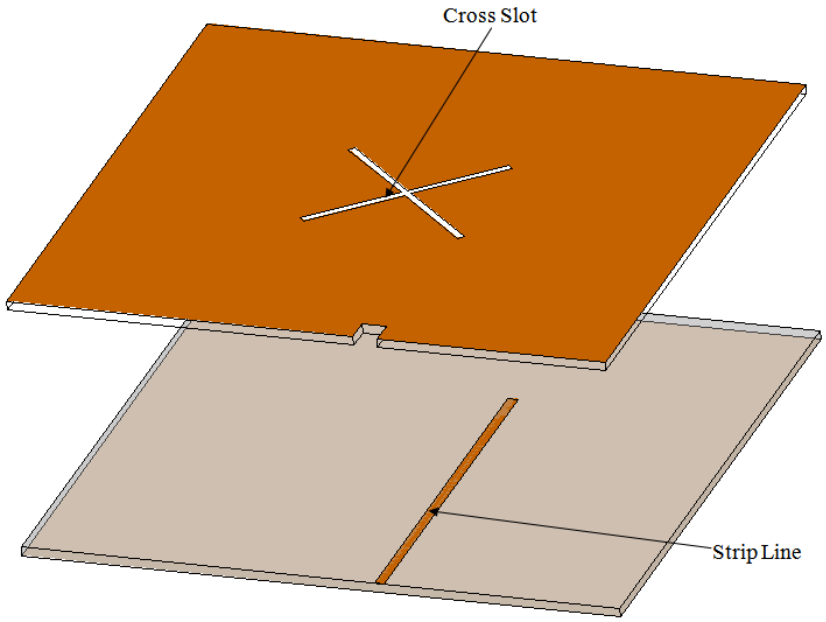

Fig. 2.27: Exploded view of the cavity-backed crossed slot antennas with straight strip line feeding.

Referring to Fig. 2.26, for both the antennas, the two slots have different lengths (l_{s5} and l_{s6}) and the same width (w_{s3}). It was found that the difference in length of two slots was needed to achieve a good CP in this design. The angle between the two slots is $\alpha_5 + \alpha_6$ and is equal to 89 degrees. The strip line has a width (w_{f3}) and is at 45 degrees with respect to the crossed slots. The phase shift needed for the CP is achieved through the offset distance O_{s3}. The impedance matching for the two slots is achieved in the same way as previous antennas by using a stub l_{f3}. Finally, a notch was cut on the top substrate in order to solder the SMA connector. All these parameters including the notch were simulated using Ansoft's HFSS.

2.4.2 Design and Fabrication of the 2.6GHz Antenna

The design frequency of this antenna is 2.6GHz. The substrate used is Roger's 4003C which is the same as that used for the previous antennas. Since this antenna has two substrates and the thickness of each substrate is 1.524mm, the overall thickness of the

antenna is 3.048mm. The antenna size is fixed to 10cm × 10cm. Slots of length l_{s5}= 37.4 mm and l_{s6} = 36.2 mm with the width w_{s3} = 1.2 mm are used for achieving a good CP from the design. The most favorable angle between the two slots to achieve good results in this design was found to be equal to 89 degrees. The width of the feeding strip line is 1.68mm to provide a 50Ω impedance. Length of the stub used for matching is established to be l_{f3} = 16.7 mm. The offset of the strip line from the center of the crossed slot to the center axis of the strip line is O_{s3} = 9mm. α_5 is the inclination angle which is equal to 43 degrees, α_6 is 46 degrees and are chosen such that the AR is reduced for the antenna. A circuit board milling machine was then used to fabricate the antenna. The sides of the antenna were grounded by applying pressure on the two stacked substrates and applying copper tape on the sides. Figure 2.28 shows the final fabricated antenna.

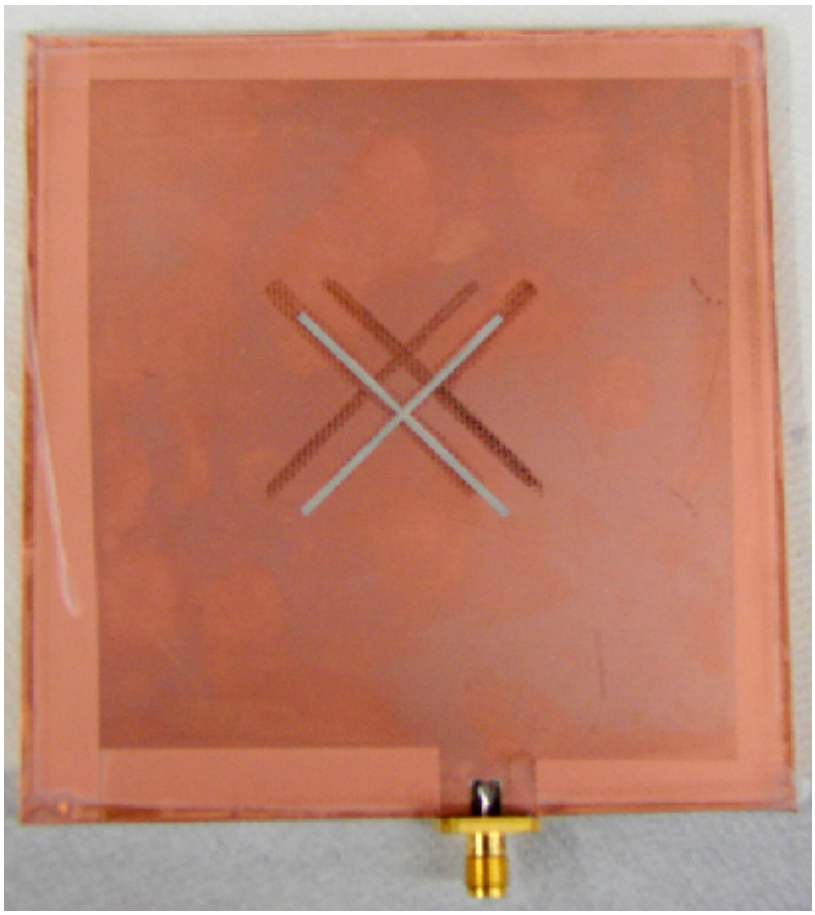

Fig. 2.28: Final fabricated 2.6GHz cavity-backed crossed slot antenna.

2.4.3 Design and Fabrication of the 2.48GHz Antenna

The design and fabrication of this antenna is same as the antenna mentioned above, but with some big differences in some of the design parameters. The design parameters affected by the change of operating frequency of this antenna are slot lengths (l_{s5} and l_{s6}) used for achieving CP, length of stub (l_{f3}) on the strip line, and offset of the strip line (O_{s3}) used to achieve matching and phase shift. The slot lengths used in this design for the operating frequency is l_{s5}= 47mm and l_{s6} = 45mm. The slots have the same widths as before. The length of the stub is changed to l_{f3} = 28.6mm and the offset distance is changed to O_{s3} = 12.6mm. These parameters along with the design as above were all simulated in Ansoft's HFSS, then fabricated using the same method, and measured. Figure 2.29 shows the final fabricated model of the antenna.

2.4.4 Simulation and Measurement Results for the 2.6GHz Antenna

After the fabrication of the antenna was completed, the S11 parameter, radiation pattern, and the AR were measured in the anechoic chamber and compared to the simulation results.

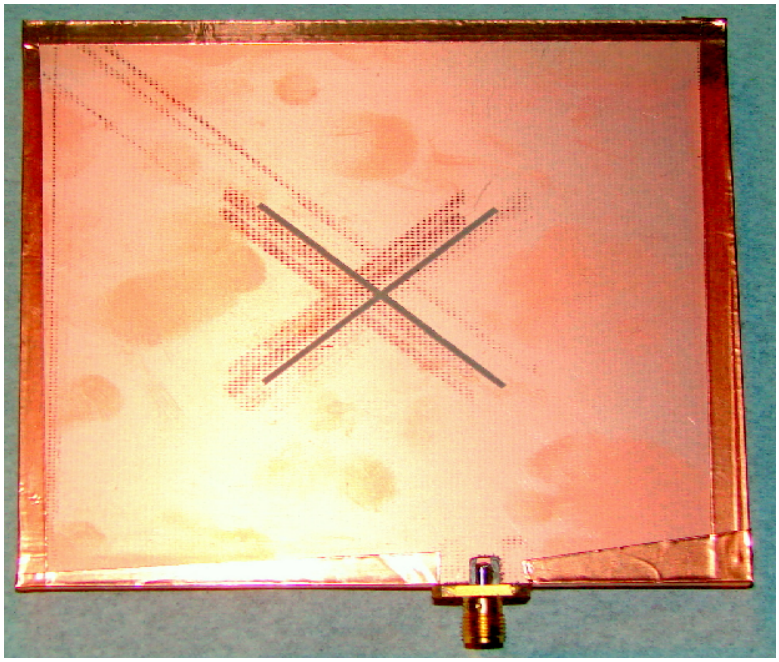

Fig. 2.29: Final fabricated 2.48GHz cavity-backed crossed slot antenna.

Figures 2.30 - 2.33 shows the results obtained in both simulated and measurement cases. In Fig. 2.30, we see that the resonant frequency conforms well for both simulation and measurement. The return loss in simulation is more than 20dB while in measurement it is less than 17dB, which is a good result. The measured and simulated radiation patterns shown in Fig. 2.31 and Fig. 2.32, also have a close resemblance in shape with each other. The antenna is found to be unidirectional and the radiation pattern is established to be symmetrical. The back radiation from the antenna is much less and thus this antenna has a good front to back ratio which is needed for use in many applications. Considering fabrication tolerance, we see that there is some loss in gain between measured and simulated gain results. The measured gain is 3.5dB and can be improved and made much closer to the simulated gain of 4.5dB with a refined fabrication process. This value of gain is high for slot antennas. The AR observed in the main beam directions in simulation and measurement is plotted in Fig. 2.33. The measured AR in the main radiation direction is 2.7dB while in simulation it is less than 0.35dB. The measured AR is fine and considered to be very good under the current fabrication process. The cross polarization level in the principal plane is measured to be more than 18dB in the fabricated antenna.

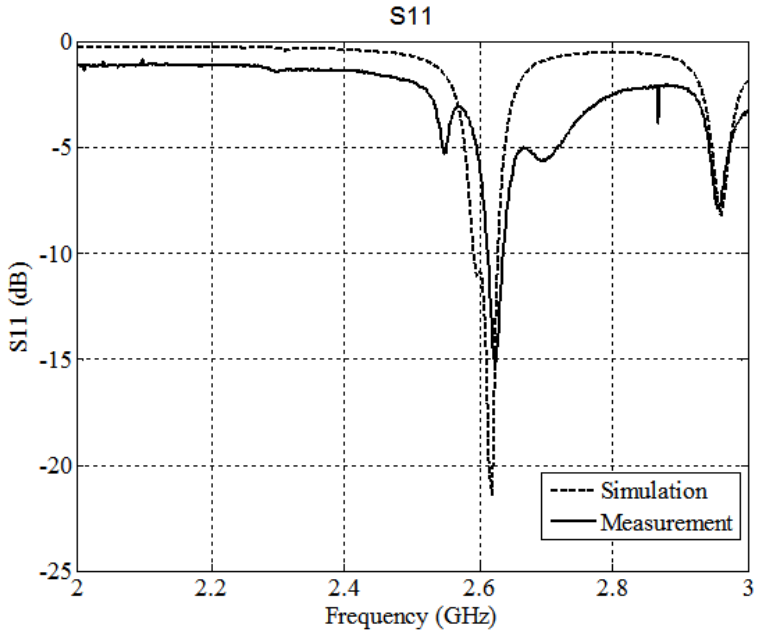

Fig. 2.30: S11 for 2.6GHz cavity-backed crossed slot antenna.

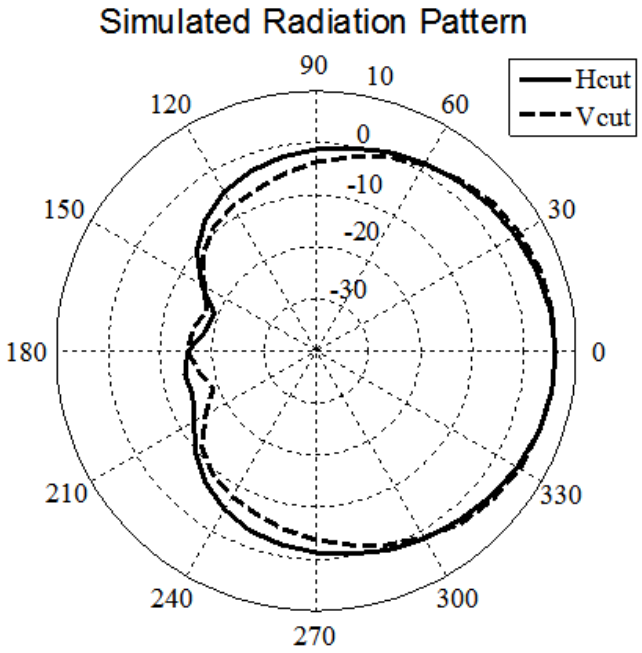

Fig. 2.31: Simulated radiation pattern for 2.6GHz cavity-backed crossed slot antenna.

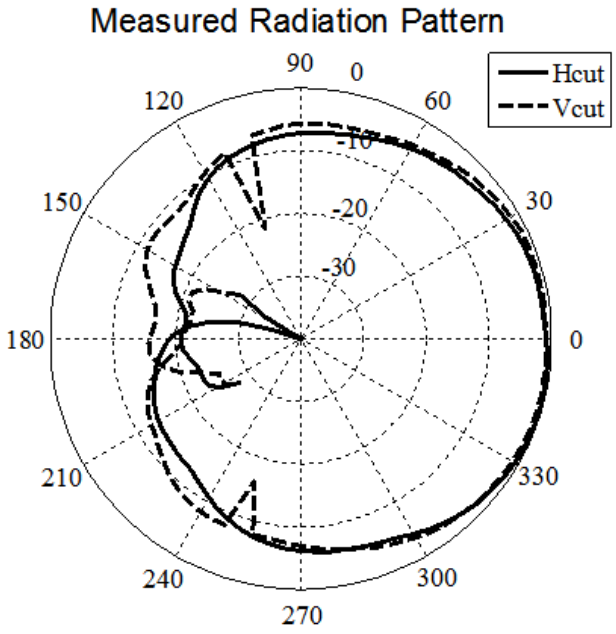

Fig. 2.32: Measured radiation pattern for 2.6GHz cavity-backed crossed slot antenna.

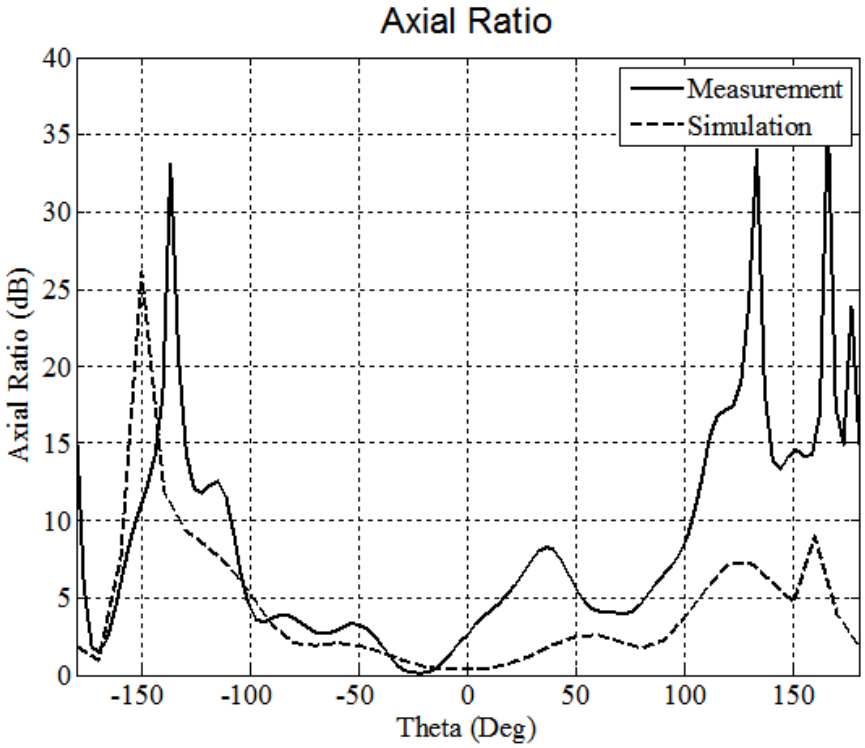

Fig. 2.33: Axial ratio for 2.6GHz cavity-backed crossed slot antenna.

2.4.5 Simulation and Measurement Results for the 2.48GHz Antenna

This antenna was also measured in the anechoic chamber after its completed fabrication and the S11 parameter, radiation pattern, and AR were quantified along with the simulation results. Figures 2.34 - 2.37 shows the results obtained in both simulated and measurement cases. Figure 2.34 shows that the return loss in both simulated and measurement cases exceeds 18dB, and is thus considered superior. The simulated and measured radiation pattern is shown in Figs. 2.35 and 2.36. It is seen that the radiation patterns conform with each other, are unidirectional, and have less back radiation just like in the previous antenna. The radiation pattern is very similar to the previous antenna. The measured gain and simulated gain values are found to be 3.6dB and 4.8dB, respectively, which is good. In Fig. 2.37, the AR determined in main beam direction, in simulation and measurement is equal to 0.63dB and 2.8dB, which is sufficient for operation of this antenna as CP. The cross polarization level for CP in measurement is found to be more than 17dB.

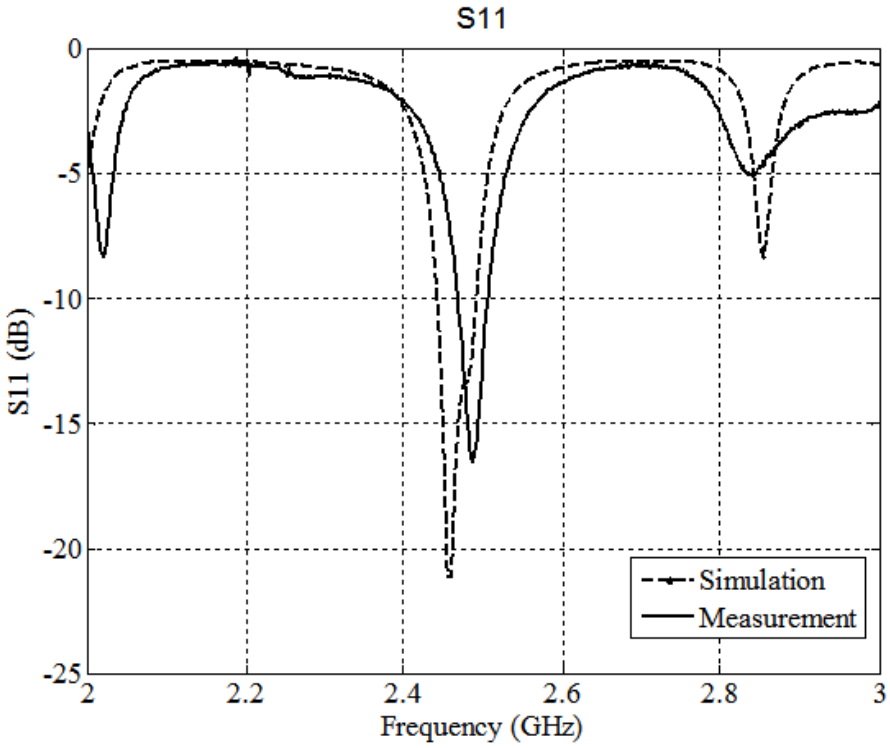

Fig. 2.34: S11 for 2.48GHz cavity-backed crossed slot antenna.

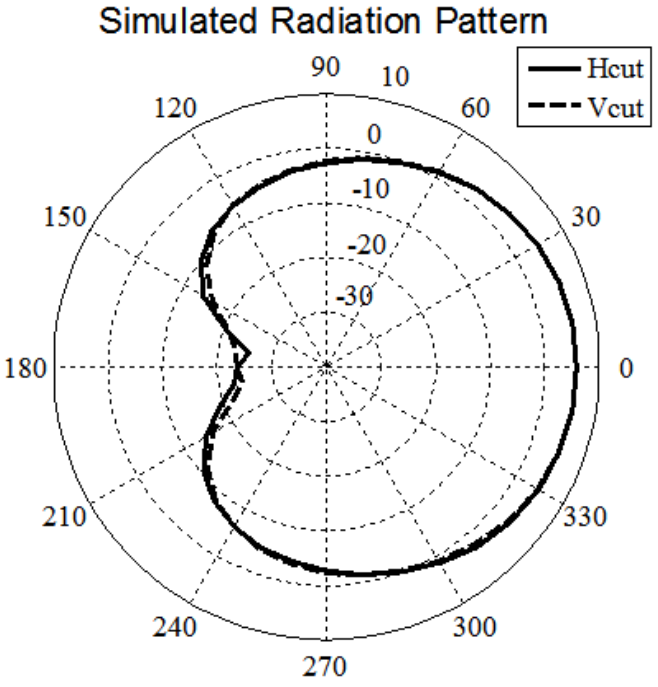

Fig. 2.35: Simulated radiation pattern for 2.48GHz cavity-backed crossed slot antenna.

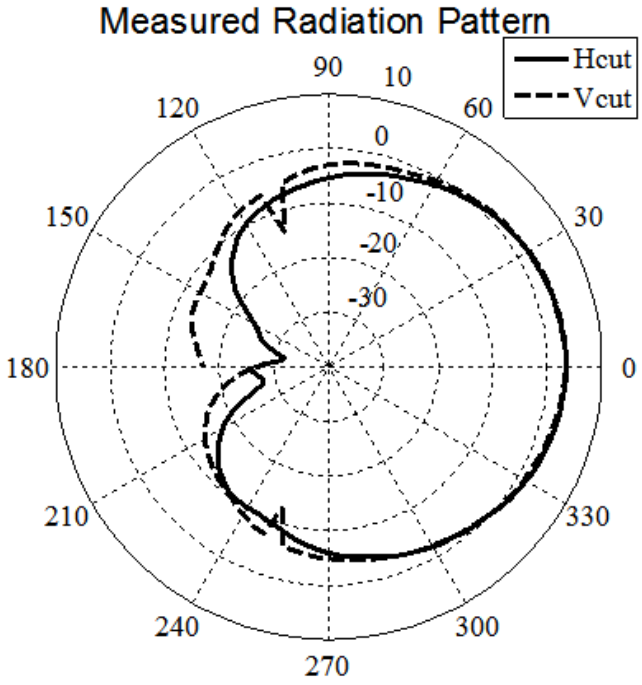

Fig. 2.36: Measured radiation pattern for 2.48GHz cavity-backed crossed slot antenna.

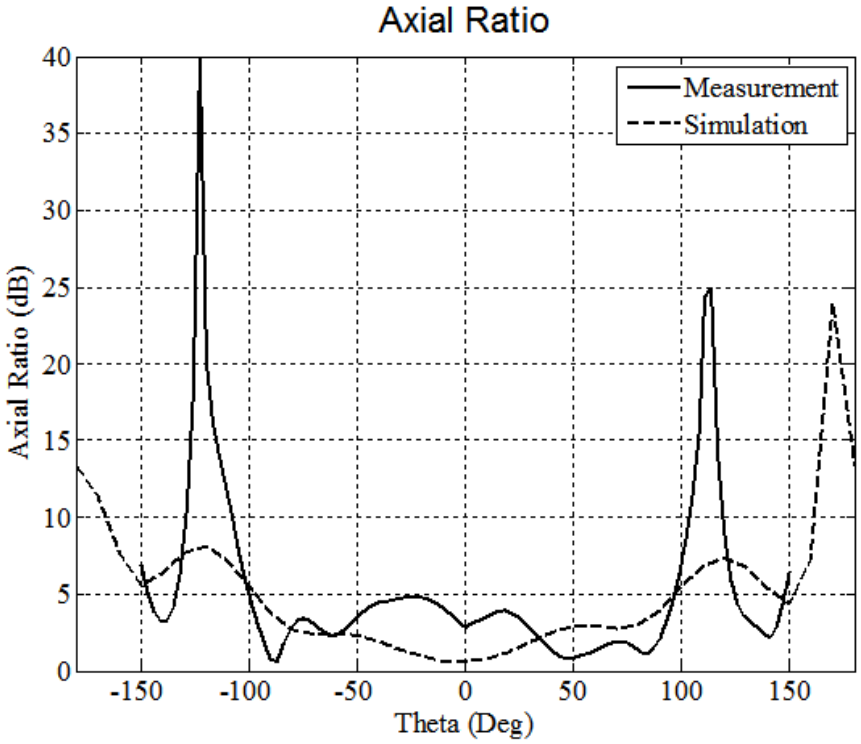

Fig. 2.37: Axial ratio for 2.48GHz cavity-backed crossed slot antenna.

2.4.6 Conclusion

Two cavity-backed crossed slot antennas with simple feeding were simulated and fabricated. Both of these antennas were found to be RHCP. It is clearly seen that compared to a reflector backing, cavity-backed crossed slot antenna has a better radiation pattern in terms of suppressing the undesired back radiation. The radiation patterns fulfilled the conditions expressed faultlessly. The gain in fabrication was a little lower than simulated gain, but it can be improved by a more refined fabrication process, such as better pressing to get rid of possible air in between substrates, better grounding of walls, and a more refined soldering of the connector. It is believed that the measured AR may also be further improved with a more accurate fabrication, such as the ones used in circuit board companies. These antennas showed how simple feed designs can be used to achieve CP and since the feed design is straightforward it can be easily extended to larger array configurations. Also, the design allows it for a better integration with various applications.

2.5 Cavity-Backed Crossed Slot Antennas with Bent Strip Line Feeding

This antenna was built so that it could be used on a cube satellite of 10cm $\times$ 10cm $\times$ 10cm, as it has a simple geometry and can be integrated with solar cells by placing solar cells around the slots [1, 4]. This cavity-backed slot antenna is an improvement over the previous one because of its easier integration with solar cells. The design frequency of this antenna was chosen to be 2.5GHz so that it can be compatible with the communication requirements of the cube satellites, which use the amateur bands. This antenna has a cavity backing, thus allowing it to radiate to only one side of the ground plane. The antenna is RHCP and has a high cross polarization level allowing for better communication [21] . The feed method although a little different from previous ones is still kept simple so as to allow for better array constructions. This antenna was designed, fabricated, and then measured in the anechoic chamber to satisfy all the conditions required.

2.5.1 Antenna Geometry

The feed is similar to before,(i.e., a strip-line is used here), but the feed design is bent

in order to properly feed the antenna. The antenna structure and the feed design is shown in Figs. 2.38 and 2.39. The antenna structure is comparable to the previous structure and has two slots and a strip line along with two substrates and copper tape walls all around the antenna, which is used for shorting the four walls of the substrates. Two slots with unequal lengths are etched on the top of the first substrate in a + shape and the feed line is printed on the second substrate. The bottom of the second substrate acts as a ground plane in this antenna, too.

The two slots have the same width (w_{s4}) and different lengths (l_{s7} and l_{s8}) (as shown in Fig. 2.38). The angle between the slots is equal to 90 degrees, and along with the length of the slots, is needed to achieve a good CP. The bent strip line even in this design is at an angle of 45 degrees with respect to the slots, and the phase shift is again achieved by the offset distance O_{s4}. Stub l_{f4} is used for impedance matching with the two slots. The place where the SMA connector is to be connected has a notch on its top substrate. All these design parameters with their values are simulated in Ansoft's HFSS.

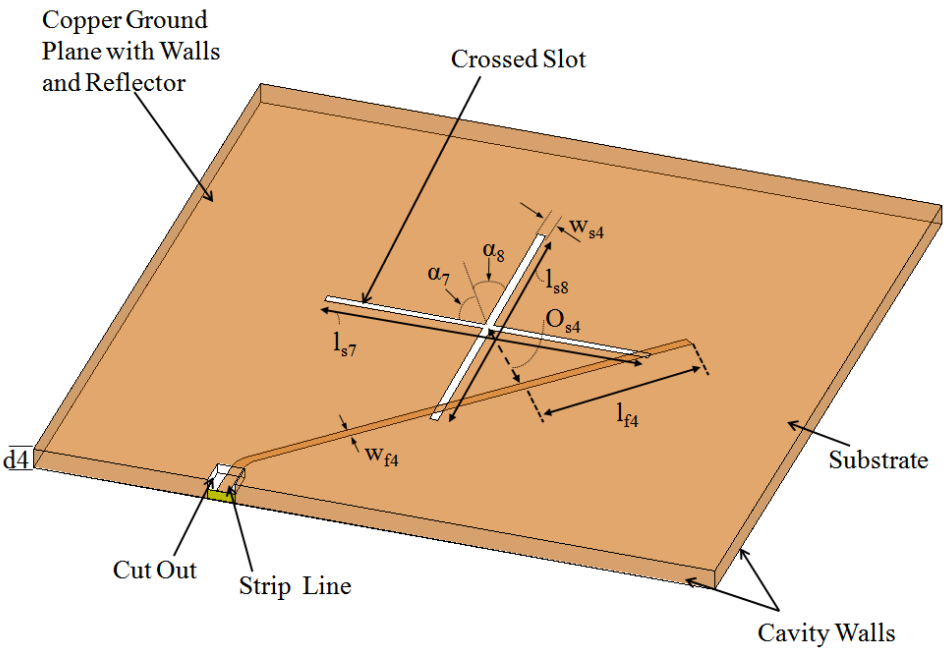

Fig. 2.38: Antenna geometry for cavity-backed crossed slot antenna with bent strip line feeding.

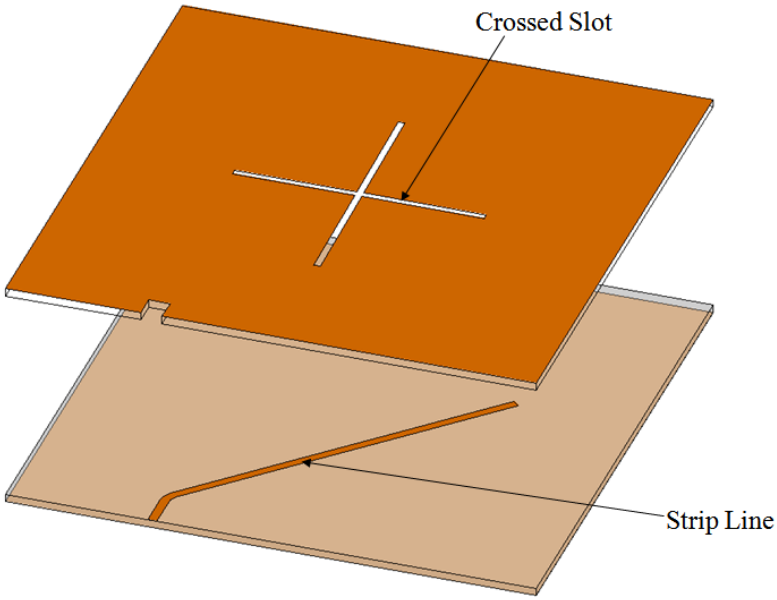

Fig. 2.39: Exploded view of the cavity-backed crossed slot antenna with bent strip line feeding.

2.5.2 Design and Fabrication

The design frequency of the antenna desired is 2.50 GHz. The substrate used for making this antenna is the same as in all other antennas, which is Roger's 4003C. The thickness of each of the two substrates is 1.524mm. Since the two substrates are combined together the total thickness of the antennas is 3.048mm. The width of the strip line is 1.68mm for a 50Ω impedance. Since the antenna is built for a cube satellite the size of the antenna is chosen to be 10cm × 10cm. The length of the two orthogonal slots were designed to be l_{s7}= 47.5 mm and l_{s8} = 50.3 mm with the width w_{s4} = 1.2 mm. Although the angle between the two slots is not always 90 degrees due to different ground sizes, in this particular design, the optimal angle was found to be 90 degrees. The offset of the strip line from the center of the crossed slot to the center axis of the strip line is O_{s4} = 12.9 mm and the inclination angle α_7 was chosen such that the AR is minimized for the CP antenna. The stub length was found to be l_{f4} = 24 mm. The antenna was fabricated using the circuit board milling machine. The two substrates were pressed together and then copper tape is used to ground the walls. Figure 2.40 shows the final fabricated bent feed crossed slot antenna.

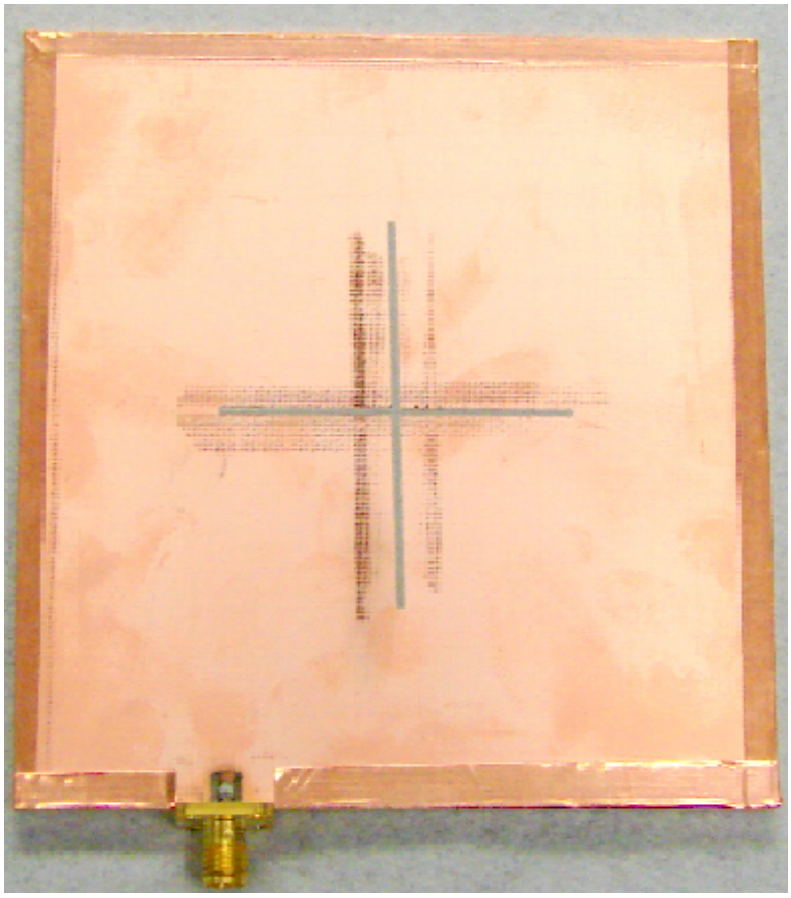

Fig. 2.40: Final fabricated cavity-backed crossed slot antenna with bent strip line feeding.

2.5.3 Results

The S11 parameter, radiation pattern, and AR were measured after the antenna was fabricated and compared to their simulation counterparts as shown in Fig. 2.41- Fig. 2.44. In Fig. 2.41, it is seen that the resonant frequency conforms well for simulation and measurement. The measured radiation patterns also have a close resemblance to the simulated ones in shape and are satisfactory for cavity backed antennas as shown in Figs. 2.42 and 2.43. There is a loss in gain, in measurement compared to the simulation, but this is mainly due to the fabrication tolerance. The measured gain is 3.5dB and it is believed that the gain can be improved and made closer to the simulated 4.55dB. The measured AR in the main radiation direction is 2.7dB while in simulation it was 0.74dB (Fig. 2.44). The measured result is considered to be very good under the current fabrication method. The cross

polarization level in the principle plane is measured to be more than 18dB. The gain and the AR can be improved by a better fabrication process and techniques as mentioned in the previous section.. This will make the antenna much closer to the simulation.

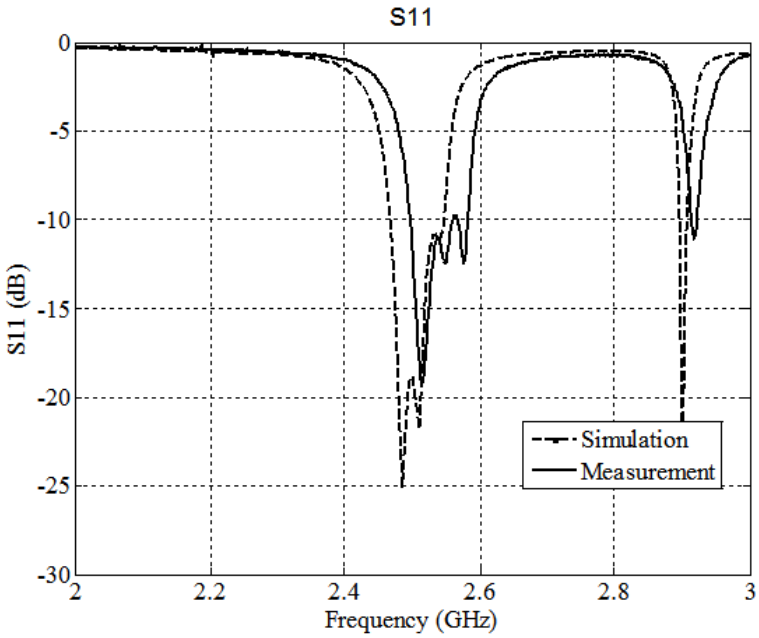

Fig. 2.41: S11 for cavity-backed crossed slot antenna with bent strip line feeding.

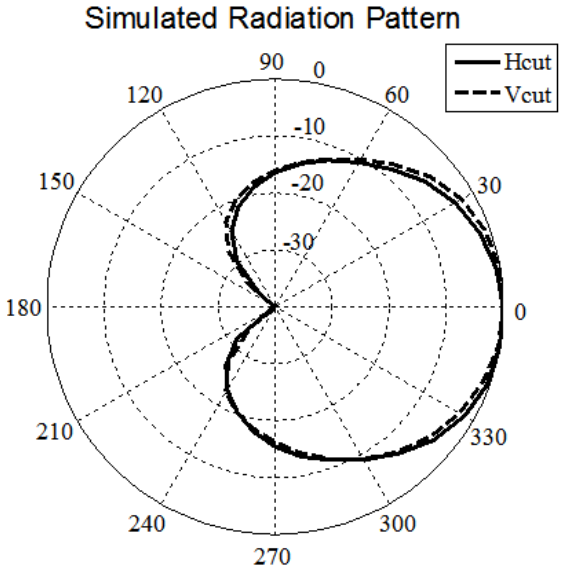

Fig. 2.42: Simulated radiation pattern for cavity-backed crossed slot antenna with bent strip line feeding.

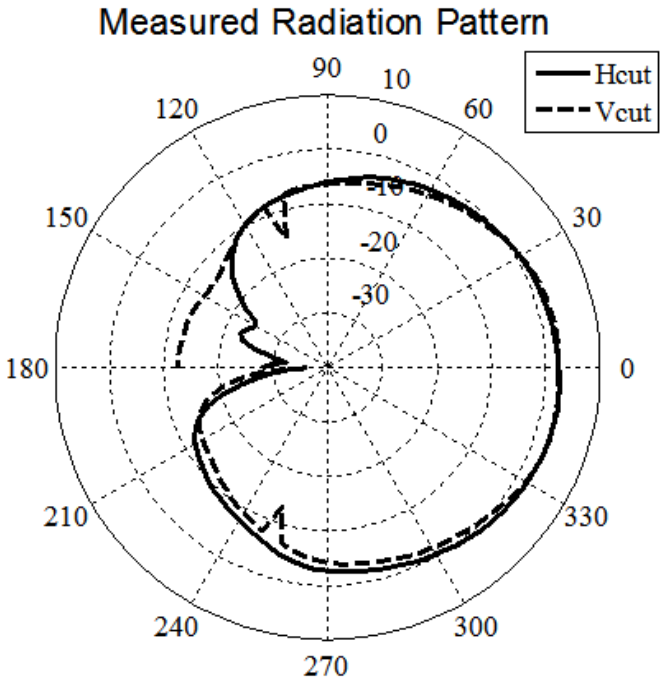

Fig. 2.43: Measured radiation pattern for cavity-backed crossed slot antenna with bent strip line feeding.

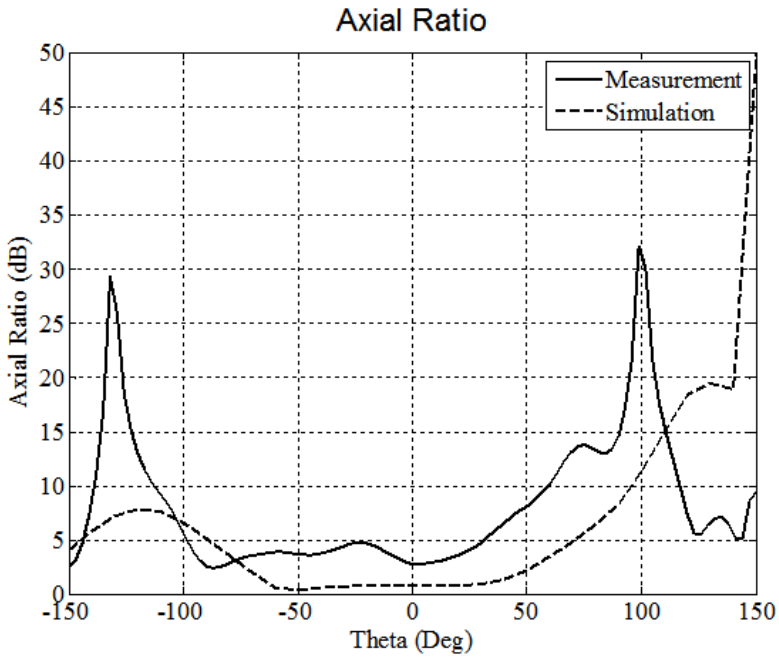

Fig. 2.44: Axial ratio for cavity-backed crossed slot antenna with bent strip line feeding.

The designed antenna has a simple geometry and can be integrated with solar cells by placing solar cells around the slots. This antenna is aimed for use on a cube satellite. But since the feed design is very simple and can be easily extended for array configuration, the proposed antenna can be conveniently used for larger solar panels too.

2.6 A Study on Shifting the Feed of Cavity-Backed Bent-Feed Crossed Slot Antenna

A study was performed to see the effects of moving the bent feed in cavity-backed antenna sideways from its original position to near the walls and to near the etched slots on the top of the substrate as shown in Figs. 2.45 and 2.46. The point where the SMA connector is connected and the strip feed line associated with it was moved in both left and right direction laterally while keeping the impedance matching and the phase matching the same. In Fig. 2.45 we see many strip lines on the substrate. After moving the strip line to different positions which is a certain distance away laterally from it original position as shown in the Fig. 2.46, it is then simulated along with the antenna to observe the change in results. It also helped us in understanding coupling of the strip line with the antenna's cross slots and walls [21]. This change in position lead to a variation in total length of the strip line as the matching was meant to be kept the same.

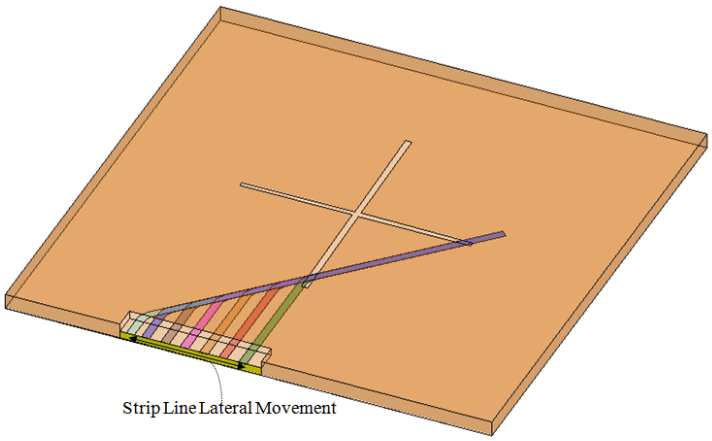

Fig. 2.45: Different shifted feeds in the cavity-backed bent feed crossed slot antenna.

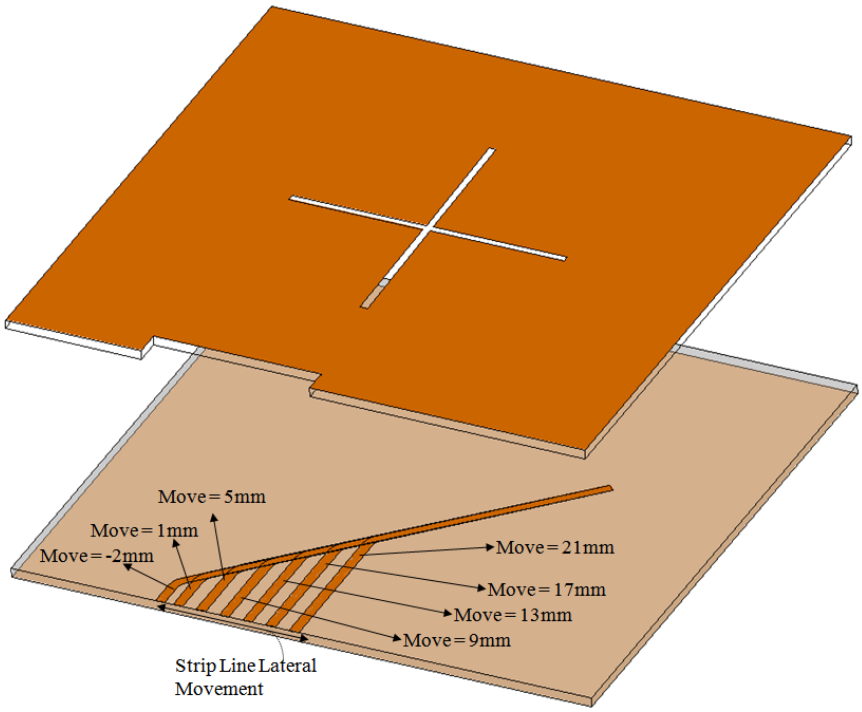

Fig. 2.46: Exploded view of the shifted feeds in the cavity-backed bent feed crossed slot antenna.

It was seen that moving the strip line from its regular position to be more near to the wall while maintaining the same matching conditions did not affect the antenna too much. The antenna still operated at the same frequency and had the same radiation pattern and gain. The AR changed a little in value, but not enough to justify the coupling of the feed to walls. The little change in AR can be attributed to minute changes in the feed line as it is dependent on the matching of it. Similarly when the feed line was moved to be more closer to the slots so that the changes in antenna parameters due to coupling between them could be studied, it was found that this also had not much effect on the antenna, and its results. This proved that whatever the position of your strip line feed in the antenna is, as long as the impedance matching and the phase matching is the done properly, the antenna will give you the nearly the same results. The movement and the length of the feed line does not affect the various characteristics of the antenna. Thus, you can place the feed line at any place in the antenna laterally as long as you match it properly. The results of this study is shown in Figs. 2.47 and 2.48.

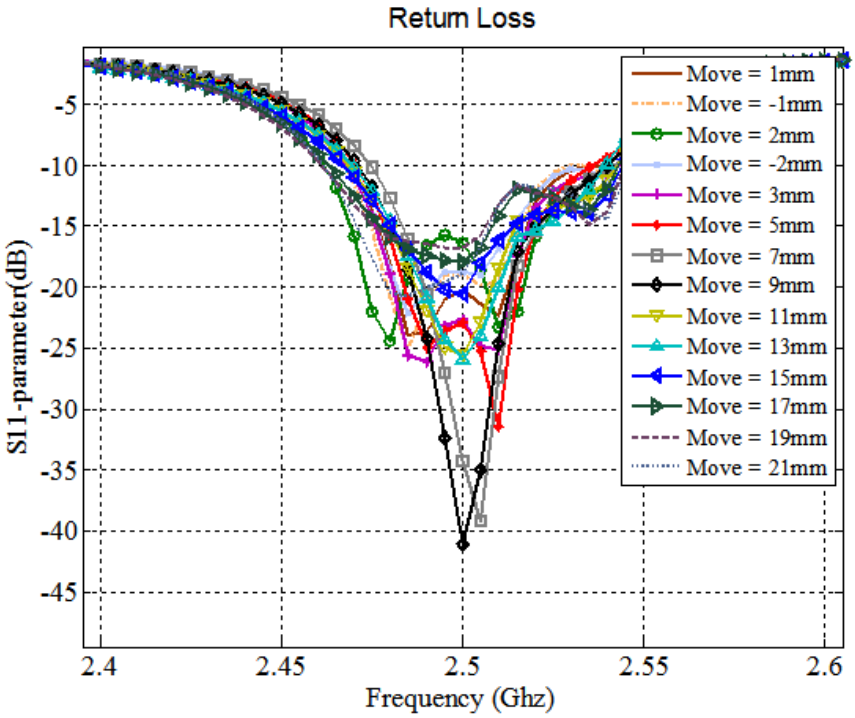

Fig. 2.47: S11 for shifted feeds in the cavity-backed bent feed crossed slot antenna.

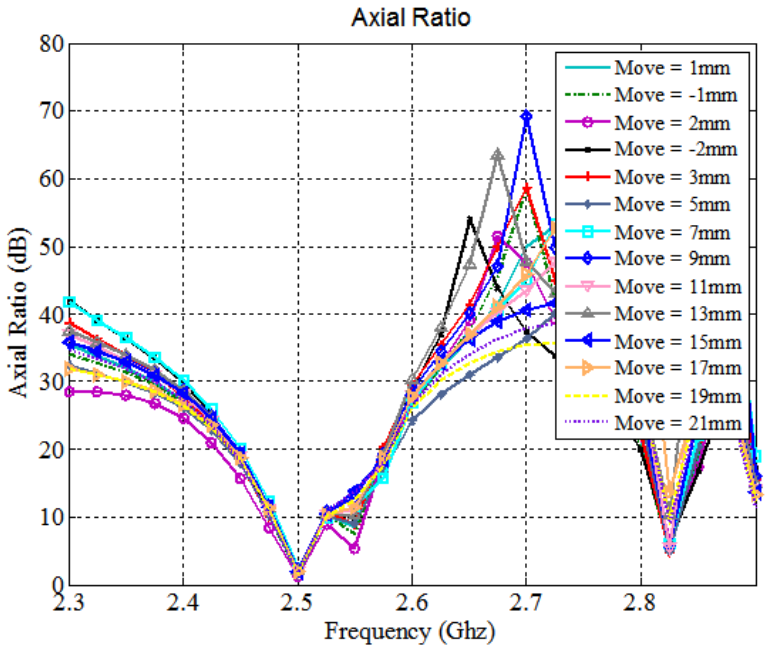

Fig. 2.48: Axial ratio for shifted feeds in the cavity-backed bent feed crossed slot antenna.

2.7 Strip Line Fed Cavity-Backed Antenna with Condensed Ground Plane Size

The effect of a finite ground plane in a simple slot antenna has been studied before [9]. Thus, we want to see the effect of condensing the ground plane on a cavity-backed antenna as it is the cavity backing which differentiates and changes its characteristics from other slot antennas. It will help us in finding more information about cavity-backed antennas and also will show how to miniaturize a cavity-backed antenna for future use. Also, all the cavity-backed and reflector-backed antennas shown above had a cavity resonance as seen in Fig. 2.49, which shows the simulated and measured S11 for cavity-backed crossed slot antennas with simple straight strip line feeding. This cavity resonance was established to be appearing due to the size of the antenna which was fixed to be of 10cm $\times$ 10cm in all of the previous antennas. Thus, a cavity-backed antenna with a condensed ground plane size was designed. This antenna is much smaller than all the previous antennas studied before, roughly just $1/4^{th}$ of their size. This antenna removes the cavity resonance found in the previous antennas while maintaining the rest of the benefits of cavity-backed antennas such as being planar, high gain, unidirectional radiation pattern, and an excellent return loss. This antenna has a circular polarization as it allows for better communications and is thus a crossed slot antenna. Since we wanted to build a smaller antenna which was cavity backed, the feed design in this antenna was not changed and it is still a strip line fed antenna.

This antenna operates at a frequency of 2.4GHz which is chosen keeping in mind communication requirements. This antenna was designed and simulated in HFSS to verify the conditions. As mentioned above this antenna is much smaller in size. The antenna is RHCP and was found to have a high cross polarization level.

2.7.1 Antenna Geometry

The antenna geometry is shown in Fig. 2.50 and is pretty comparable to other cavity-backed antennas with the difference being that this antenna has a size of 5.6cm $\times$ 5.6cm, which is pretty small. This antenna is fed in a similar way to other cavity-backed antennas (i.e., with a straight strip line sandwiched between two substrates). Two orthogonal slots of equal size are etched on the top of the first substrate, while the strip line is printed on the

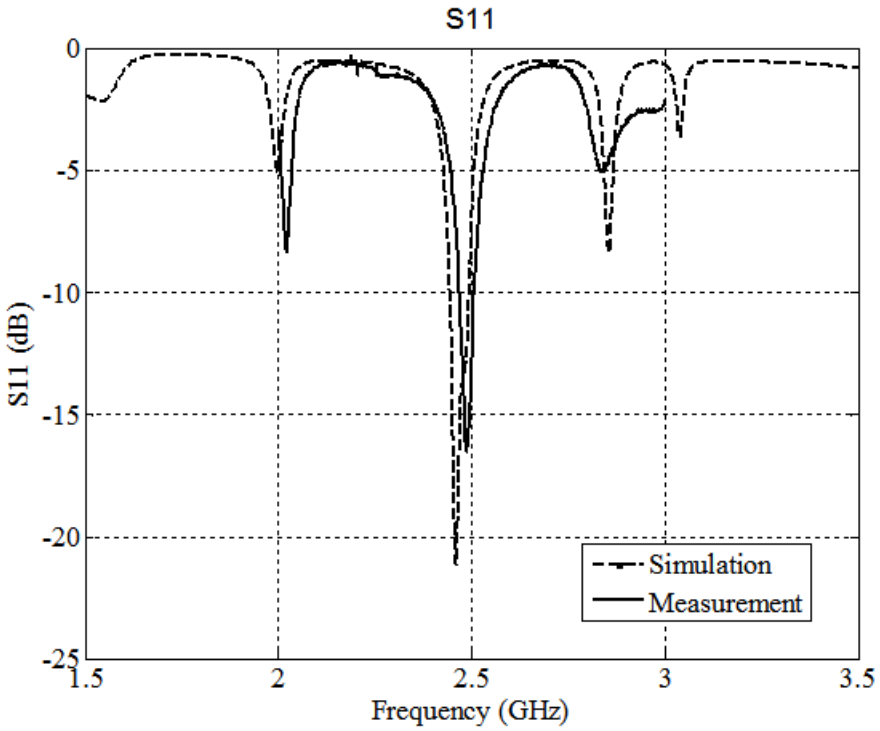

Fig. 2.49: S11 for cavity-backed crossed slot antenna with simple straight strip line feed.

top of the second substrate. The orthogonal slots etched are in an X shape in this antenna. The bottom plane of the second substrate again acts as a ground plane. The two substrates are then combined by putting conductive walls on the sides of the antennas to make them into one entity.

As shown in Fig. 2.50, in this antenna the slots are realized to be of equal length and width. The length of the slots is given by l_{s9} and the width is given as w_{s5}. The angle between the slots needed to achieve a good CP is a combination of $\alpha_9 + \alpha_{10}$. The width of the strip line is given as w_{f5} and it has an offset of O_{s5} from the center of the slots which is used for achieving phase shift. The strip line as seen in Fig. 2.50 is at 45 degrees with respect to the slots. The size of the stub used for impedance matching is given by l_{f5}. This antenna also has a notch simulated in it to make sure of the connection to the SMA connector. All the above designs and parameters were then simulated in Ansoft's HFSS to obtain the required results.

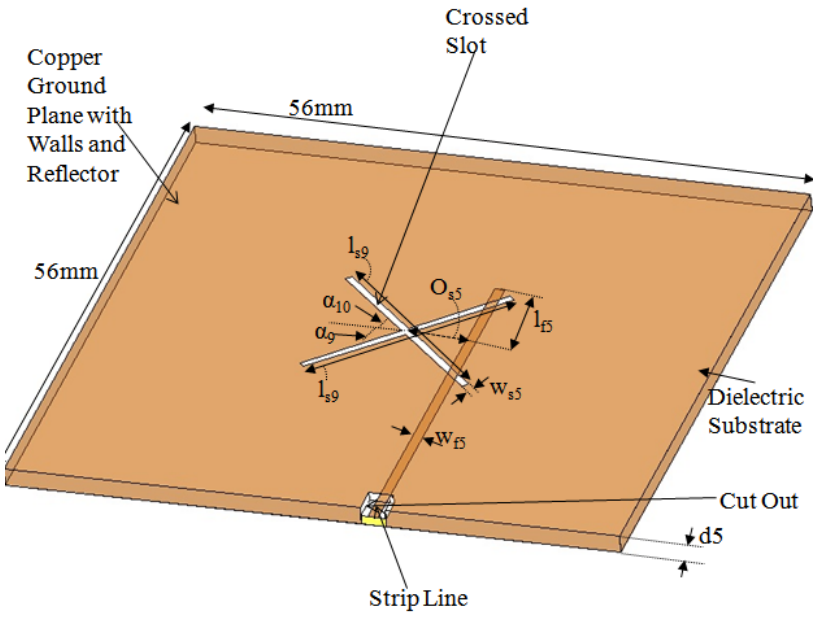

Fig. 2.50: Antenna structure for strip line fed cavity-backed antenna with condensed ground plane size.

2.7.2 Design

The design frequency of this antenna is 2.4GHz. The overall size of the miniaturized cavity backed antenna is 56mm × 56mm × 3.048mm. The two substrates used in designing this antenna are Roger's 4003C, with each substrate being 1.524mm thick, which is the same as previous antennas. The width of the strip line is 1.68mm for 50Ω impedance. The length of the strip line is 42.1mm with the stub size for open stub matching being 14.1mm. The offset of the strip line from the center of the slots for the requisite phase shift is 9.02mm. The slots on the antenna are etched at the center of the antenna. The length of the equal slots is 38.3mm and the width is 1.2mm. The angle between the two slots is not exactly 90 degrees and is equal to 89.1 degrees with the inclination angle α_9 chosen to be 43.1 degrees so that the AR is minimized for the antenna. The antenna with its design values was then simulated in HFSS.

2.7.3 Results

The simulated results of this antenna is shown in Figs. 2.51 - 2.53. The simulation results show the S11 parameter, the radiation pattern, the gain, and the AR of the antenna designed. In Fig. 2.51 we can see that this antenna has a good return loss which is below 25dB and has adequate bandwidth at the frequency designed. Also seen in Fig. 2.51, there is no cavity resonance in this antenna as there was in the previous antennas. The radiation pattern for this antenna is shown in Fig. 2.52. The radiation pattern is really good with very less back radiation and a very small back lobe. This makes the front to back ratio of the antenna very good and desirable. In addition to this, the antenna has high gain of around 5dB in simulated measurements which is considered as superior. The AR simulated is shown in Fig. 2.53. The AR of the antenna simulated is 0.3dB which is very low, and thus will have an excellent CP. The antenna is RHCP with a cross polarization level in excess of 25dB.

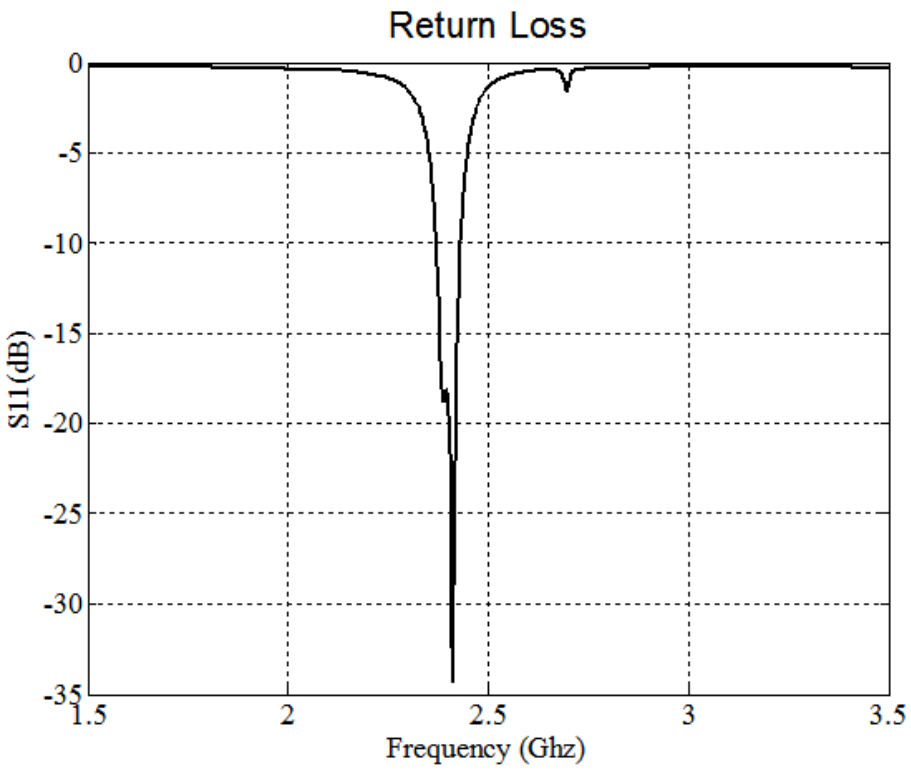

Fig. 2.51: S11 for strip line fed cavity-backed antenna with condensed ground plane size.

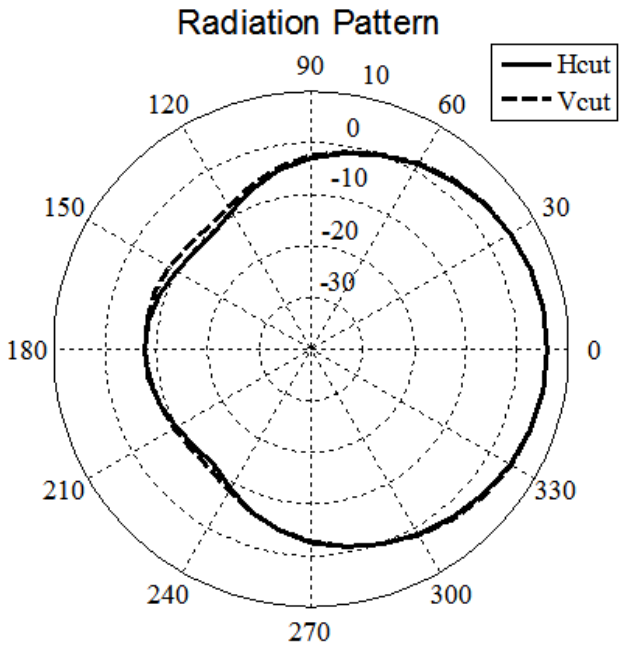

Fig. 2.52: Radiation pattern for strip line fed cavity-backed antenna with condensed ground plane size.

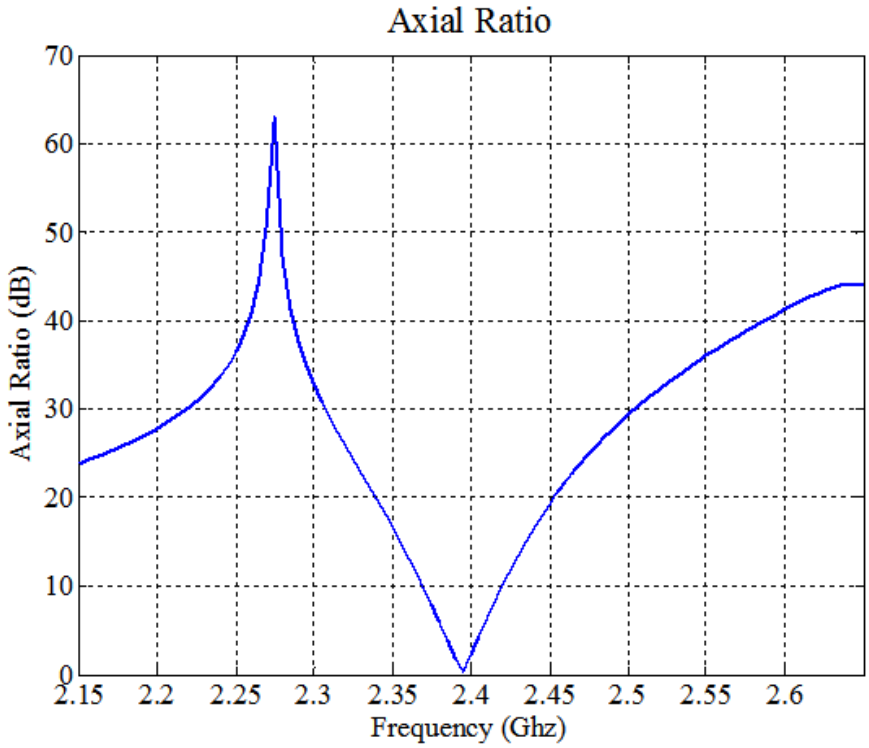

Fig. 2.53: Axial ratio for strip line fed cavity-backed antenna with condensed ground plane size.

Thus, in this study a miniaturized cavity-backed crossed slot antenna was designed and simulated and its effects were seen. The results of condensing the ground size of antenna were also seen in this antenna.

2.8 Prototyping of Cavity-Backed Antennas

The cavity-backed antennas described above were prototyped to observe how close to simulation they worked. Different prototypes were developed and tested for the antennas. At least two to three prototypes were developed for every cavity-backed antenna and then it was compared to the simulated antenna. All the new prototypes were an improvement over the previous ones to make the results of this antenna closer to the simulation results. The measurement of the prototypes was done in the anechoic chamber as mentioned above to make sure that the antennas were tested in controlled surroundings. Since these antennas are cavity-backed, and CP the most important result to be measured of these antennas were the S11 and the AR, these will get most affected. The first prototype of the antennas always had a higher AR and lower S11 than the next prototype. While making prototypes of the cavity-backed CP antennas, it was realized that certain steps needed to be followed while fabricating the antennas to make a lesser number of prototypes and better prototypes faster. Based on these steps being followed, a better cavity-backed antenna with CP can be fabricated much faster. The steps are:

- While fabricating the cavity-backed antenna on the milling machine, make sure to fabricate the strip line and crossed slots on top of two separate Roger's 4003C substrates and make sure that they are etched properly. Peeling of the copper layers on the substrates should be done as cleanly as possible. For fabrication, the copper layer below the substrate containing the crossed slots and the copper layer on top of the subtrate containing the strip line are peeled away. The copper in the crossed slots is also peeled away.

- The two substrates are then put together with the etched strip line sandwiched between them and in the notch on the top substrate and the crossed slot on the first

substrate being the top of the antenna.

- A lot of pressure is put on this configuration then to make sure that no air remains in between the substrates and that both the two substrates are properly joined together.
- Copper tape is put on the sides of the configuration to make copper walls for the cavity-backed antenna while the pressure is still being applied. The copper walls were made as smooth as possible to remove any air from the antenna and to make sure that it bound the antenna tightly.
- The SMA connector is then connected to the strip line of the antenna in the notch to finally fabricate the antenna. The connection of the SMA connector to the antenna should be as smooth as possible to make sure that spurious effects do not crop up.

After all the above steps are done, the cavity-backed antenna is ready to work and be measured. The quality of the antenna depends on how good you make it and how close to simulation design you can go. As long as there is no air in the antenna and all the connections are well made, the antenna will provide results very close to the simulation results. Figures 2.28, 2.29, and 2.40 show some of the cavity-backed slot antennas fabricated.

Chapter 3

The Anechoic Chamber

An anechoic chamber meaning non-echoic or echo-free chamber is a room designed to stop reflections of either sound waves or electromagnetic waves. The chamber is also insulated from external sources of noise. The combination of both aspects means that it simulates a quiet open space of infinite dimension, which is useful when exterior influences will otherwise give false results [7]. Anechoic chambers are generally used to minimize reflections from a room mostly in context of acoustics. Recently, rooms that are designed to reduce reflection and external noise in radio frequencies have been used to test antennas, radars, and electromagnetic interference.

An anechoic chamber can be as small as a small compartment to as large as an aircraft hanger depending on the size of the object to be tested and the frequency range of the signals used, although scaled models can also be used by testing at shorter wavelengths.

There are generally two kinds of anechoic chambers:

- Acoustic Anechoic Chamber - These kind of chambers are used to conduct experiments in nominally "free field" conditions. All sound energy will be travelling away from the source with almost none reflected back.

- Radio Frequency Anechoic Chamber - The internal appearance of the Radio Frequency (RF) chamber is sometimes similar to that of an acoustic anechoic chamber but these kind of chambers are generally used to conduct experiments in nominally "free space" conditions. All radiation will be travelling away from the source with almost none reflected back [13].

In this work, we are generally concerned only with the second type of anechoic chamber which is the RF Anechoic Chamber.

3.1 Radio Frequency (RF) Anechoic Chamber

In these types of chambers, the interior surfaces of the anechoic chambers are covered with Radiation Absorbent Material (RAM). The chambers are typically used to house the equipment for performing measurements of antenna radiation patterns, electromagnetic compatibility (EMC), and radar cross-section measurements. Testing can be conducted on full scale objects including aircrafts or on scaled models where the wavelength of the measuring radiation is scaled proportional to the target size. This family of chambers also exhibit some properties of the acoustic anechoic chamber such as sound attenuation and shielding from the outside noise.

3.2 How do RF Anechoic Chambers Work?

The workings of anechoic chambers is really simple and can be explained by considering it to be as a signal passing down transmission line where the plane electromagnetic wave is the signal and the walls along with the free space impedance 377ohms form a transmission line with characteristic impedance [13]. Thus to create a reflectionless chamber, we need to model it as sending a signal down a transmission line with no reflections. Since the shell off the anechoic chamber is metal, our transmission line model will have a short circuit at its termination which means that all the signals sent down the transmission line will be reflected back. Thus, our task will be to find something that can be put up on the wall and absorbs or scatters these radiations or energy.

One of the methods proposed to achieve this effect was by the use of "Salisbury Screen," but although it is an elegant solution it has a lot of limitations such as, it works at only one frequency for a single sheet and in order to make it work for a range of frequencies several sheets need to be used. Another method is the "Jaumann Sandwich" in which both the resistances and the distances from the metal walls are tapered [13].

The modern techniques borrowing from these concepts employ pyramidal absorbers or Radiation Absorbent Material (RAM). The tapered material of these absorbers performs in a similar way to the above techniques. Many small reflections are created as the electromagnetic wave passes into the pyramid and these reflections tend to cancel out and to be

effective, the pyramids must be at least one half wavelength long at the lowest frequency of interest [13]. The size of the pyramid needed to achieve this effect is mitigated somewhat by the fact that the wavelength of the radio frequency signal as it passes through the pyramidal material is shorter than the free space. It is reduced by a factor of

$$\lambda_r = \frac{1}{\sqrt{\epsilon_r}}, \tag{3.1}$$

where λ_r is the wavelength in media and ϵ_r is the electric permittivity relative to the free space.

For frequencies below 100 MHz, different technologies other than pyramidal absorbers are used for compensating for anechoic effects.

3.3 Requirements for Building an Anechoic Chamber

Anechoic chambers are usually rectangular or tapered. For making an anechoic chamber, we usually require extra room than that which is required to simply house the test equipment, the hardware under test, and associated cables. The far field criterion is used to find the minimum distance from antenna in terms of wavelength to be observed when measuring antenna far field radiation patterns, which is given by

$$R = \frac{2D^2}{\lambda}, \tag{3.2}$$

where R is the distance from the antenna and D is the largest dimension of the antenna and λ is the wavelength in free space. If R is found to be greater than 3λ from the antenna, then the antenna is supposed to be radiating in the far field. Thus considering the distance between the transmitter and the receiver to be greater than three times the wavelength of radiation and allowing for this at the lowest frequency of desire and the extra space that may be required for the pyramidal RAM, gives us the dimensions of the chamber required for measurement purposes. The dimensions of the chamber should be such that the angle of incidence on sidewalls is less than 60 degrees [7].

An RF anechoic chamber is usually built into a screened room designed using the

Faraday Cage Principle. A Faraday cage's operations depends on the fact that an external static electrical field will cause the electrical charges within the cage's conducting material to redistribute themselves so as to cancel the field's effects in the cage's interior [22]. A Faraday Cage is best understood as an approximation to an ideal hollow conductor. Most of the RF tests that require an anechoic chamber to minimize reflections from the inner surfaces also require the properties of a screened room to attenuate unwanted signals penetrating inwards and causing interference to the equipment under test and prevent leakage from tests penetrating outside.

3.4 Radiation Absorbent Material (RAM)

The RAM is designed and shaped to absorb incident RF radiation as effectively as possible from as many incident directions as possible. The more effective the RAM is the less will be the level of reflected RF radiation. Many measurements require that the spurious signals arising from the test setup, including reflections are negligible to avoid the risk of causing measurement errors and ambiguities. They are used both in measurement ranges and also as antenna components for reducing side lobe and back lobe radiation.

One of the most effective RAM's comprise of arrays of pyramid shaped pieces as shown in Fig. 3.1, each of which is constructed form a suitably lossy material such as carbon loaded polyurethane foam [7]. To achieve this, RAM can neither be a good electrical conductor nor a good electrical insulator as they both do not absorb any power. Generally, Pyramidal RAM will comprise a rubberized foam material impregnated with controlled mixtures of carbon and iron [7]. For low frequency damping the distance is often 24 inches, while high frequency panels are as short as 3-4 inches. Panels of RAM are installed with tips pointing inward to the chamber. RAM attenuates signals by two ways: scattering and absorption. Scattering can occur both coherently, when reflected waves are in phase but directed away from the receiver or incoherently when waves are picked up by the receiver but are out of phase and thus have lower signal strength. This scattering also occurs within the material with carbon particles promoting destructive interference. Internal scattering can cause as much as 10 dB of attenuation. The pyramids are cut at angles that maximizes the number

of bounces the wave makes inside the structure. With each bounce the wave loses energy to the absorbers.

Waves of higher frequencies have shorter wavelengths and are higher in energy while lower frequency waves have longer wavelength and lower energy as given by

$$\lambda = \frac{v}{f}, \tag{3.3}$$

where λ is the wavelength, v is the phase velocity, and f is the frequency of the wave. The performance quality of an RF anechoic chamber is determined by its lowest test frequency of operation. Pyramidal RAM is at its most absorptive when the incident wave is at normal incidence to the internal chamber surface and the pyramid height is equal to quarter wavelength of free space. At microwave frequencies, the reflection coefficient may be below -50dB at normal incidence [7]. At higher frequencies the reflection coefficient is larger. By increasing the height or increasing the thickness of the pyramid structure we can improve its working at lower frequencies but might reduce the working area in the chamber.

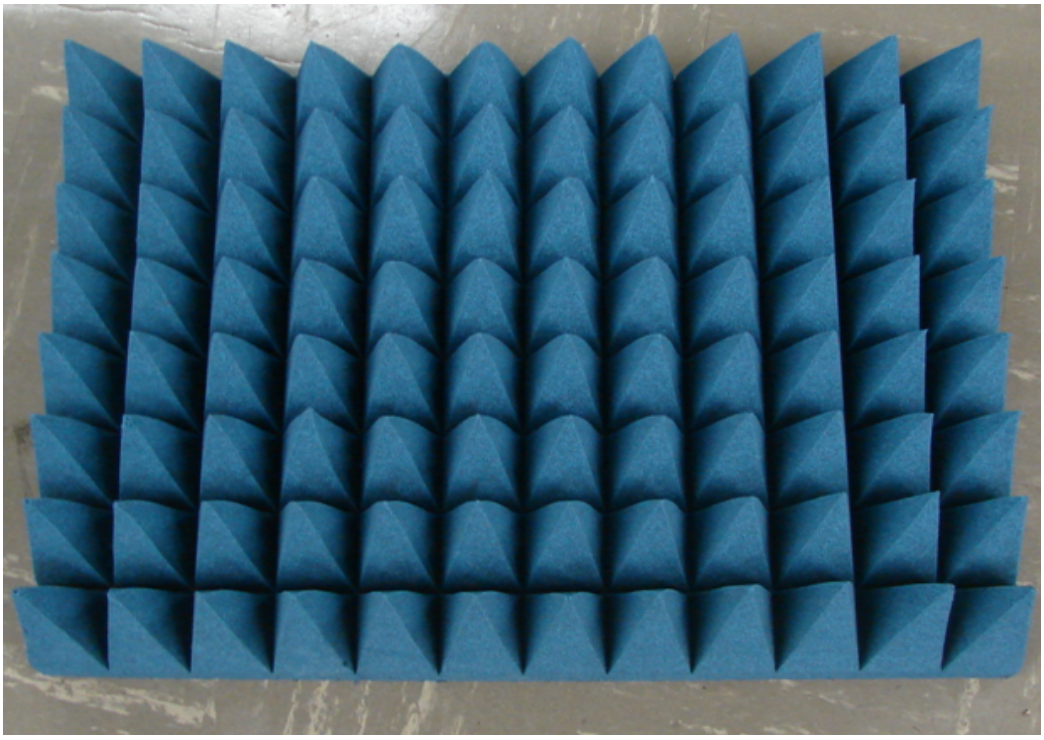

Fig. 3.1: A section of pyramidal RAM.

3.5 The State of Art Anechoic Chamber at Utah State University

Utah State University has a state of the art anechoic chamber capable of measuring antennas from frequency range of 2GHz and above. The anechoic chamber in the university is completely insulated. The chamber was built in 2010 and has since then been used to measure antennas in a free space environment with RAM on all sides inside the chamber. The NSI Near Field Range has been placed inside the chamber and is calibrated for measuring for frequencies above 2GHz. All the equipment besides the cables and NSI Near Field Range have been placed outside the chamber, thus reducing the number of reflecting surfaces in the room. The power and the signal connection to the equipment inside the chamber has been made through specified holes so that there is no radiation leakage from the room. Any reflecting surface still left in the room is covered by RAM so that the reflections are reduced to a very low level. The measurements done in the anechoic chamber are more precise and have none of the spurious effects when compared with a normal environment measurement.

3.6 Design Specifications of the Chamber

The size ($length \times width \times height$) of the screened room used for building the Anechoic Chamber at USU is

$$12ft \times 10ft \times 8ft.$$

The walls, the ceiling and the floor are all made up of 1 inch thick aluminum metal with copper lining on the corners and at the edges of the chamber walls for extra screening protection. There is a door in one of the sidewalls for entering and placing the equipment and antenna in the chamber. The size ($width \times height$) of the door is

$$7ft \times 3ft.$$

The door also has copper shielding on its sides for better RF shielding in the chamber. Based on the size of the chamber and the absorbing material to be placed in it along with the equipment, the minimum frequency at which the chamber can be successfully operated was found to be 2GHz. There is no maximum frequency range as wavelength of electromagnetic waves decreases with increase in frequency and thus the minimum distance required for measuring any type of antenna or device also decreases, thus allowing effective measurement

of any antenna or device operating at frequencies of 2GHz and above. Three holes of 3" diameter each were made in the walls of the chamber for data and power connection to the equipment inside the chamber from the outside setup. The holes were drilled and insulated to avoid any damage to the cables, at locations which provided an easy and smooth path to the cables going in and out of the chamber for measurement purposes.

3.7 Materials Used for the Inside Shielding of the Chamber

The RAM's of different types, shapes, and sizes were used for shielding the walls on the interior side of the anechoic chamber. These RAM's were stuck on the walls of the chamber with the help of a specially made high strength contact adhesive. All of the different kinds of RAM's in various shapes and sizes and adhesive were ordered from Advanced Electromagnetics Inc (AEMI). AEMI designed, manufactured, and tested the RF absorber material to be supplied to USU for quality and effectiveness and shipped it to the university for the purposes of installation. A combination of the Broadband Pyramidal Absorbers AEP-06 and AEP-04 were supplied by AEMI for this purpose. Below is a list of all the different types, shapes, sizes, and properties of the absorbers and the adhesive which were used for the construction of the Anechoic chamber at USU.

- 50 AEP-06 pyramidal absorbers with standard AEP-06 configuration size of 24" × 24" × 6"
- 95 AEP-04 pyramidal absorbers with standard AEP-04 configuration size of 24" × 24" × 4"
- 8 AEP-06 diagonal one half piece from a standard AEP-06 pyramidal absorber cut into two pieces with a diagonal cut with standard AEP-06 configuration size of 24" × 24" × 6"
- 16 AEP-06 diagonal one half piece from a standard AEP-04 pyramidal absorber cut into two pieces with a diagonal cut with standard AEP-04 configuration size of 24" × 24" × 4"

- 20 AEPF-06 picture frame material with a size of 24" × 6" × 4" cut from AEPF-24
- 28 AEPF-04 picture frame material with a size of 24" × 4" × 4" cut from AEPF-24
- 25 SP AES 0.5" × 1" and SP SLAB 24" × 0.5" × 1"
- 5 AEWW-04 walkway absorbers with standard AEWW-04 configuration size of 24" × 24" × 5.5"
- 3M(TM) Scotch-Weld (TM) hi-strength 94 CA postforming bulk adhesive

3.8 Building of the Anechoic Chamber

A plan was developed for the sticking of the absorbers on each of the sides of the anechoic chamber. The absorbers were identified for treating each of the six sides separately and the design pattern for each side based on the generalized radiation pattern of the antennas was thought of. Each side had its own absorber structure plan based on the requirement of that side. AEMI helped a lot with the proposed designing process of sticking the absorbers in the chamber and also helped in the final drawing of designs for the sides of the chamber. After the plans for each side of the chamber were finalized, designs were drawn to indicate the required structure of the sides. The shape, width, length, and the cuts required on each of the absorber to be used were calculated and identified based on the design. More detailed designs were then made based on the various values computed for the absorbers above. The absorbers were then classified according to the design structure and any more absorbers needed were ordered from AEMI, to fulfill the requirements of the design plan. During the design process it was decided to complete each of the sides of the chamber as a single entity by itself. The corners on all of the sides and the holes in the wall for the insertion of cables for various functioning of equipment inside the chamber was also taken into account during the design process. Once the exhaustive design process was finished, the sticking of the absorbers on the wall according to the design commenced. The absorbers were stuck on the sides of the chamber by first applying the high strength adhesive using rollers, on the back side of each of the absorbers to be used during the completion of

a particular side of the chamber and then putting a little pressure on them to make sure that they stay at their designated places. All six sides of the chamber were done separately. The six different sides of the chamber are listed below.

3.8.1 Reflected Ceiling

The most important part of the chamber as the absorbers placed here are the ones most in danger of falling down and damaging themselves. The ceiling design was made with considerable attention to the radiation pattern as it is important to attenuate the radiation here so that there is no reflection from the ceiling whatsoever. The proposed design for the ceiling is shown in Fig. 3.2. The design finalized for the center of the ceiling based on the radiation pattern was a tetrahedron design as it helps in better attenuation of radiation as shown in Fig. 3.2. The edges of the ceiling were treated with AEPF-06 and AEPF-04 picture frame material as shown in Fig. 3.2 with the one edge behind the receiving antenna being treated with AEPF-06 and the rest of the three edges of the ceiling being treated with AEPF-04. Once all of the absorbers were put into place using the hi-strength adhesive, the edges of the ceiling became shielded and the ceiling looked like a picture frame. This picture frame configuration was chosen to make certain that the wall which receives higher radiation has better absorbers to achieve good attenuation. The tetrahedron was composed of the longer AEP-06 and AEP-06 diagonal absorbers which attenuate more radiation and thus provide lesser reflection. The tetrahedron absorbers were then stuck to the ceiling in the shape shown in Fig. 3.2. Four AEP-04 diagonal absorbers then covered the diametrically opposite ends of the tetrahedron and four other AEP-04 absorbers were cut using a saw to accommodate the rest of the corners of the tetrahedron. The above structure was then surrounded by sticking the AEP-04 absorbers around it and between the picture frame absorbers and the tetrahedron. Any adjustment to the absorbers if necessary was made by cutting them into shape using a saw. The final completed picture of the ceiling is shown in Fig. 3.3.

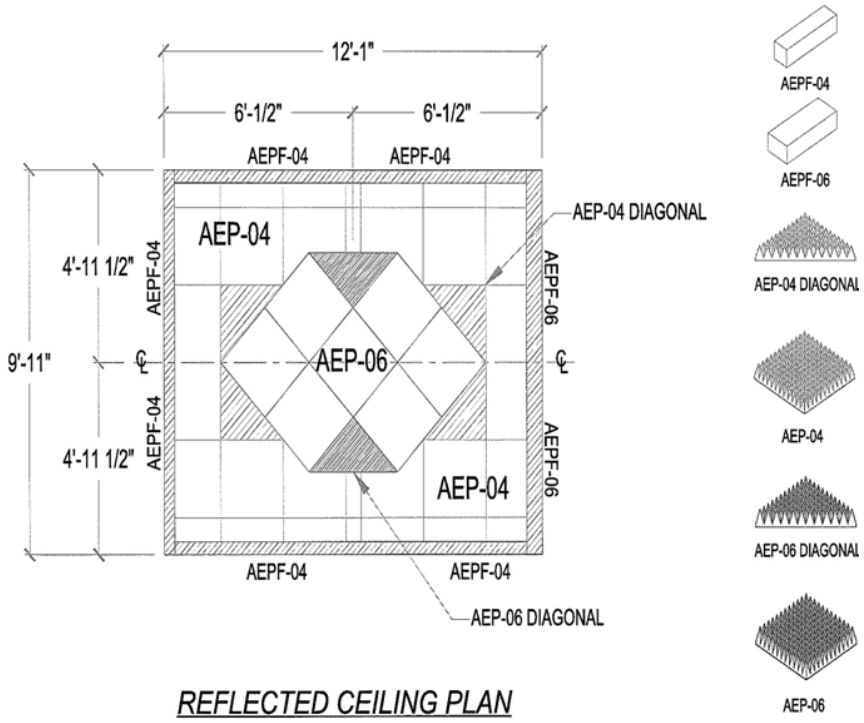

Fig. 3.2: Proposed reflected ceiling design.

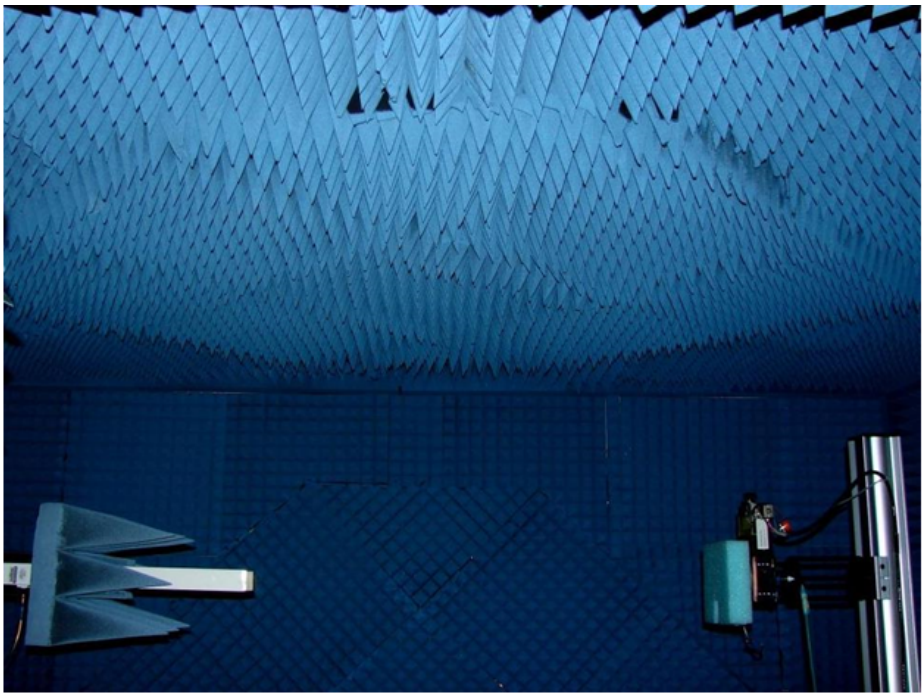

Fig. 3.3: Final completed picture of anechoic chamber's ceiling.

3.8.2 Sidewall A

Sidewall A is the wall opposite to the door of the chamber. The design of this wall including the edges, with one edge shielded by AEPF-06 and the other three edges being shielded by AEPF-04, is similar to the reflected ceiling design with one exception. The AEP-04 surrounding the tetrahedron structure on this wall has a small little gap where two 3" holes are made for the power cables to enter into the chamber. These holes are insulated from all sides by absorber and allows power and data cables for the equipment to come easily into the room. The proposed design for Sidewall A is shown in Fig. 3.4 and the final completed Sidewall A is shown in Fig. 3.5.

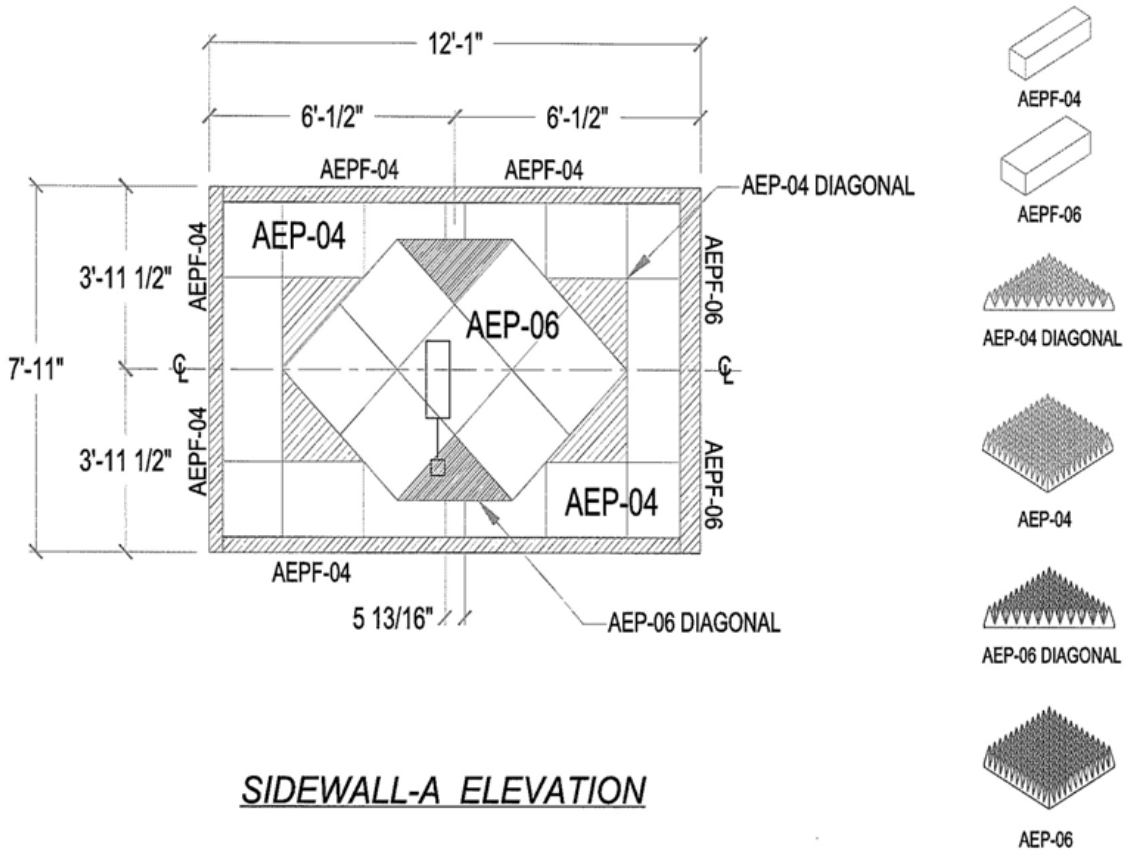

Fig. 3.4: Proposed sidewall A design.

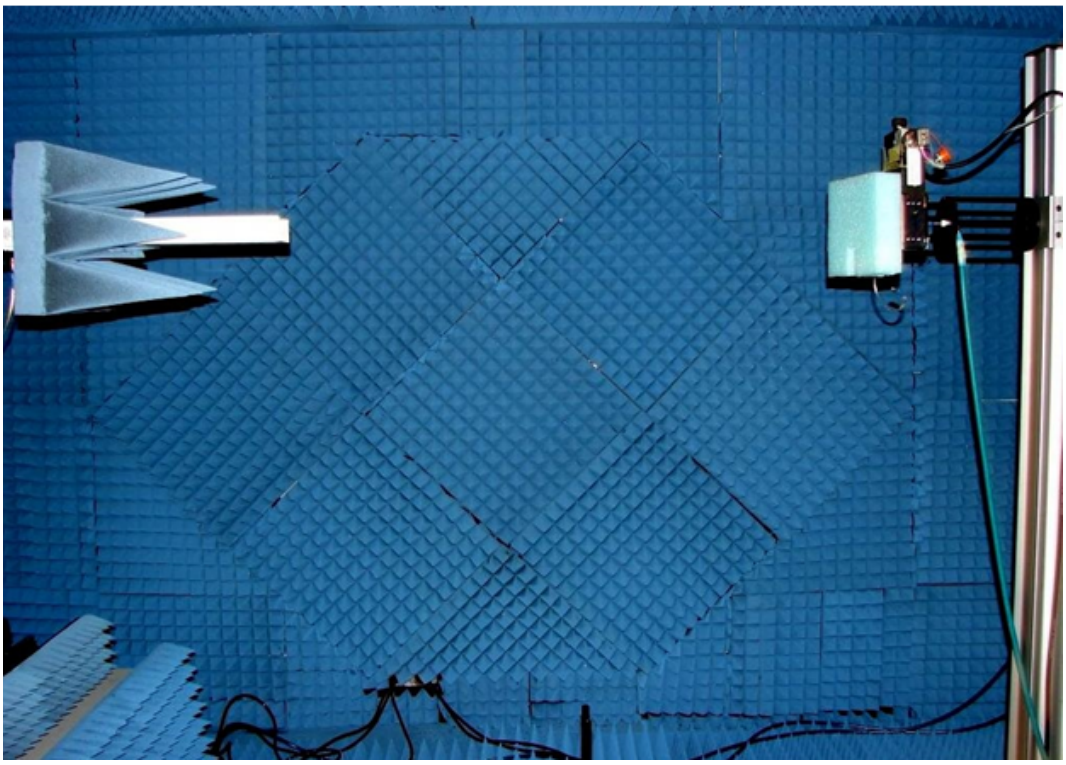

Fig. 3.5: Final completed picture of anechoic chamber's sidewall A.

3.8.3 Sidewall C

Sidewall C is the wall containing the door of the anechoic chamber. The final design for this wall is also the same as the design for the reflected ceiling, but with a cut in the absorber configuration where the door is present. The design of absorbers on this wall is shown in Fig. 3.6. The figure shows a cut where the door should be. While sticking the tetrahedron AEP-06 absorbers and the surrounding AEP-04 absorbers on the wall using the adhesive, the door position has been calculated before hand and suitable cuts are made in the configuration of absorbers to accommodate the door in the wall. The cuts were made using a saw and in such a way that they do not hinder the closing of the door of the chamber while providing suitable shielding all over the wall. The final completed configuration of the absorbers on the sidewall C is shown in Fig. 3.7. As can be seen from the figure the gap due to the presence of door is very negligible and thus can be neglected for all practical purposes.

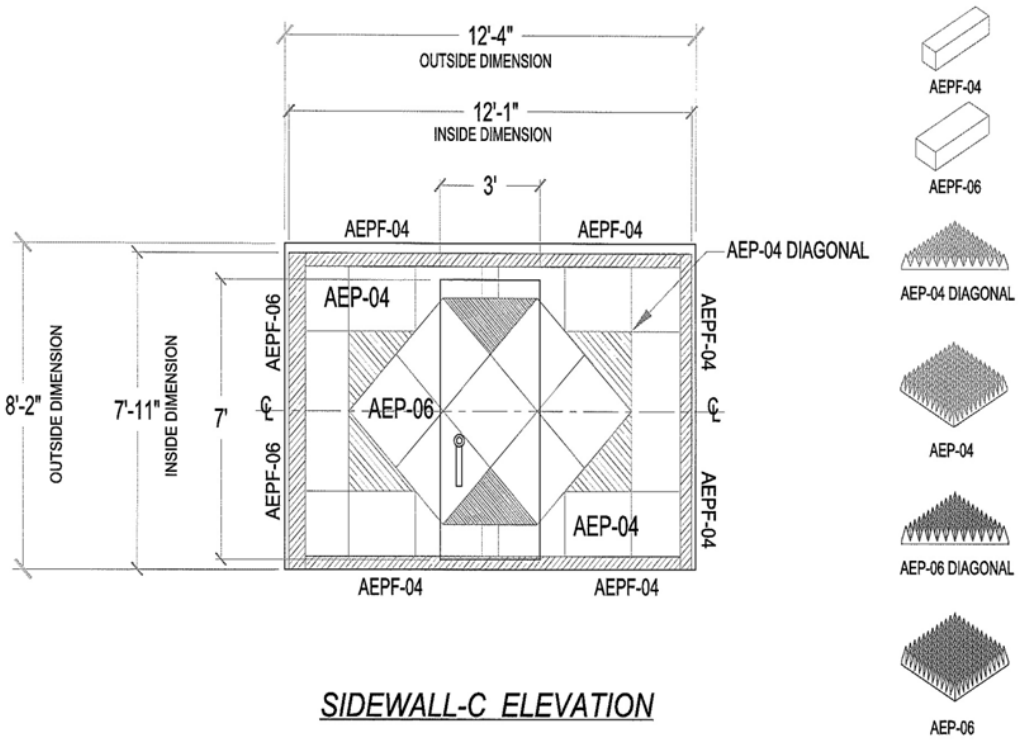

Fig. 3.6: Proposed sidewall C design.

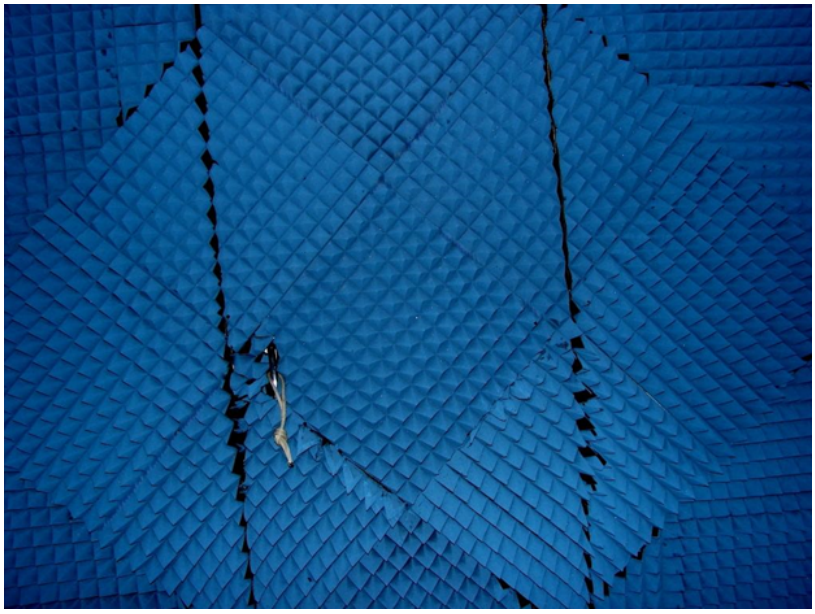

Fig. 3.7: Final completed picture of anechoic chamber's sidewall C.

3.8.4 Transmit Wall

Transmit wall is the wall in the chamber behind the transmitter of the NSI Near Field Systems Inc range. The final recommended design of the transmit wall is shown in Fig. 3.8. The edges of the transmit wall are all treated with AEPF-04 picture frame absorbers giving it a look like a picture frame configuration. AEP-04 absorbers are then used to treat the area between the picture frame on the transmit wall. AEP-04 absorbers are used to absorb and attenuate any back radiation occuring from the antenna so that proper measurement can be carried out and accurate results can be obtained. There is no special pattern on this wall and all the absorbers used are stuck using the adhesive in the standard manner. They are just stuck in proper rows and columns piece by piece. The final completed transmit wall is shown in Fig. 3.9.

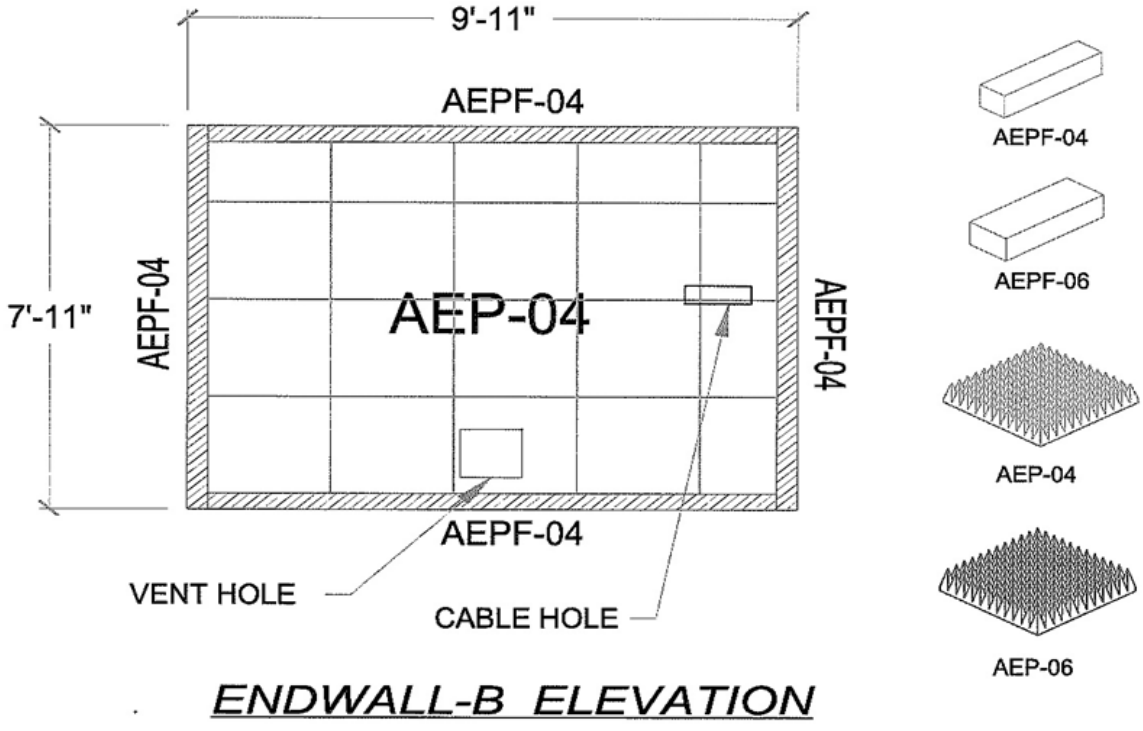

Fig. 3.8: Proposed transmit wall design.

Fig. 3.9: Final completed picture of anechoic chamber's transmit wall.

3.8.5 Receive Wall

Receive wall is the wall in the anechoic chamber behind the receiver assembly of the NSI System. The final design for this wall is shown in Fig. 3.10. The edges of the receive wall are all treated with AEPF-06 picture frame absorbers giving it a look like a picture frame. The area between the picture frame on the receiving wall is then treated by AEP-06 absorbers which can absorb more radiation due to their larger size of pyramids in the absorbers. The receive wall needs to have bigger pyramidal absorbers than the transmit wall because it is in the direction of maximum radiation. Thus, the recieve wall needs to absorb more radiation and reflect back much less radiation than the other walls in the anechoic chamber. The receiver wall design is very similar to the transmit wall design with the exception of the absorbers used on this wall. The final completed receive wall with absorbers placed is shown in Fig. 3.11.

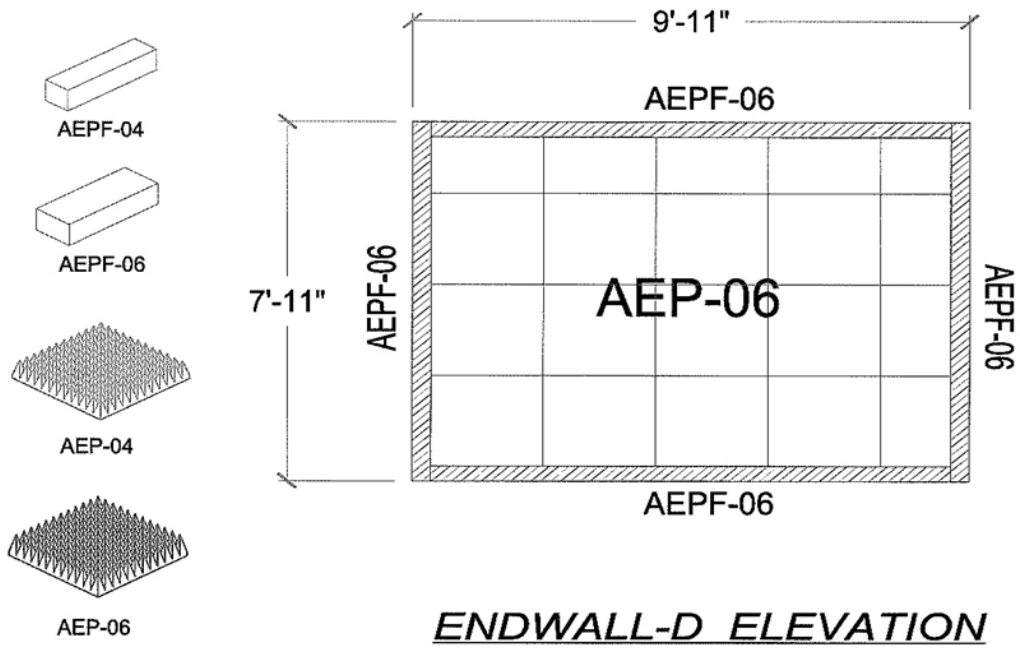

Fig. 3.10: Proposed receive wall design.

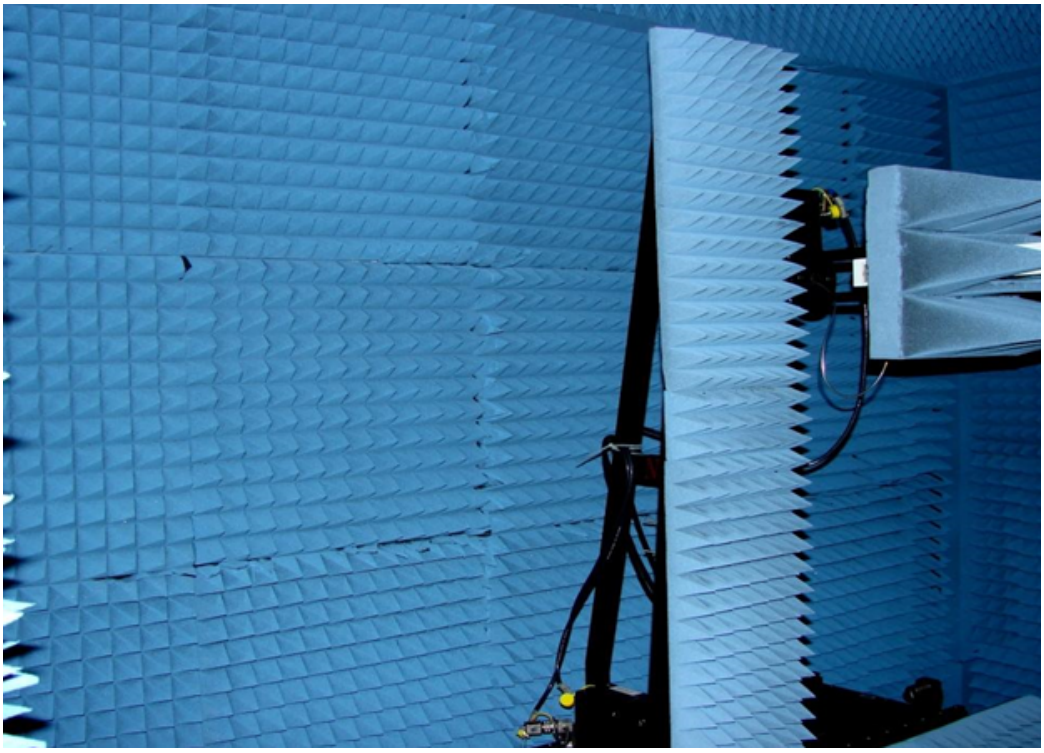

Fig. 3.11: Final completed picture of anechoic chamber's receive wall.

3.8.6 Edges of the Chamber

All the edges of the chamber as mentioned above were treated with a unique picture frame design approach. This approach takes care of all the edges on all sides of the chamber, which can be the ceiling-wall edges or the wall-wall edges, etc. In this approach, the edges on each side is treated with 3" to 4" thick flat absorbers that extends to the full length of absorber size along the wall surface. This method is the most efficient method to load the edges to eliminate any corner reflections and interaction between adjacent sides of a chamber. This approach also takes care of the pyramidal absorbers stuck on the sides of the chamber as it allows for suitable placing of these absorbers without them affecting each other on adjacent sides. Figures 3.12 and 3.13 show some of the edges made on the sides inside the chamber.

Fig. 3.12: A ceiling wall edge of the anechoic chamber.

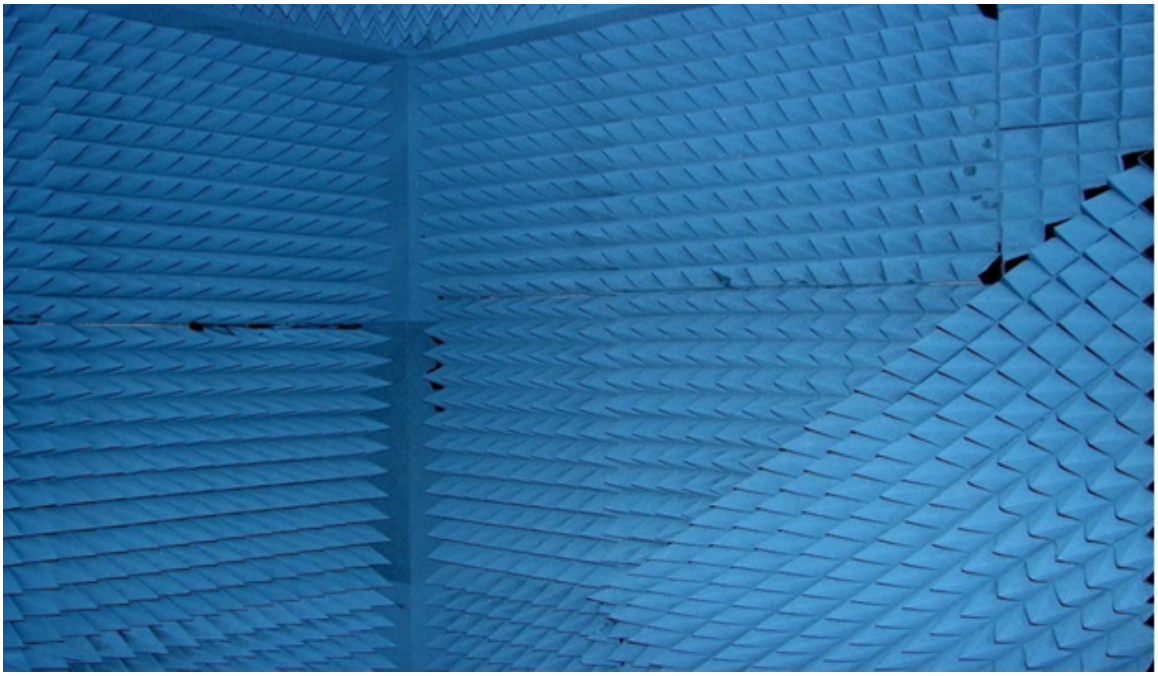

Fig. 3.13: Another shielded edge of the anechoic chamber.

3.8.7 Floor

The floor of the anechoic chamber was done last in the making of the chamber. It was done after the NSI equipment required to measure the antennas was placed inside the chamber and was suitably calibrated. The absorbers on the floor in the chamber were not stuck to the floor and were just simply placed on the floor making sure that there was no gap between them. This was done as this allows for changing of the absorber pattern on the floor based on the antenna type that is being measured and it allows users more mobility in the room as they can just remove the absorbers when they want to do some changes in measurement process. The final completed floor, as shown in Fig. 3.15, is very different from the suggested floor design that was thought of initially as shown in Fig. 3.14. This is due to the practical considerations regarding the antennas and to allow for better ease of access to the measuring system when the chamber is being used. The suggested design for the floor that was thought of, was similar to the one made on the reflected ceiling but the final completed floor structure (as seen in Fig. 3.15) is different and is a combination of AEP-06, AEP-04, and AEWW-04 absorbers. The walkway absorbers placed extend from the door

of the anechoic chamber close to the transmitter equipment in the current configuration to allow users easier access and to stand near the transmitter and fix their antennas and do calibrations based on it. The absorbers between walkway absorbers and the receive wall were AEP-06 and the absorbers between the transmit wall and walkway absorbers were AEP-04. The absorbers on the floor were just placed in a simple fashion (as shown in Fig. 3.15) with space between them where the transmitter and the receiver for NSI were placed. The absorbers surround the receiver scanner and the transmitter scanner of the NSI Near Field Range from all sides to make sure that there was proper absorption from the floor of the anechoic chamber and no radiation was reflected back. The edges between floor and walls are also covered with picture frame absorbers as explained previously to give the floor a picture frame look, too.

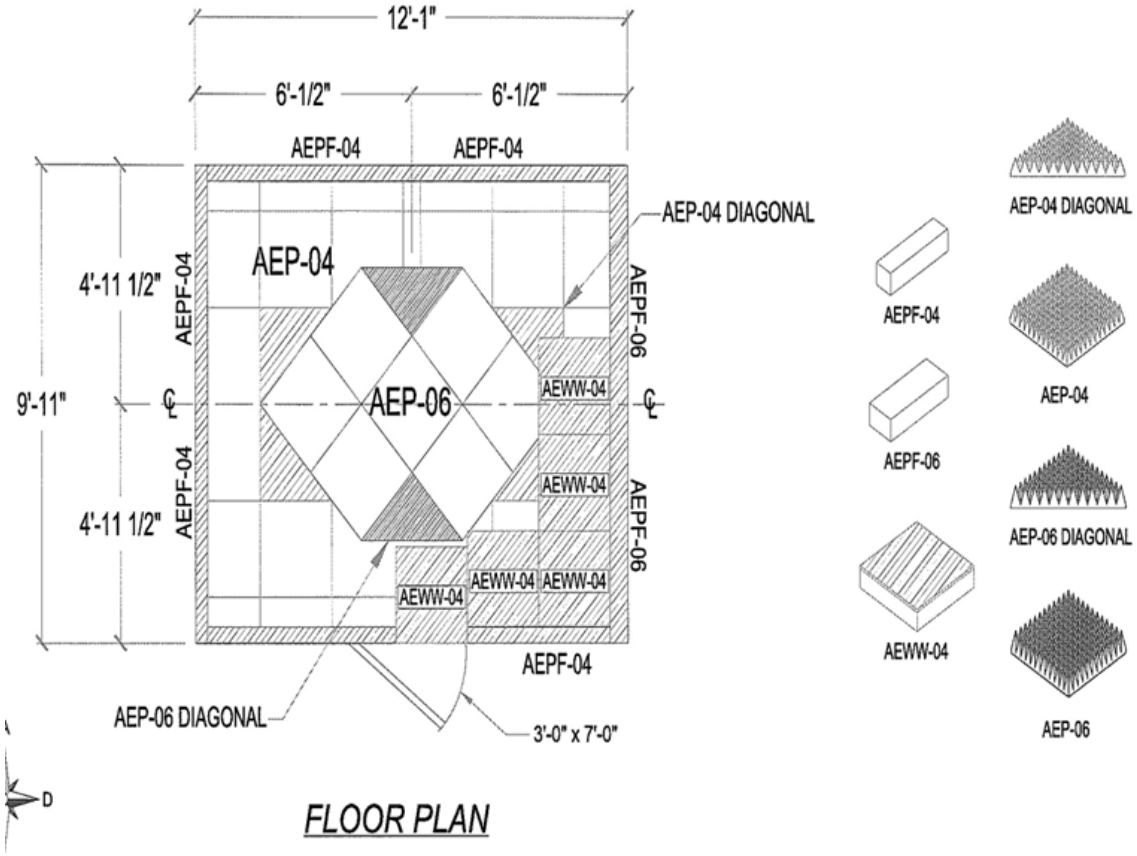

Fig. 3.14: Proposed anechoic chamber floor design.

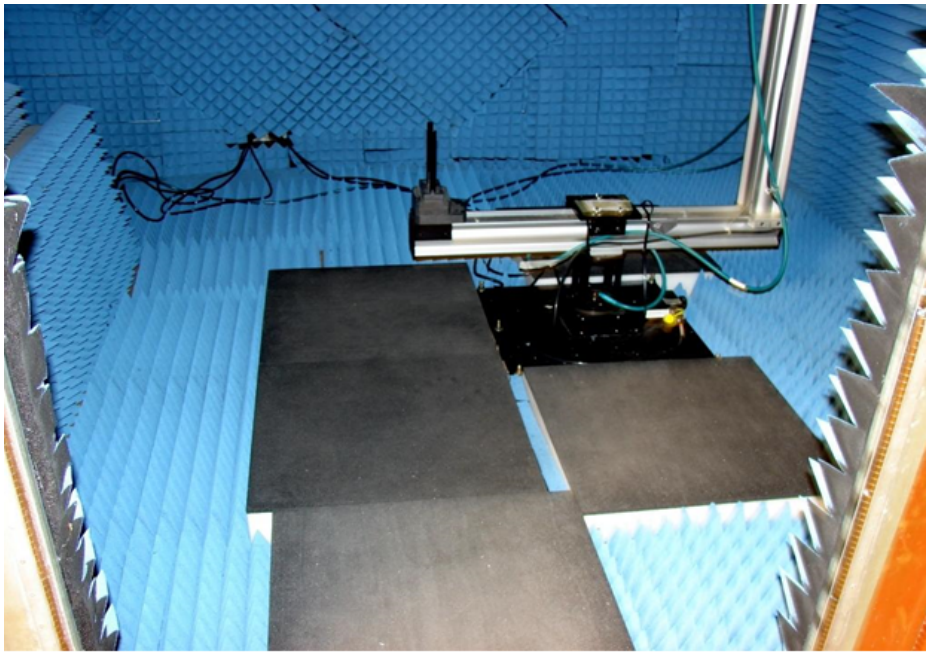

Fig. 3.15: Final completed anechoic chamber floor.

3.8.8 Receiver Scanner Bench

The receiver of NSI near field range requires a bench so that it can be properly aligned to the transmitter for appropriate measurement work. The receiver is a little smaller than the transmitter thus arising the need for a receiver bench. The receiver bench on which the receiver scanner would be placed is made of metal and has a wood top on it. The height, width, and size of the bench were made considering that it fits into the chamber and aligns the receiver to the transmitter perfectly without damaging any absorbers. The placing of the bench in the chamber increases the number of reflecting surfaces in the room and can thus cause spurious results in measurements. Thus, it is required to make sure that the number of surfaces of the bench exposed was much less. To achieve this a wooden board of width and height just a little more than the dimensions of the bench was taken and was treated with AEP-04 absorbers. These absorbers after being stuck firmly on the board were taken together with the board and placed in front of the receiver bench, which helped in reducing reflection from it as shown in Fig. 3.16. Also, absorbers were placed on the side of the receiver bench to reduce its spurious effects.

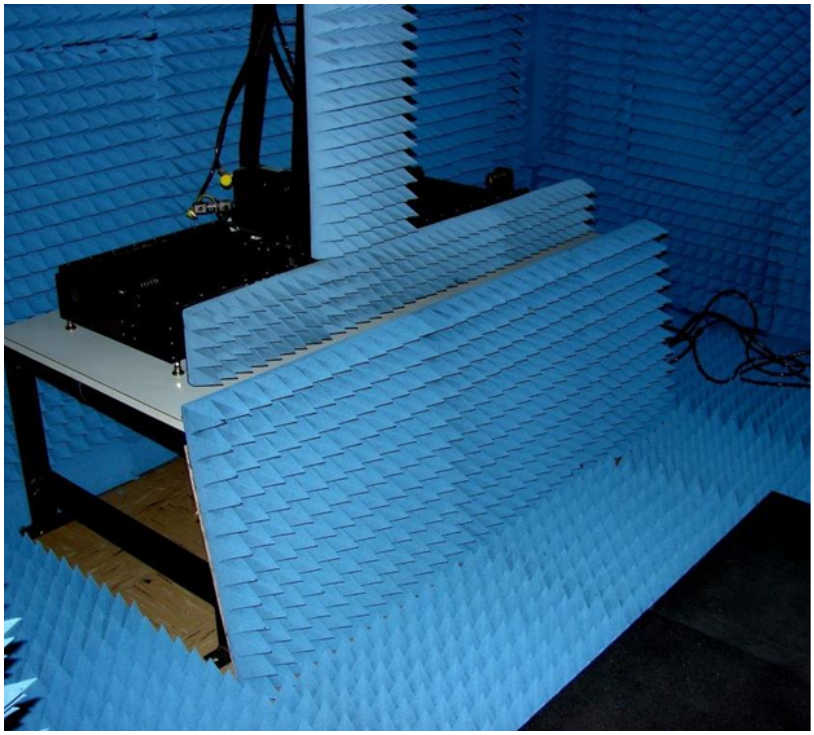

Fig. 3.16: Receiver scanner bench.

3.9 Equipment Installation

The following equipments and cables were used for smooth operation of the anechoic chamber built:

- Agilent Network Analyzer,
- Vertical Scanner or Receiver Scanner,
- Spherical Scanner or Transmitter Scanner,
- Antenna Range Controller Boxes (ARC),
- NSF Scanner Hardlock Computer Subsystems,
- Data Cables,
- Power Cables,
- Open Ended Waveguide Cables (OEWG).

After all of the absorbers on the wall and the ceiling of the chamber were stuck, some of the NSI equipment was moved into the chamber. The two major parts of the NSI range in the chamber is the transmitter scanner and the receiver scanner. The transmitter of NSI range is a spherical scanner and the spot where any measuring antenna is fixed and the receiver is the vertical scanner and the position where the probe is fixed to measure the antenna based on its frequency [14]. Figure 3.17 shows an antenna placed on the transmitter ready for measurement. The best readings are achieved when both of them are aligned with each other on a perfectly flat ground. The transmitter and receiver scanner are shown in Figs. 1.2 and 1.3. The receiver is placed on the bench mentioned before, to make sure that it aligns the receiver to the transmitter while creating much less disturbance to the absorbers placed in the room. The separation between the transmitter and the receiver is kept in excess of 3λ at a frequency of 2GHz. Based on this separation between the transmitter and the receiver, the chamber's lowest operating frequency is specified.

It is then made sure that the NSI equipment is placed flatly on the surface by using level balances on both the receiver and the transmitter. The power cables from both the transmitter and the receiver are then taken out through one of the holes in sidewall1 for power connection from the power port. The data cables connected to the receiver and the transmitter in the chamber, which controls the scanning of the equipment is then passed through the other hole in sidewall 1 and connected to ARC boxes. The transmitter of the NSI range is then connected to port 1 of the network analyzer using a OEWG cable for a particular frequency range which in this case is from 2.2GHz to 3.3GHz. The receiver of the NSI range is then connected in a similar fashion to port 2 of the network analyzer using another OEWG cable. These OEWG cables are placed in the chamber in such a way that they cause minimum disorder and are brought out of the chamber to connect to the network analyzer by using the hole made in the transmit wall of the chamber.

The equipment placed outside of the chamber and used for measurements includes the network analyzer, the ARC boxes, and the computer subsystems. The network analyzer is used to send power to the antenna connected to the transmitter in the chamber and to

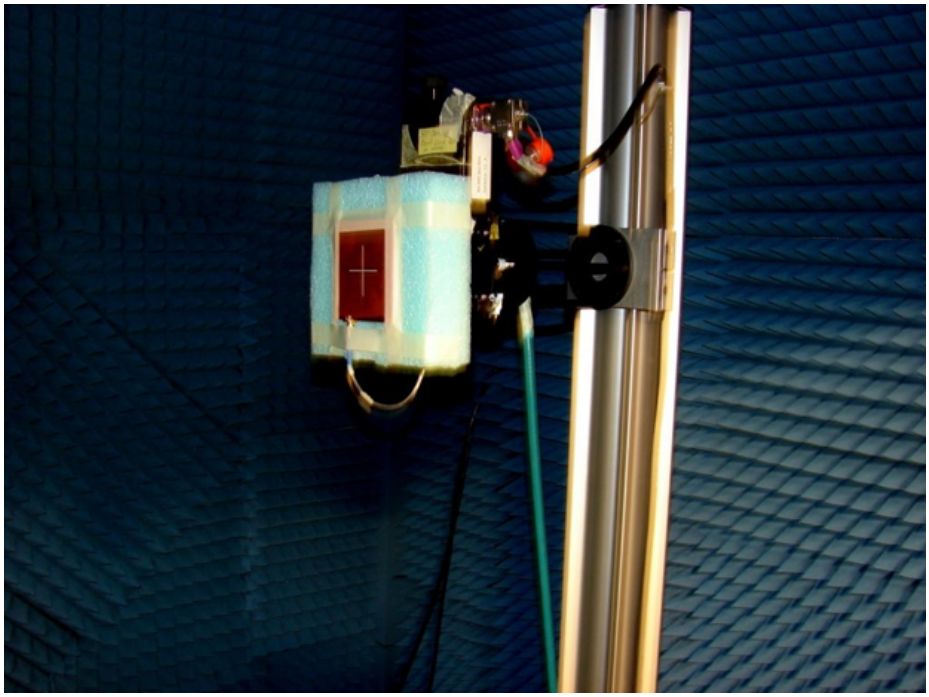

Fig. 3.17: Antenna placed on the transmitter scanner.

receive the radiated power back from the probe connected to the receiver. Data cables and a trigger cable connects the ARC boxes and the computer subsystems to the network analyzer for transfer of data from it and for triggering the network analyzer while in measurement mode. The ARC boxes placed outside the chamber control the movement of the scanners inside the chamber based on the settings made in the software and thus interact with both the computer subsystems and the scanners inside. The computer subsystem is the major controller of the measuring system, and it is from here that the user decides what kind of scanning and measurement process to do and how to do it. It also does all the computations required for the results and generates, saves and shows the results to the user. The computer subsystem thus can be said to be the brain of the system. It sends the controlling instructions to the ARC boxes and the network analyzer and then interprets the data received to show the results to the user. After all the above equipment is installed and connected, the chamber is ready to begin the measurement process. Figure 3.18 shows the equipment placed outside the chamber for the measurement process and the cables connected to the equipment.

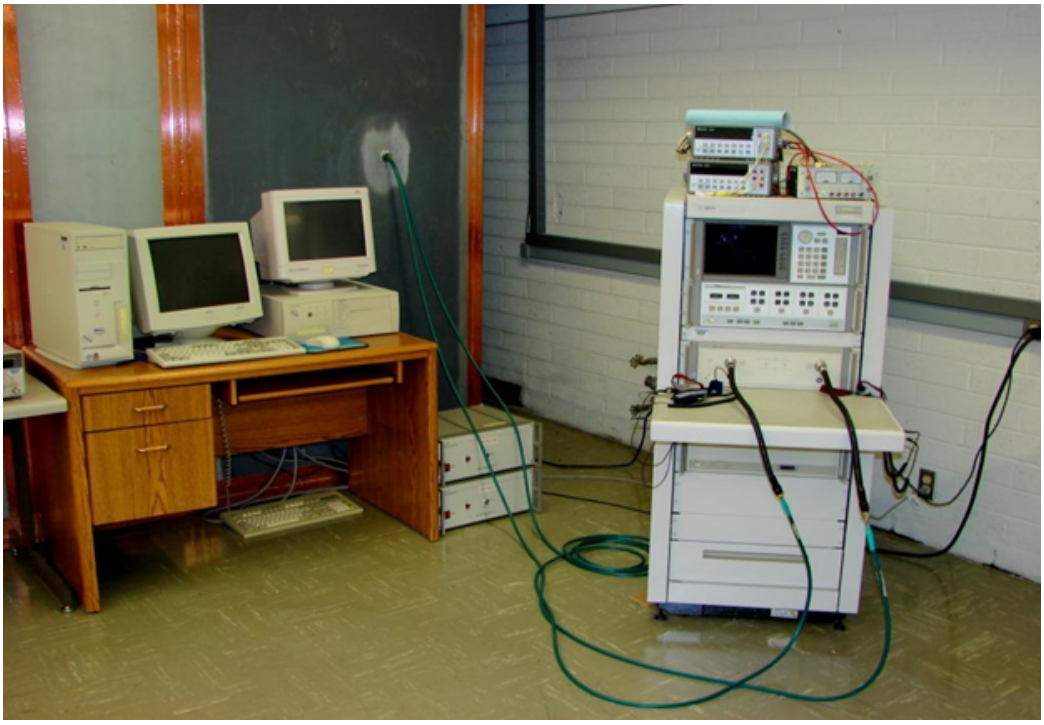

Fig. 3.18: NSI equipment placed outside for controlling the measurment process.

3.10 Usage

After all the above setup is done, the chamber is ready to begin the measurement process for an antenna. The chamber is currently used for measuring antennas of different types such as slot antennas and patch antennas. It is used to calculate the actual radiation pattern, directivity, gain, and polarization of an antenna in normal environment and compare it with simulation to see the difference in results. The chamber reduces the spurious effects to minimum and helps in better characterization of the antennas measured. The radiation pattern obtained can be seen in both 3D and 2D patterns, thus giving a better representation of the antenna. Thus, an anechoic chamber makes practical measurement realizable and possible and helps in better understanding of radiating structures.

Chapter 4

Measurements in Anechoic Chamber

After the antennas are simulated and fabricated, they are measured in a real environment to see whether they fulfill the requirements that are expected of them in reality and how much they differ from the simulation results obtained. The measurement environment is generally some controlled surroundings in which the antenna performance is not hindered and one which makes the antenna performance the best, such as the anechoic chamber as mentioned before. The measurements on antennas done in the anechoic chamber are usually genuine and do not have any spurious results. The measurements done at USU were all done in the anechoic chamber.

Special equipment is needed for measurement of different parameters of antennas and the ones used for measurement purposes here are called the NSI near field range. This range is placed inside the anechoic chamber for the best results out of measurement methods. The antennas to be measured are placed on the range and tested for their various parameters such as radiation pattern, cross polarization level, AR, gain, etc. These measurement results are then noted and the antenna specifications are given whenever the antenna is used.

The measurements carried out using the NSI near field range to achieve the various parameters of antenna are generally done in two steps:

- Pattern Measurement,
- Gain Measurement.

Pattern measurement, as defined before, is the relative power density of the electromagnetic wave transmitted by the antenna in a given direction. Pattern measurement is done to view and validate the radiation pattern of an antenna in far field region of free space. It also gives us the axial ratio of the antenna and the cross polarization level between different

components of the polarization of the antenna. Pattern measurement is the most important measurement of the antenna and all the basic results of measurement of antennas comes from it.

To measure the gain of the particular antenna being tested, gain measurement is done. It is important as it is one of the most important characterizing factors of the antenna and is related to both the efficiency of the antenna and its directivity. Gain measurement using NSI is generally done in two ways:

- Comparison Gain Measurement,
- Direct Gain Measurement.

This thesis shows the way to perform direct gain measurement as it does not require an antenna of comparative parameters and can be easily modified to be used for other kinds of antennas. The gain measured by this method is correct to the accuracy of ± 0.5dB for all practical antennas. Before doing gain measurement, it is necessary to have the results of pattern measurement; otherwise, it is not possible to measure the gain of the antenna.

To perform the pattern measurement, the AUT is placed on the transmitter of the NSI near field range and near field techniques are then applied to measure the radiation pattern of the antenna in the far field. Spherical near field measurement techniques are generally used for this purpose. The measurement is carried out in the anechoic chamber and its setup is shown in the following steps:

- Based on the known design frequency of the antenna, the near field region is calculated, which is generally 3 to 10 times the wavelength of the antenna, and the transmitter is then placed in that range for the antenna to be setup on it. The range distance also includes the length of the receiver probe. Thus, the total distance to find the range is a total of the length of the receiver probe and the distance between the transmitter and the receiver probe.
- The transmitter alignment is checked next. This is done by making sure that the transmitter setup is placed flat on the surface. The balances are placed on the bottom

plane of the transmitter to see if it is perfectly flat or not. If it is not perfectly flat, the screws below the plane are tightened or loosened to make sure that the bottom plane is perfectly flat as shown by the balances so that the transmitter is aligned.

- The AUT is then put on the transmitter as shown in Fig. 2.17, which is then connected to Port 1 of the network analyzer using a OEWG cable. The receiver is connected to Port 2 of the network analyzer using another OEWG cable. The OEWG cables have a frequency range, and the one which is desirable for use is used.

- The trigger cable from the ARC boxes is then connected to the network analyzer.

- The network analyzer, the ARC boxes and the computer subsystems are then started. After the NSI software is opened, the network analyzer displays the message "System in fast-ch mode."

- Indexing of all the axes of the system is then done by selecting the hardware option in the NSI software, then selecting the hardware axes in it and then choosing the index all option in the scanner subsystem dialog box.

- The transmitter AUT and the receiver probe alignment is now checked using a laser [14]. If any mismatch is found, it is compensated by adjusting the x-axis and y-axis in the scanner subsystem in the dialog box hardware axes in the software so that the receiver probe exactly matches the transmitter.

- The pol axis, phi axis, and the azimuth axis are then setup by double clicking on them in the scanner subsystem and then setting them up based on your requirement. Generally all the limit switch in all the three axes is ignored while moving.

- An existing file is then opened and a new scan is created in it.

- Dimension of the antenna are then put in the length and width blanks of the measurement box as shown in Fig. 4.1.

- Maximum far field angle is then set to 180 degrees.

- The parameters for AUT scan radius is then put in, where the distance between the probe tip and the antenna center is the width and the expanse between the antenna center and the bottom hole in transmitter is the distance to be put in as the parameters.

- Sampling is done as per your measurement desires, and the spherical near field system is selected from the box below it.

- If the AUT is to be tested for various frequencies, then the multibeam setup option is now used. The start frequency is put in by the user, and then the step size by which the frequency will shift is put in the delta frequency box. To put in the stop frequency you just calculate the number of steps you need to get there from the start frequency using the delta frequency steps. The outer loop is then selected and the generate frequency list tab is pressed to generate the frequencies of operation. Scan speed and dwell time can also be set up as per requirement.

- The type of probe is put in the probe setup then. The probe setup requires the definition of the probe and its model.

- The door of the anechoic chamber is now closed for final settings to take place on the software.

- Now in RF Subsystem in hardware axes we press edit and select the control to 4096Ave, 824.00msec. This helps us in maintaining a good S/N ratio. The source setup is then done as per requirements.

- The frequency is now chosen as per requirement.

- When the S/N ratio exceeds 40dB, acquire is pressed to start the measurement.

The above pattern measurement method remains the same for both linear polarization and CP. Polarization is not considered when pattern measurement is setup. After the pattern measurement is done, direct gain measurement is carried out. To do the direct gain

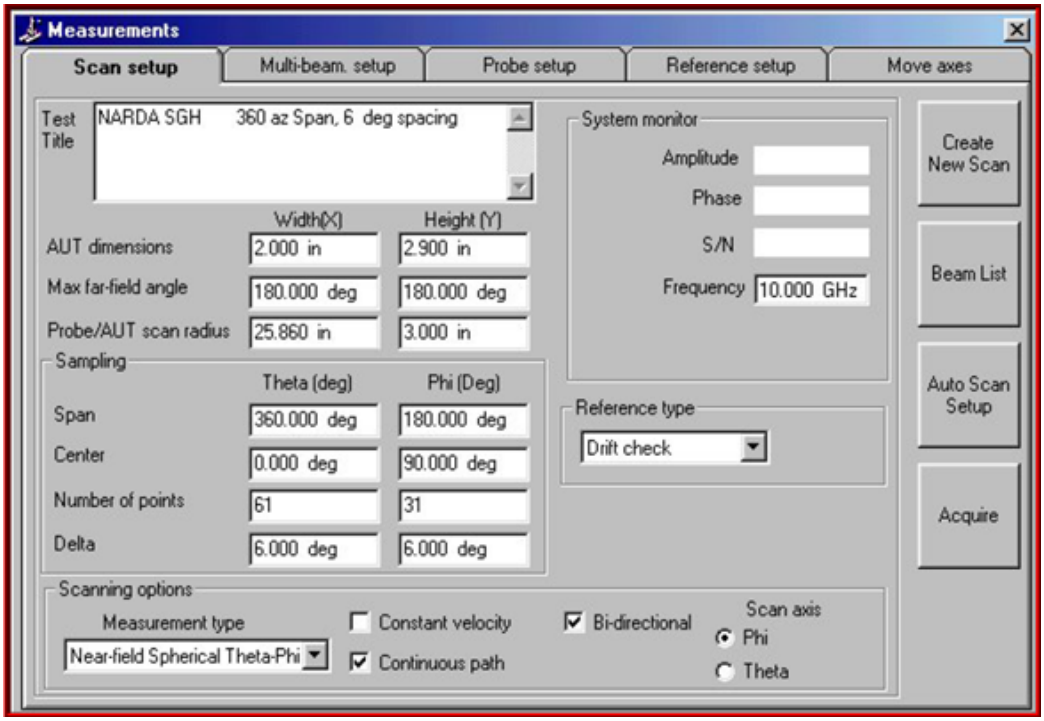

Fig. 4.1: Measurement box in NSI software.

measurement, probe gain, and bypass measurement values are established in advance. This is shown to be done in the following steps:

- Probe gain of the probe being used is found out for that particular frequency by using the probe data sheet. In this case our probe is a OEWG with a frequency range of 2.2-3.3GHz. The probe gain was found out for this particular probe at the corresponding frequencies. Generally 5dB is used as an approximate probe gain for this probe for approximate calculations.

- Bypass measurement is done by connecting a cable between the AUT and probe mounts, thereby bypassing both AUT and probe in the RF path. This will give a peak amplitude reading. This amplitude reading is considered to be all the power radiated in the RF path without any losses present. This is the bypass measurement value to be used in the direct gain method. If any increase in accuracy is needed, the effects of losses in the cable can also be included in calculations. This is done by inserting the value of losses of cable in the network offset box in dB in the plot parameters tab

in measurement of far field. Also, the mode in which bypass measurement is done does not matter as it is only a single amplitude reading and does not depend on the acquisition mode or position of the scanners.

After all the values are known and the pattern measurement is finished, the radiation pattern in far field is plotted using the far field tab in NSI as shown in Fig. 4.2. Here you can plot the radiation pattern for different far field spans with a center angle and the number of points as desired by you. The known polarization of the antenna is selected from the principal pol reference box, where you can select all the three types of polarizations that a antenna can have which are LHCP, RHCP, and LP. As long as the option is on amplitude, radiation pattern in both principal and cross plane in both horizontal and vertical cuts can be plotted. If the antenna is CP, then setting the option to AR and choosing the principal pol reference as either RHCP or LHCP will give you the measured AR of the antenna and tell you how good the CP of the antenna is.

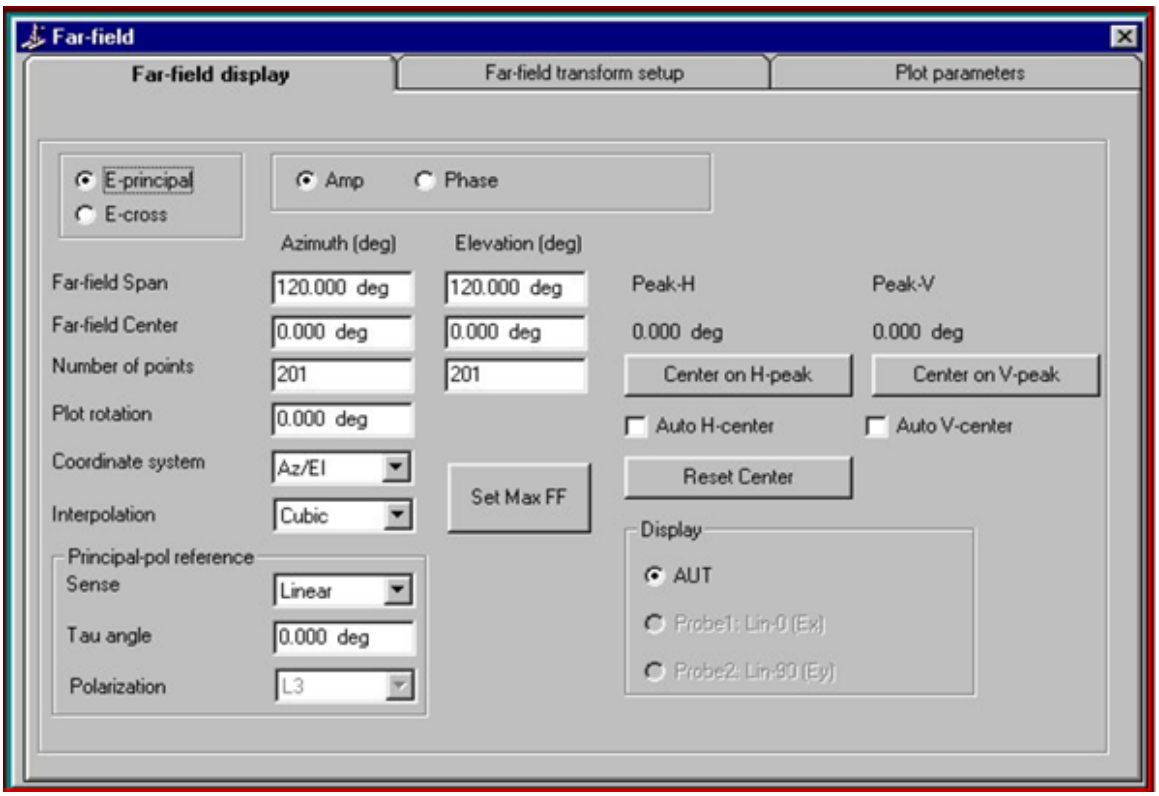

Fig. 4.2: Far field box in NSI software.

The gain can be found out from the plot parameters tab in the same dialog box. The box is shown in Fig. 4.3. The option, in this case, in far field display tab is set to amplitude. In the plot parameters tab then the probe gain and bypass measurement values are put in. After the amplitude in either of the cut is plotted the gain value appears in the calculated AUT gain box. This is the gain of the antenna. Directivity is also mentioned above and based on it the efficiency of the antenna can be computed. It is important to remember that the polarization sense is set up based on the polarization of your antenna; otherwise, the gain may differ from its original value.

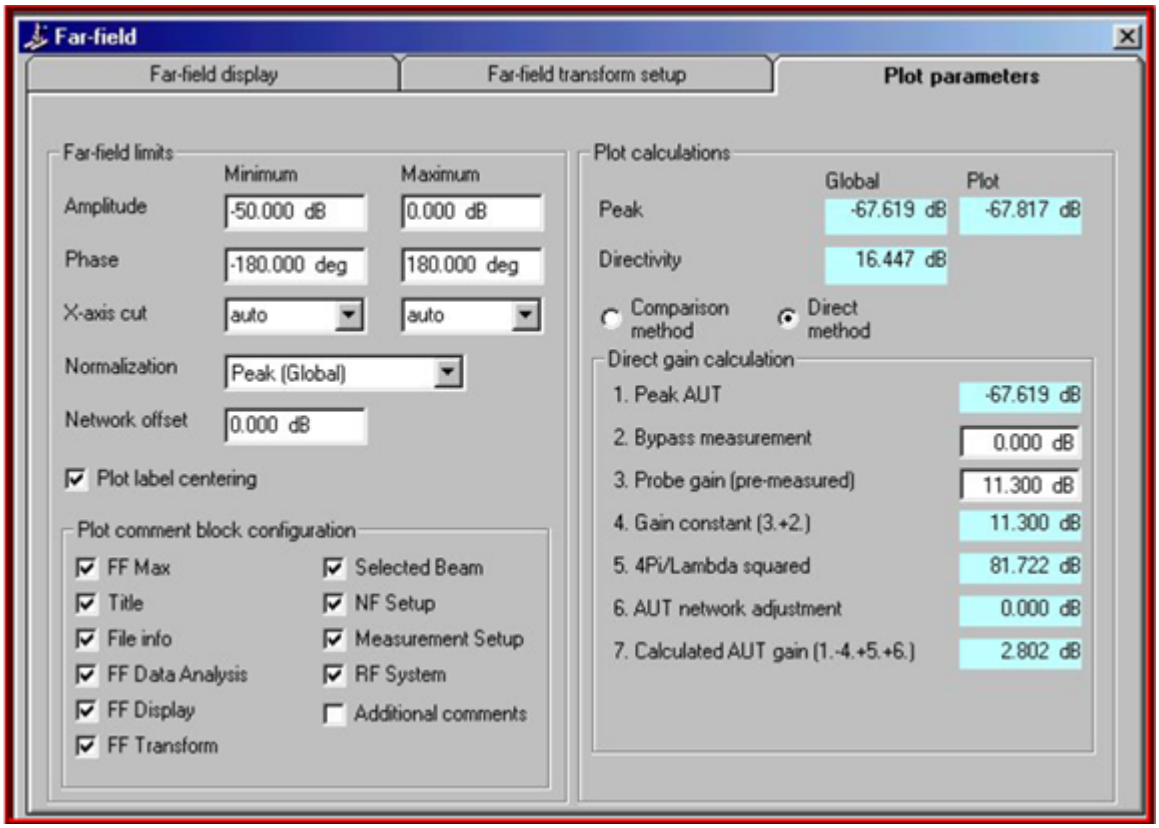

Fig. 4.3: Direct gain measurement box in NSI software.

Table 4.1 shows the bypass measurement values for a frequency range of 2.2-3.3GHz. All the values are in dB and have been calculated for two source power levels of 10dBm and 15dBm.

Table 4.2 shows cross polarization level in terms of axial ratio.

Table 4.1: Bypass measurement values using OEWG cable for NSI from frequency of 2.2Ghz - 3.3GHz.

Frequency (GHz)	Bypass Measurement(dB) @10dBm	Bypass Measurement(dB) @15dBm
2.2	-5.61	-5.61
2.25	-5.63	-5.63
2.3	-5.73	-5.73
2.35	-5.77	-5.77
2.4	-5.80	-5.80
2.45	-5.80	-5.80
2.5	-5.72	-5.73
2.55	-5.77	-5.77
2.6	-5.80	-5.80
2.65	-5.73	-5.73
2.7	-5.75	-5.75
2.75	-5.78	-5.79
2.8	-5.76	-5.77
2.85	-5.81	-5.81
2.9	-5.93	-5.93
2.95	-5.94	-5.94
3	-6.05	-6.05
3.05	-6.20	-6.20
3.10	-6.29	-6.29
3.15	-6.47	-6.47
3.20	-6.67	-6.67
3.25	-6.71	-6.71
3.30	-6.91	-6.91

Table 4.2: Axial ratio in terms of cross polarization level.

Cross Polarization Level	Axial Ratio
-10	5.69
-15	3.12
-20	1.74
-25	0.98
-30	0.55
-35	0.31
-40	0.17
-45	0.10

References

[1] C. Kakoyiannis and P. Constantinou, "Electrically small microstrip antennas targeting miniaturized satellites: the cubesat paradigm," in *Microstrip Antennas*, N. Nasimuddin, Ed., Vienna, Austria: InTech, 2011, pp. 273–316.

[2] S. Vaccaro, J. Mosig, and P. De Maagt, "Making planar antennas out of solar cells," *Electronics Letters*, vol. 38, no. 17, pp. 945–947, 2002.

[3] T. Turpin and R. Baktur, "Meshed patch antennas integrated on solar cells," *Antennas and Wireless Propagation Letters, IEEE*, vol. 8, pp. 693–696, 2009.

[4] M. Mahmoud, "Integrated solar panel antennas for cube satellites," Master's thesis, Utah State University, Logan, UT, 2010.

[5] J. James and J. James, *Handbook of Microstrip Antennas.* London, UK: Peregrinus, 1989.

[6] C. Balanis, *Antenna Theory: Analysis and Design.* Hoboken, NJ: John Wiley and Sons, 2005.

[7] J. Kraus and R. Marhefka, *Antennas for all applications.* New York: McGraw-Hill, 2002.

[8] P. Bhartia, I. Bahl, R. Garg, and A. Ittipiboon, *Microstrip Antenna Design Handbook.* Norwood, MA: Artech House Publishers, 2001.

[9] J. Yun and R. Vaughan, "Open slot antenna in a small ground plane," *Microwaves, Antennas & Propagation, IET*, vol. 5, no. 2, pp. 200–213, 2011.

[10] D. J. v. Rensburg, *Rotating Linear Source CP Testing*, Torrance, CA: Nearfield Systems, Inc., 2011.

[11] S. Thierauf, *Understanding Signal Integrity.* Norwood, MA: Artech House Publishers, 2010.

[12] D. Pozar, *Microwave Engineering*, 3rd ed. Danvers, MA: John Wiley and Sons, 2005.

[13] G. Dash and L. Ampyx, "How rf anechoic chambers work," *dashfoundation.com*, 2005.

[14] *NSI 2000 Operating Manual Version 4*, Torrance, CA: Nearfield Systems, Inc., 2005.

[15] J. Seybold, *Introduction to RF propagation.* Hoboken, NJ: John Wiley and Sons, 2005.

[16] M. Katayama, M. Yamamoto, T. Nojima, and K. Itoh, "Microstrip-fed crossed-slot array antenna," *Electronics Letters*, vol. 40, no. 4, pp. 223–224, 2004.

[17] M. Katayama, M. Yamamoto, K. Itoh, and T. Nojima, "Microstrip-fed slot array antenna having 45 inclined linear polarisation," *Electronics Letters*, vol. 39, no. 21, pp. 1492–1493, 2003.

[18] S. Vaccaro, J. Mosig, and P. de Maagt, "Two advanced solar antenna solant designs for satellite and terrestrial communications," *Antennas and Propagation, IEEE Transactions*, vol. 51, no. 8, pp. 2028–2034, 2003.

[19] Y. Yoshimura, "A microstripline slot antenna (short papers)," *Microwave Theory and Techniques, IEEE Transactions*, vol. 20, no. 11, pp. 760–762, 1972.

[20] M. Mahmoud and R. Baktur, "A dual band microstrip fed slot antenna," *Antennas and Propagation, IEEE Transactions*, no. 99, pp. 1–1, 2011.

[21] B. Porter and S. Gearhart, "Theoretical analysis of coupling and cross polarization of perpendicular slot antennas on a dielectric half-space," *Antennas and Propagation, IEEE Transactions*, vol. 46, no. 3, pp. 383–390, 1998.

[22] J. Kraus, *Electromagnetics*, 4th ed. New York: McGraw-Hill, 1992.